Synthesis, *In vitro* Antimicrobial Activity and *In silico* Studies of Schiff Base Derivatives of Isonicotinic Acid Hydrazide

By: Mulugeta Ayele (B. Pharm.)

Advisors: Dr. Daniel Bisrat (PhD.)

Prof. Kaleab Asres (PhD.)

A Thesis Submitted to the Department of Pharmaceutical Chemistry and Pharmacognosy, School of Pharmacy, College of Health Sciences, Addis Ababa University in Partial Fulfilment of the Requirements for the Degree of Master of Sciences in Medicinal Chemistry

Addis Ababa, Ethiopia

February, 2024

Addis Ababa University

School of Graduate Studies

This is to certify that the thesis prepared by Mulugeta Ayele, entitled: "**Synthesis, *In vitro* Antimicrobial Activity and *In silico* Studies of Schiff Base Derivatives of Isonicotinic Acid Hydrazide**" and submitted in partial fulfilment of the requirements for the Degree of Master of Science in Medicinal Chemistry complies with the regulations of the university and meets the accepted standards with respect to originality and quality.

Signed by the Examining Committee:

Name	**Signature**	**Date**
External examiner: Dr. Wondmagegn Tamiru (PhD)	……	**.**…..……
Internal examiner: Mr. Biniam Paulos	……	**...**……
Advisors: Dr. Daniel Bisrat (PhD)	…….....	……
Prof. Kaleab Asres (PhD)	……..	..……..**.....**

Abstract

Synthesis, *In vitro* Antimicrobial Activity and *In silico* Studies of Schiff Base Derivatives of Isonicotinic Acid Hydrazide

Mulugeta Ayele

Addis Ababa University, 2024

Infectious diseases pose a significant global health burden due to growing antimicrobial resistance and the emergence and spread of new and existing pathogens. These continuing challenges demand for the development of potent drugs with high biological activity. In drug development, compounds featuring diverse structures, like Schiff bases, exhibit remarkable pharmacological effects. Isonicotinic acid hydrazide is used to treat tuberculosis (TB), which is caused by *Mycobacterium tuberculosis*. However, its effectiveness is limited against common Gram-positive and Gram-negative bacteria. Therefore, the objective of this study is to extend the antimicrobial efficacy of isonicotinic acid hydrazide by structurally modifying it through synthesis. Using the conventional Schiff base synthesis method, three compounds were synthesized by employing isonicotinic acid hydrazide (**15**) as a scaffold and incorporating imine functional groups through specific ketones or aldehydes. The chemical structures of three derivatives, namely (E)-N'-(2-hydroxy-1,2-diphenylethylidene) isonicotinohydrazide (compound **27**), (E)-N'-(4-hydroxy-3-methoxybenzylidene) isonicotinohydrazide (compound **28**), and (E)-N'-(4-(dimethylamino)benzylidene)isonicotinohydrazide (compound **29**), were determined through ^{1}H, ^{13}C-NMR, DEPT-90 and DEPT-135 spectral data. The antimicrobial activity of these synthesized compounds was assessed against twenty-six bacterial and four fungal strains using disk diffusion and broth dilution methods. Using the disk diffusion method, compound **27** demonstrated the highest antibacterial activity against *S. aureus* ML 267 at a concentration of 200 µg/ml, resulting in a 17.0 mm zone of inhibition (ZOI), which was

comparable to the standard ciprofloxacin (ZOI= 18.0mm). Additionally, the minimum inhibitory concentration (MIC) of compound **27** was determined to be 25 µg/ml using the broth dilution method. Notably, compounds **28** and **29** also displayed antibacterial activity, showing ZOI values ranging from 7.5-15.0 mm and MIC values within the range of 10-400 µg/ml. Moreover, compound **29** demonstrated the highest antifungal activity against *Candida albicans* ATCC 10231 and *Aspergillus niger* ATCC 6275, with ZOI value of 13.0 mm for both microorganisms at a concentration of 1500 µg/ml, and an MIC value of 400 µg/ml for each. Antimicrobial drugs target specific enzymes crucial for the biosynthesis pathways of pathogenic microbes. In this study, FabF of *Escherichia coli* (*E. coli*) was selected for molecular docking analysis to predict ligand-protein interactions for antibacterial purposes. Molecular docking of compounds **27-29** on the FabF (PDB ID: 3HNZ) of *E. coli* showed favorable docking scores within the range of –8.665 to –5.070 Kcal/mol. Among the compounds, compound **27** demonstrated the strongest binding affinity (–8.665 Kcal/mol) with FabF, establishing multiple hydrogen bonds and pi-pi stacking interactions at specific binding sites of the 3HNZ enzyme. The presence of imine functional groups in these compounds seemingly contributes to their antimicrobial activities. Overall, these findings underline the potential of the synthesized compounds, particularly the Schiff bases of isonicotinic acid hydrazide, in addressing bacterial and fungal infections.

Keywords: Antimicrobial resistance, isonicotinic acid hydrazide, Schiff bases, antimicrobial activity, molecular docking, pharmacokinetic properties

Acknowledgments

I want to start by expressing my gratitude to the Almighty God for providing me with resilience, health, and strength during this study and throughout my entire life.

I would like to express my deepest appreciation to Dr. Daniel Bisrat, my advisor and Head of Department of Pharmaceutical Chemistry & Pharmacognosy, for his incredible support and valuable guidance throughout the research period. He continually conveyed the knowledge of research and provided the guidance to complete my research work despite his busy schedule. I will always be indebted for his constant support in technical and non-technical issues, kind supervision, and priceless suggestions.

I express my gratitude to Prof. Kaleab Asres for his assistance, insightful feedback, and direction on this research. Also I am grateful to Prof. Arivijit Mazmuder for performing the antimicrobial activity assay; without his invaluable assistance, this study would not have been possible.

I am grateful to the Department of Pharmaceutical Chemistry and Pharmacognosy for the opportunity I have got to proceed in the research area I am highly interested. Also I would like to thank my family; friends; my sincere appreciation goes out to all who have contributed to the successful completion of this research work.

Thank you all!

Table of Contents

Contents Page No.

List of Figures

List of Tables

List of Schemes

Abbreviations

^{13}C-NMR	Carbon thirteen nuclear magnetic resonance
^{1}H-NMR	Proton nuclear magnetic resonance
ACP	Acyl carrier protein
ADME	Absorption, distribution, metabolism and excretion
AMR	Antimicrobial resistance
DABA	4-(dimethylamino)benzaldehyde
DEPT	Distortionless Enhancement by Polarization Transfer
DMSO-d_6	Deuterated dimethylsulfoxide
FAS	Fatty acid biosynthesis
FAS-I	Fatty acid synthase I
FAS-II	Fatty acid synthase II
GNB	Gram-negative bacteria
GPB	Gram-positive bacteria
INH	Isonicotinic acid hydrazide
MDR	Multidrug resistance
MIC	Minimum inhibitory concentration
OPLS4	Optimized Potentials for Liquid Simulations 4
PDB	Protein data bank
SB	Schiff's bases
TB	Tuberculosis
TLC	Thin layer chromatography
TMS	Tetramethylsaline
UTI	Urinary tract infection
WHO	World Health Organization
ZOI	Zone of inhibition

1. Introduction

Global health is under threat from infectious diseases, especially in developing countries. While advancements in antimicrobial agents have reduced morbidity and mortality, the surge in antimicrobial resistance and the emergence of new pathogens challenge existing treatments (Rock *et al.*, 2014). In response to this, our study aimed to synthesize and assess the antimicrobial potential of Schiff base derivatives from isonicotinic acid hydrazide. The introduction section highlights the background of infectious diseases, outlines literature reviews and research problems, and emphasizing the critical need for novel anti-infective agents.

1.1. Overview of Infectious Diseases

An infectious disease is characterized as an illness caused by a pathogen or its toxic product that spreads to a susceptible host via transmission from an infected person, infected animal, or contaminated inanimate object (Van Seventer and Hochberg, 2017). While most microorganisms peacefully coexist with hosts, some can become pathogenic, causing illnesses (Vijaya *et al.*, 2012). Despite their existence in abundant diversity, only a small number of microorganisms are identified as causing infections in individuals who are otherwise healthy. Various pathogens, such as viruses, bacteria, fungi, protozoa, multicellular parasites, and prions, can cause infections (Vijaya *et al*., 2012; Van Seventer and Hochberg, 2017). Globally, infectious diseases rank as the leading cause of morbidity and the second leading cause of death, carrying substantial economic consequences (M'ikanatha *et al.*, 2007). The impact of these illnesses varies widely across populations and regions, with low-income nations experiencing the most severe effects (Khabbaz *et al.*, 2014). For instance, in 2019, communicable diseases accounted for over half of all deaths in Africa (52.9%), 24.3% in the Eastern Mediterranean, and 22.6% in South-East Asia (World Health Statistics 2021)(WHO, 2021). Despite Ethiopia's progress in the past 25 years, lower respiratory infections, diarrheal

diseases, tuberculosis, and HIV/AIDS continue to be significant contributors to premature mortality (Misganaw *et al.*, 2017). Research by Meles *et al*. (2009 to 2017) affirms that communicable diseases remain the leading causes of adult mortality in southern Ethiopia, accounting for about half of all fatalities (Meles *et al.*, 2023).

1.1.1. Bacterial Infections

Since bacteria can infect nearly all host tissues, they are the primary cause of morbidity and mortality in the world (Asadi *et al.*, 2019). Recurrence is a critical aspect of bacterial infections which occurs in around30% of cases (Qi *et al.*, 2017). In 2019, 33 bacterial pathogens associated with 11 infectious syndromes resulted in 7.7 million deaths (Ikuta *et al.*, 2022). Lower respiratory and diarrheal infections, often bacterial in origin, rank among the top causes of death worldwide (Doron and Gorbach, 2008). Healthcare-associated infections, such as skin and soft tissue infections, pneumonia, and bloodstream infections, driven by bacteria, are on the rise (Los *et al.*, 2013; Jia *et al.*, 2019). The second most common infectious disease is urinary tract infection (UTI), which is typically caused by bacteria. Each year, 150 million people worldwide get UTIs (Flores-Mireles *et al.*, 2015; Klein and Hultgren, 2020). Ikuta *et al*.'s study (2022) highlights that five major bacterial pathogens, including *Staphylococcus aureus* (S. aureus), *Escherichia coli (E. coli)* and *Pseudomonas aeruginosa (P. aeruginosa)* contribute to 54.9% of deaths (Ikuta *et al*., 2022). Gram-negative bacteria(GNB) pose a significant public health risk, affecting both healthy and comorbid individuals, with *E. coli*, *Klebsiella pneumonia* (*K. pneumonia*), *P. aeruginosa*, and *Acinetobacter baumannii* (*A. baumannii*) playing a major role (Holmes *et al.*, 2021). *P. aeruginosa*, implicated in various infections, further intensifies health concerns (M Campos *et al.*, 2020).

Despite tetracyclines, macrolides, and other antibacterial drugs still being widely used, antibacterial resistance is rising with increasing number of bacteria resistant to multiple

antibacterial drugs (Selvarajan *et al.*, 2020). Repeated antibacterial use for recurrent infections heightens the risk of antibacterial resistance (Qi *et al*., 2017).

1.1.2. Fungal Infections

Fungi are abundant in the environment. However, only a few species are commonly found in close proximity to humans and are capable of causing disease. Some fungi act as true pathogens, while most are opportunistic (Hall and Noverr, 2017). In contrast to acute bacterial diseases, fungal infections are chronic, often requiring lengthy treatments due to heightened resistance (Casadevall, 2018). Early detection is rare, complicating treatment. With a surge in fungal infections, swift action is imperative (Reddy *et al.*, 2022). The prevalence of fungal diseases is expected to rise, driven by factors like increased immunocompromised hosts, and antifungal drug use and climate change-induced drug resistance (Casadevall, 2018).

Fungal diseases such as *Cryptococcal meningitis*, *Pneumocystis pneumonia*, disseminated histoplasmosis, chronic pulmonary aspergillosis, and fungal keratitis are among the priority fungal diseases that are important for public health (Bongomin *et al.*, 2017). Over 90% of fungal-related deaths stem from *Cryptococcus*, *Candida*, *Aspergillus*, and *Pneumocystis* species (Brown *et al.*, 2012). *Candida* species are major culprits in invasive fungal infections, ranging from non-life-threatening disorders to severe organ-related diseases (Pappas *et al.*, 2009). *Aspergillus fumigatus* (*A. fumigatus*) and *Aspergillus flavus* (*A. flavus*), though non-pathogenic, contribute to a substantial global burden annually (Rokas, 2022).

Despite advancements in antifungal medications, mortality rates remain high, reaching 30-50% (Netea and Brown, 2012). Current antifungal therapies comprise azoles, polyenes, echinocandins, allylamines, and pyrimidine analogs, but the rising resistance in fungal pathogens poses a clinical challenge (Reddy *et al*., 2022).

1.2. Statement of the Problem

Global concerns are mounting over bacterial and fungal resistance to current chemotherapeutic agents, particularly the uncontrolled growth of antimicrobial resistance (AMR). AMR is estimated to cause 10 million deaths annually and incur a staggering cost of $100 trillion (Tagliabue and Rappuoli, 2018). The challenges are exacerbated by increasing antimicrobial resistance, a shortage in antimicrobial discovery, and the emergence of new pathogens, posing significant hurdles in treating infectious diseases worldwide (Wilson *et al.*, 2002). In the last few years, the emergence of viral infections like Ebola, Middle East respiratory disease, and severe acute respiratory syndrome has become the norm. Not only are viral infections becoming more common, but bacterial infectious diseases are also increasing. A few noteworthy examples of these include the devastating cholera epidemic in Haiti, the 2011 foodborne *E. Coli* outbreak in Germany, and the invasive non-typhoidal *Salmonella* in Africa (Bloom *et al*., 2017). Furthermore, *Streptococcus suis* (*S. suis*), which was first identified in 19542, appears to be a human pathogen that was previously ignored but has recently come to light. Infections due to *S. suis* has become increasingly severe, particularly in southeast Asian nations like Thailand, Vietnam, and China (Feng *et al.*, 2014). The resurgence of deadly infectious diseases and the prevalence of antimicrobial-resistant strains further heighten the threat to public health (Townsend *et al.*, 2020). Current antimicrobial drugs pose challenges due to adverse effects that can significantly impact patient health. While antimicrobials are vital for treating infectious diseases, their use is often linked to unwanted side effects, ranging from mild to severe. Therefore, there is an urgent need for search effective, safe and affordable drugs with potent antimicrobial activity to reduce infection-related deaths. To address these challenges, it is crucial to synthesize compounds with diverse structures, such as Schiff bases. In this study, three Schiff base derivatives were synthesized from isonicotinic acid hydrazide, aiming to improve antimicrobial efficacy and broaden the spectrum of activity.

1.3. Literature Review

1.3.1. Schiff Bases and Their Biological Activities

1.3.1.1. Schiff Bases

Schiff's bases (SB), named after chemist Hugo Schiff, result from the reaction of primary amines with carbonyl compounds. First described in 1864, SB feature an azomethine group (-HC=N-) shown in Figure 1 (where: $\mathbf{R_1}$, $\mathbf{R_2}$, and $\mathbf{R_3}$ can be alkyl or aryl groups, but $\mathbf{R_1} \neq H$). The distinctive -N=CH- (imine) group in SB aids in understanding transamination and racemisation reactions in biological systems (Abirami and Nadaraj, 2014; Raczuk *et al.*, 2022).

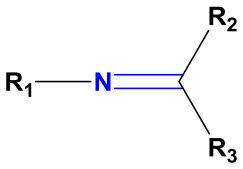

Figure 1: General structure of Schiff base

The synthesis of SB from aldehydes or ketones is a reversible process, typically occurring under acid or base catalysis. Completion of the formation is often achieved by product separation or water removal. Aqueous acid or base can hydrolyze many SB back to their aldehydes or ketones and amines. Scheme 1 outlines the general synthetic pathway for SB formation (Xavier and Srividhya, 2014). The commonly used technique involves reactions between primary amines and either aldehydes or ketones (Tsacheva *et al.*, 2023).

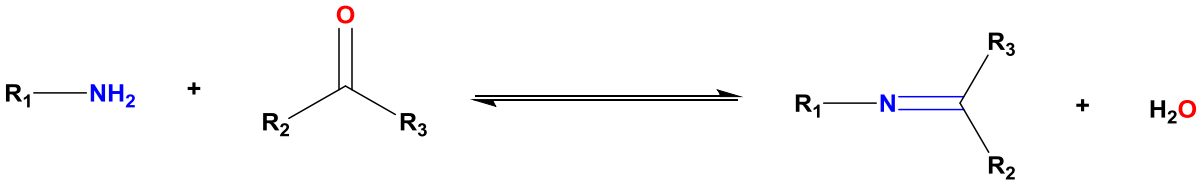

Scheme 1: General reaction method of Schiff base formation

1.3.1.2. Biological Activities of Schiff Bases

Because of the presence of bioactive azomethine core, SB have become important in medicine (Uddin *et al.*, 2020). The active centres of cell components may form hydrogen bonds with the nitrogen atom of azomethine, causing a disruption in cell activity. The nitrogen of the azomethine group [C=N] serves as an effective donor site because the nitrogen atom has one lone pair, the double bond is electron-donating, and nitrogen has a low electronegativity.(Slaihim *et al.*, 2023). Indeed, the azomethine group can be found in some marketed drugs, such as dantrolene ((compound **1**), Figure 2) a muscle relaxant used for treatment of skeletal muscle spasticity (Krause *et al.*, 2004), nitrofurantoin ((compound **2**), Figure 2) a drug used to treat uncomplicated UTI (Porreca *et al.*, 2021), furazolidone ((compound **3**), Figure 2), a drug active against a broad spectrum of bacteria and *Giardia lamblia* (Phillips and Hailey, 1987), nifurtimox ((compound **4**), Figure 2), an antiprotozoal drug used to treat Chagas disease, a disease caused by the parasite *Trypanosoma cruzi* (Falk *et al.*, 2022). Because the majority of the drugs mentioned above are anti-infective agents, compounds with an imine functional group may be promising antimicrobial agents.

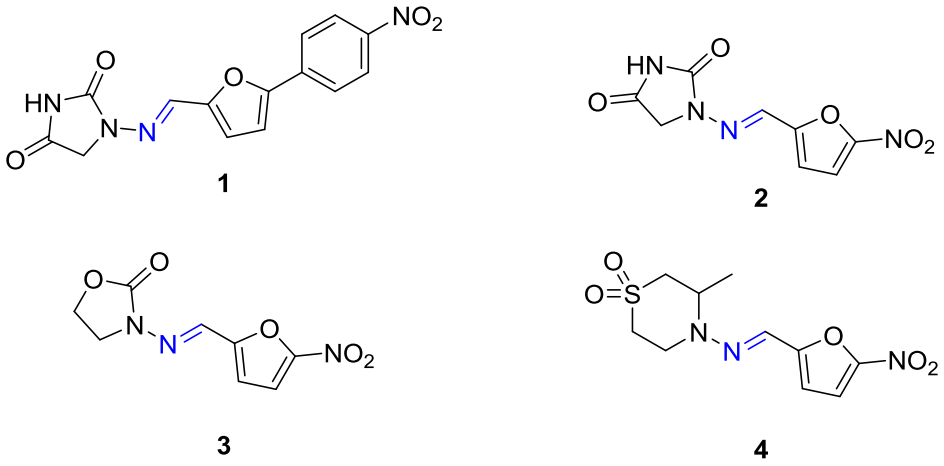

Figure 2: Some of marketed drugs having imine functional group

In addition to commercially available drugs, there are also studies that offer documented data on SB of diverse compounds with wide scope of biological activities; such as antiviral activity

(Mojzych and Sebela, 2015; Lazar *et al.*, 2018), anthelminthic (Hemalatha and Madhumitha, 2016; Manjunath *et al.*, 2016), analgesic and anti-inflammatory (Kadhim *et al.*, 2020; Afridi *et al.*, 2021), antioxidant (Kumar *et al.*, 2017; Kizilkaya *et al.*, 2020), anticancer (Uddin *et al.*, 2020; Sadia *et al.*, 2021), antidiabetic (Kapoor *et al.*, 2019; Szklarzewicz *et al.*, 2021), antimalarial (Rathelot *et al.*, 1995; Fonkui *et al.*, 2019), leishmanicidal activities (Teran *et al.*, 2019), antischistosomiasis (Amorim *et al.*, 2020), antidepressant (Thomas *et al.*, 2016), antitrypanosomal activity (Fonkui *et al.*, 2019), anti-tubercular activities (Aboul-Fadl *et al.*, 2012; Uzzaman *et al.*, 2020), antibacterial (Dewangan *et al.*, 2021; Salihović *et al.*, 2021), antifungal activities (Fonkui *et al.*, 2019; Aochar *et al.*, 2022), etc.

1.3.2. Biological Activities of Hydrazide-Hydrazones

Hydrazide-hydrazones are a class of organic compounds that have fascinated the interest of medicinal chemists due to the presence of an azomethine group linked to a carbonyl group, which is responsible for their various pharmaceutical applications and allows for the synthesis of various heterocyclic scaffolds (Popiołek, 2017). Hydrazones, a common class of SB compounds, are important class of compounds for the development of novel drugs (Asif and Husain, 2013). Hydrazones characterize as resourceful compounds having a basic structure $R_1R_2C{=}NNR_3R_4$ (Figure 3) and their properties are imprinted by the presence of the >C=N-N< structural unit, which contains two nitrogen atoms with nucleophilic character and a carbon atom which may act as either electrophile or nucleophile according to the reaction environment (Desai and Desai, 2014; Sharma *et al.*, 2020).

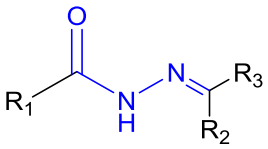

Figure 3: A moiety characteristic of hydrazones

The hydrazone moiety is present in some approved drugs; such as nitrofurazone ((compound **5**), Figure 4), a drug used to treat uncomplicated UTI (Johnson *et al.*, 1999), nifuroxazide ((compound **6**), Figure 4) is an oral antibiotic used to treat infectious colitis, diarrhoea, and schistosomiasis (Roquini *et al.*, 2023), thiacetazone ((compound **7**), Figure 4) a prodrug used for the treatment of tuberculosis (Grzegorzewicz *et al.*, 2015), methisazone ((compound **8**), Figure 4) inhibits structural viral protein synthesis and disrupts viral assembly in pox viruses (Bauer *et al.*, 1970; West *et al.*, 1998).

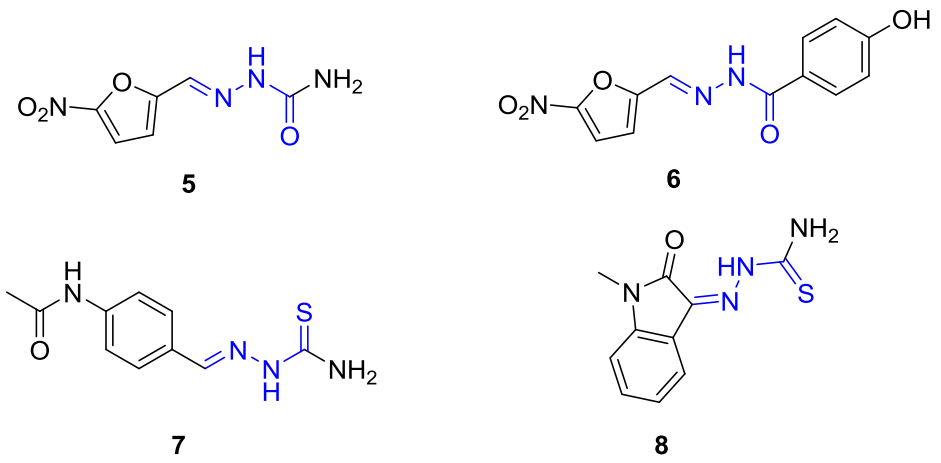

Figure 4: Commercially available drugs that contain hydrazone moiety

Furthermore, it is well known that the hydrazone community plays an important role in anti-infective activity (Sharma *et al.*, 2020). Yilmaz and Cukurovali (2019) synthesised some hydrazones and screened their antibacterial activity against *E. coli*, *S. aureus*, *E. faecalis* and *P. aeuroginosa*, and all demonstrated significant activity. Among them, (compound **9,** Figure 5) was observed to be the most effective against E. *coli* with minimum inhibitory concentration (MIC) of 1µg/ml. Besides, hydrazones were shown to have greater antibacterial activity than hydrazides. For example, (compound **10**, Figure 5) exhibits superior antibacterial activity than (compound **11**, Figure 5), an hydrazide, against *S. aureus*, *E. coli*, and *P. auroginosa* (Wang *et*

al., 2014). Among the studied hydrazones derived from 4-(trifluoromethyl)benzohydrazide, (compound **12,** Figure 5) has very good antibacterial activity against *S. aureus*, methicillin resistant strain of *S. aureus* (MRSA), *Staphylococcus epidermidis*, *Enterococcus sp.*, *E. coli* with MIC 1.98, 1.98,3.0, 3.0, 250 µM respectively and antifungal activities against *Candida glabrata* with MIC of 0.98 µM (Krátký *et al.*, 2017).

Different hydrazide-hydrazones were synthesised and evaluated against various *Candida* strains using microdilution method. In comparing MIC values with the standard reference drug, ketoconazole, (compound **13,** Figure 5) showed equal activity (125 µg/ml) against *C. albicans* (Koçyiğit-Kaymakçıoğlu *et al.*, 2012). Thirty three hydrazone derivatives were evaluated against different strains of *Candida*. One of them, (compound **14**, Figure 5) was found to be the most potent derivative against *C. albicans* and *Candida krusei* (Altıntop *et al*., 2012).

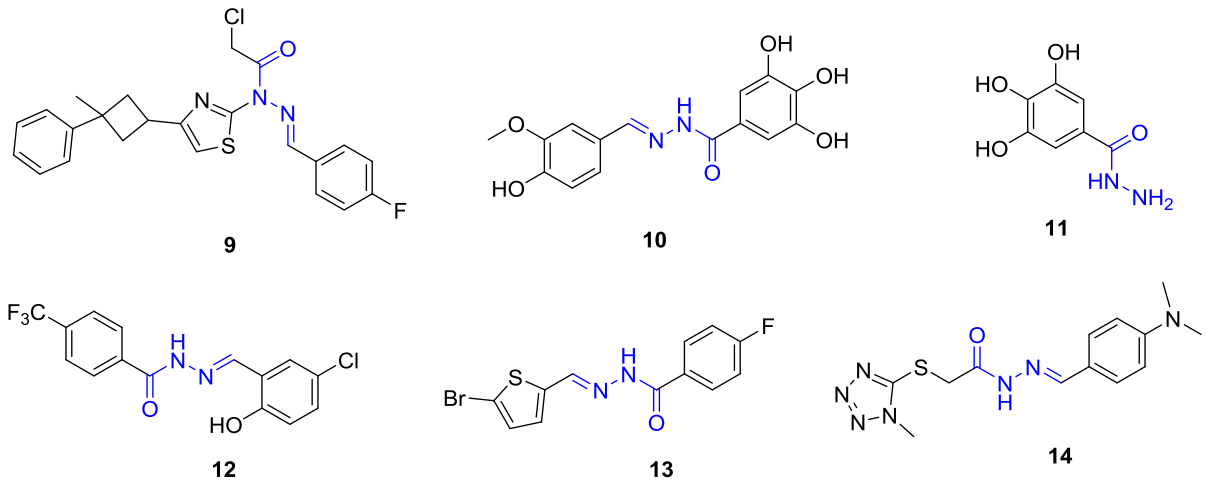

Figure 5: Examples of hydrazide-hydrazones that have antibacterial and antifungal activities

1.3.3. Antimicrobial Activities of Isonicotinic Acid Hydrazide Schiff Base Derivatives

Isonicotinic acid hydrazide (INH) has a relatively simple chemical structure consisting of a pyridine ring and a hydrazide group attached at para position to the pyridine nitrogen (Figure 6). It is still one of the most important drugs for tuberculosis treatment (Fernandes *et al.*, 2017).

Though INH is effective and potent drug with MIC in the range of 0.03-.1µg/ml against *M. tuberculosis*, it shows limited action in latent mycobacteria and does not have antibacterial activity to non-mycobacterial species with no inhibition of growth observed even at the maximal concentration of drug tested (100 µM). Moreover INH has weak antifungal activities against *Cryptococcus neoformans* and *C. albicans* with MIC between 25-100 µM (Hegde *et al.*, 2021). The precise mode of action of INH is still up for discussion, considering that it generally acts on a variety of targets (Slayden and Barry III, 2000). Enoyl acyl carrier protein (ACP) reductase and β-ketoacyl ACP synthase, the most well-known targets of INH, were found to be elements in the cell wall pathway synthesis of mycolic acid (Unissa *et al.*, 2016).

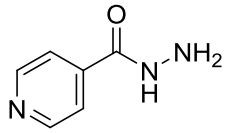

15

Figure 6: Structure of isonicotinic acid hydrazide

It was mentioned that in recent years, INH and its derivatives have generated interest and have been the focus of substantial research. The biological activities of SB derivatives made from INH have been studied by many scientists.

Sethiya *et al.* (2023) synthesised 15 INH based SB derivatives and screened for their antibacterial and antifungal activities. Almost all exhibited significant activity against both GPB and GNB of the tested strain. Among the derivatives, (compound **16** and **17,** Figure 7) were more active against *E. coli* (with MIC of 31.25µg/ml) than the reference drug ciprofloxacin (MIC 62.5µg/ml). Three INH SB were synthesized and tested for antibacterial activity against *S. aureus* and *E. coli*. The findings revealed that the synthesized compounds have significant antibacterial activity (Al-Hiyari *et al.*, 2021). Malhotra *et al.* (2012) synthesised some INH based SB and studied their antibacterial and antifungal activities. All

show good antibacterial activity against *B. subtilis*, *S. aureus*, *P. aeruginosa*, and *E. coli*. The best activity was displayed by (compound **18**, Figure 7) against all strains of bacteria (MIC 1.56-6.25 µg/mL) and against *C. albicans* and *A. niger* with MIC 3.25,3.12µg/ml respectively. Shah *et al.* (2022) synthesised six INH SB compounds and were screened for their antibacterial activity against *S. aureus*, *B. subtilus*, and *E. coli* using disc diffusion method. The results verified appreciable antibacterial activities against the applied strains.

The antimicrobial activity of SB and Cu(II) complexes was assessed against strains of the bacteria *S. aureus* and *E. coli* as well as the fungus *C. albicans*. The SB (compound **19**, Figure 7) demonstrated good activity (MIC 9.37 µM) against *E. Coli* and excellent activity (MIC 3.7 µM) against *C. albican* (Habala *et al.*, 2016). Pahlavani *et al.* (2015) synthesised an INH SB derivative (Compound **20,** Figure 7) and evaluated its antibacterial as well as its antimycobacterial activities using a serial broth micro dilution method. The results were compared with standard antibacterial drugs ciprofloxacin and ceftriaxone, and isoniazid respectively. The compound has shown higher activity against *S. aureus* (MIC 8 µg/mL), *E. coli* (MIC 4 µg/mL) and good activity against *M. tuberculosis* (4 µg/mL). Nalini *et al*. (2023) synthesized 5-chloro isatin-INH SB ligand (compound **21**, Figure 7) and its metal complex. *In vitro* antibacterial activities were examined for the ligand and its metal complexes against some bacterial species using ciprofloxacin as a standard antibiotic by the agar diffusion method. The ligand has shown moderate to good activity against *E. coli* (with MIC of 25 µg/ml) when compared to the standard drug ciprofloxacin. The pyrimidine-incorporated SB of INH were synthesized by Soni and Patel (2017), and the compounds' antimicrobial activities against a variety of bacterial and fungal strains were assessed *in vitro*. The majority of the compounds showed strong antifungal, antibacterial, and antitubercular properties.

Studies on a curcumin-based SB of INH (compound **22**, Figure 7) and its metal complexes displayed antibacterial activity against *S. aureus, Bacillus subtilis* (*B.subtilis*), *Salmonella typhi*

(*S. typhi)*, *K. pneumonia*, *E. coli* with MIC of 10.3, 11.6, 11.7, 13,and 12.6µM respectively and its antifungal activity against *Aspergillus niger* (*A. niger*), *A. flavus, Curvularia lunata, Rhizoctonia bataticola, C. albicans* having MIC of 20.4, 22.1, 20.6, 21.5, 22.7 µM respectively (Jeyaraman *et al*., 2020).

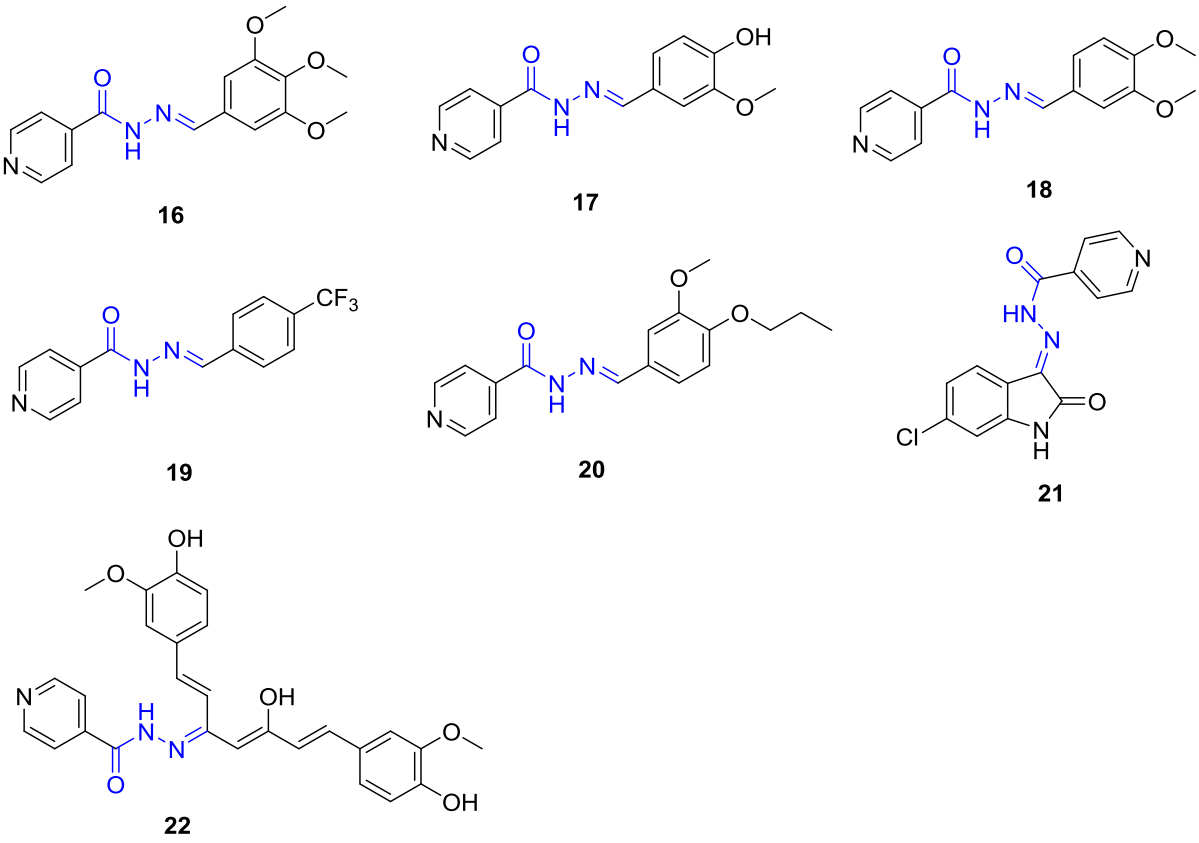

Figure 7: Schiff bases of isonicotinic acid hydrazide that have antibacterial and antifungal activities

1.3.4. Potential Antimicrobial Drugs Target

Antimicrobial agents disrupt crucial elements of bacterial metabolism, incapacitating the bacteria (Coates *et al.*, 2002; García-Lara *et al.*, 2005). A promising target for novel antibacterial agents is the fatty acid biosynthesis (FAS) pathway (Zhang *et al*., 2011). Two enzymes that are commonly involved in FAS and necessary for the phospholipid production process are fatty acid synthase I (FAS-I), found in mammals, and fatty acid synthase II (FAS-

II), found in bacteria. Due to this difference, antibacterial drugs may target FAS-II (Belete, 2019). Three enzymes, 3-ketoacyl-acyl carrier protein (ACP) synthase I (FabB), 3-ketoacyl-ACP synthase II (FabF), and 3-ketoacyl-ACP synthase III (FabH) involve in condensation reactions in FAS. In subsequent rounds of fatty acid elongation, the process is initiated by FabH, followed by FabB and FabF carrying out the elongation reactions (Davies *et al.*, 2000). Despite the absence of clinically utilized drugs targeting condensing enzymes, thiolactomycin (compounds **23**, Figure 8) demonstrates selective inhibition with MIC values of 1.6µg/ml against *P. aeruginosa* and 6.3 µg/ml against *S. flexneri*. Similarly, cerulenin (compound **24**, Figure 8) selectively inhibits condensation enzymes FabH and FabF/B (Wang *et al.*, 2006). Moreover, platensimycin (compound **25**, Figure 8) exhibits selective inhibition of FabF with MIC values ranging from 0.1 to 0.32 µg/ml against GPB. In contrast, platensin (compound **26**, Figure 8) acts as a balanced dual inhibitor, with MIC values ranging from 0.5 to 32 µg/ml against GPB, targeting both FabF and FabH simultaneously (Martens and Demain, 2011; Das *et al.*, 2016).

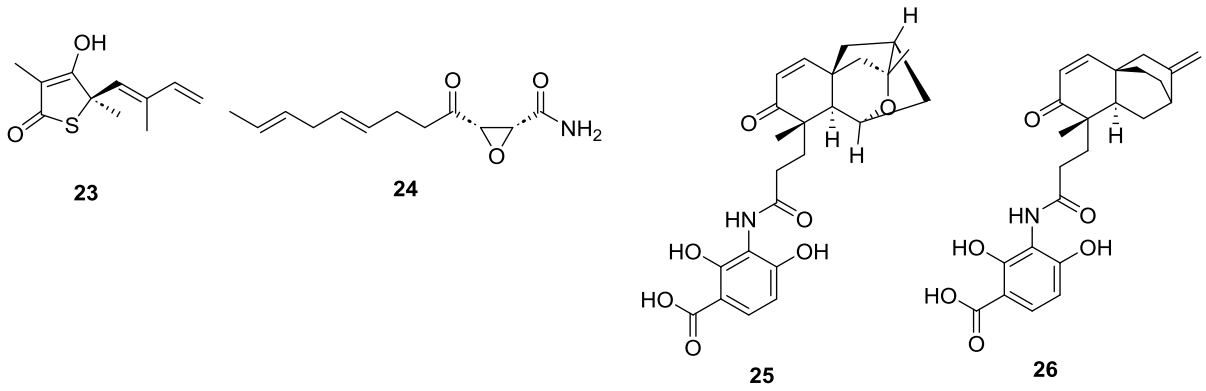

Figure 8: Compounds potentially binding to Fab enzymes

1.4. Significance of the Study

The present study is significant as it addresses the limitations of isonicotinic acid hydrazide, an anti-tubercular drug, which lacks effectiveness against common microbes. By structurally

modifying isonicotinic acid hydrazide through the synthesis of Schiff base derivatives, the antimicrobial activity extended against a broader range of microbes. The safety, affordability, and effectiveness of existing antimicrobials raise concerns, emphasizing the critical need for the exploration of new compounds. This study contributes to this vital search for novel antimicrobial agents. In the context of Africa, where infectious diseases remain a leading cause of death, including limited research on antimicrobial drug development, the significance of seeking new drugs within the continent is underlined. By introducing an imine functional group into the core structure of the currently available drug isonicotinic acid hydrazide, this research may provide valuable insights into enhancing the spectrum of antimicrobial activity. Additionally, it is anticipated that the study will contribute scientific data beneficial to those interested in the fields of synthesis, antimicrobials, and infectious diseases.

2. Objectives

2.1. General Objective

The general objective of this study was to synthesize and characterize some Schiff base derivatives of isonicotinic acid hydrazide, assess their *in vitro* antimicrobial activity, and conduct *in silico* studies.

2.2. Specific Objectives

- To synthesise Schiff base derivatives of isonicotinic acid hydrazide
- To characterize the synthesized isonicotinic acid hydrazide Schiff base derivatives
- To evaluate *in vitro* antibacterial and antifungal activities of the synthesized compounds
- To conduct *in silico* studies of isonicotinic acid hydrazide Schiff base derivatives

3. Materials and Methods

3.1. Materials

3.1.1. Chemicals and Reagents

The following chemicals and reagents were used in this study: chloroform, ethyl acetate, methanol, ethanol, distilled water, glacial acetic acid, n-hexane (all Indenta, India), vanillin (BDH, England), INH (BDH, England), benzoin (BDH, England), and 4-(dimethylamino) benzaldehyde (Hopkin & Williams, England). All the solvents were of analytical grade. The chemicals and reagents were used without further purification process.

3.1.2. Instruments

Silica gel analytical thin layer chromatography (TLC) plates (60 F254, 0.2 mm thick, Merck KGaA, Darmstadt, Germany) and Watman no.1 filter paper were used for analysis and purification purpose. Magnetic stirrer, refluxer, electric heater, electronic weighing balance, measuring cylinder, reaction flasks, glass beaker, refrigerator were used for the synthesis, purification and reaction workup. UV-Visible (ultraviolet-visible) Spectrophotometer (Evlution 60S, Germany) was used to visualize the TLC chromatogram plates. Nuclear Magnetic Resonance (NMR) spectra were recorded using 400 MHz for proton NMR (^{1}H-NMR) and 100 MHz for carbon-13 NMR (^{13}C-NMR) on a Bruker Avance DMX400 FT-NMR spectrometer (Bruker, Billerica, Massachusetts, USA).

3.1.3. Microorganisms

Bacillus pumilus (*B. pumilus*) (82), *B. subtilis* (ATCC 6633), *S. aureus* (ML 267) *S. aureus* MDR 1, and *S. aureus* MDR 2 were the Gram-positive bacterial (GPB) strains against which antibacterial assays were performed. The GNB strains that were employed were *E. coli* (3:37C), *E. coli* (7360), *E. coli* (872), *E. coli* (CD/99/1), *E. coli* (K88), *E. coli* (LT37), *E. coli* (ROW 7/12), *E. coli* (5933), *P. aeruginosa* MDR 1, *Salmonella enterica* (*S. enterica*) (TD 01), *S. typhi* (Ty2), *Shigella boydii* (*S. boydii*) (D13629), *S. dysentery* (8), *Shigella flexneri* (*S.*

flexneri) (Type 6), *S. soneii* (1), *V. cholera*e (NCTC 5596), *V. cholerae* (NCTC 10732), *V. cholerae* (NCTC 11501), and *V. cholerae* (NCTC 4693).

The Department of Technology at Jadavpur University, the Central Drugs Laboratory in Kolkata, and the Institute of Microbial Technology in Chandigarh, India were the sources of all the bacterial strains. The stains were used to determine their sensitivity to the test samples after their purity was initially assessed using conventional microbiological, cultural, and biochemical tests.

The following fungal pathogens were tested for antifungal activity: *P. notatum* (ATCC 11625), *A. niger* (ATCC 6275), *C. albicans* (ATCC 10231), and *Penicillum funiclosum* (*P. funiclosum*) (NCTC 287). All of the fungal strains were obtained from Central Drugs Laboratory in Kolkata, India.

3.2. Methods

3.2.1. Synthesis of Compounds

3.2.1.1 Synthesis of Compound 27

Compound **27** ((E)-N'-(2-hydroxy-1, 2-diphenylethylidene) isonicotinohydrazide) was synthesized via an SB condensation reaction. Benzoin solution was initially prepared by dissolving 2.122 g (10 mmol) of benzoin (2-hydroxy-1,2-diphenylethan-1-one) in 15 ml of methanol in a 250 mL round bottom reaction flask. 2 ml of glacial acetic acid was then added to a benzoin solution. Separately, 1.371g (10 mmol) of INH was dissolved in 15 ml of methanol in a separate beaker and gradually introduced into the above benzoin-glacial acetic acid solution. The mixture was refluxed for approximately 12 hours at 80 ºC. The reaction progress was monitored using analytical TLC with chloroform: methanol (7:1) as a mobile phase. After the reaction completion, the mixture was left at room temperature to cool, and crystal growth was observed after 2 days. The crystals was separated, purified by washing with chloroform:

methanol (1:1), and filtered using Whatman no.1 filter paper, yielding 0.701g (24%; yield, w/w).

3.2.1.2. Synthesis of Compound 28

Compound **28** ((E)-N'-(4-hydroxy-3methoxybenzylidene) isonicotinohydrazide) was synthesized using the same procedure as described above. 2 ml of glacial acetic acid was added to a vanillin solution. The vanillin solution was initially prepared by dissolving 1.521 g (10 mmol) of vanillin (4-hydroxy-3-methoxybenzaldehyde) in 20 ml of methanol in a 250 mL round bottom reaction flask. Separately, 1.371g (10 mmol) of INH was dissolved in 20 ml of methanol in a separate beaker and gradually introduced into the vanillin-glacial acetic acid solution. The mixture was refluxed for about 8 hours at 78 ºC. The reaction progress was monitored by analytical TLC using chloroform: methanol (7:1) as a mobile phase. After completion of the reaction, the mixture was allowed to cool at room temperature and was filtered using Whatman no.1 filter paper to obtain a yellowish-white precipitate (2.020 g), yielding 92% w/w.

3.2.1.3. Synthesis of Compound 29

Compound **29** ((E)-N'-(4-(dimethylamino) benzylidene)isonicotinohydrazide) was synthesized using a similar procedure as described above. To a solution of 4-(dimethylamino) benzaldehyde (DABA), 2 ml of glacial acetic acid was added. The DABA solution was initially prepared by dissolving 0.373g (2.5 mmol) of DABA in 15 ml of methanol in a 250 mL round bottom reaction flask. Separately, 0.343 g (02.5 mmol) of INH was dissolved in 15 ml of methanol in a separate beaker and gradually added to the above DABA-glacial acetic acid solution. The reaction mixture was monitored by TLC using chloroform: methanol (7:1) as a mobile phase. After the reaction completion, the mixture was allowed to cool at room temperature for about five days and was filtered using Whatman no.1 filter paper to obtain a yellow-colored crystals (0.663g), yielding 84% (%;w/w).

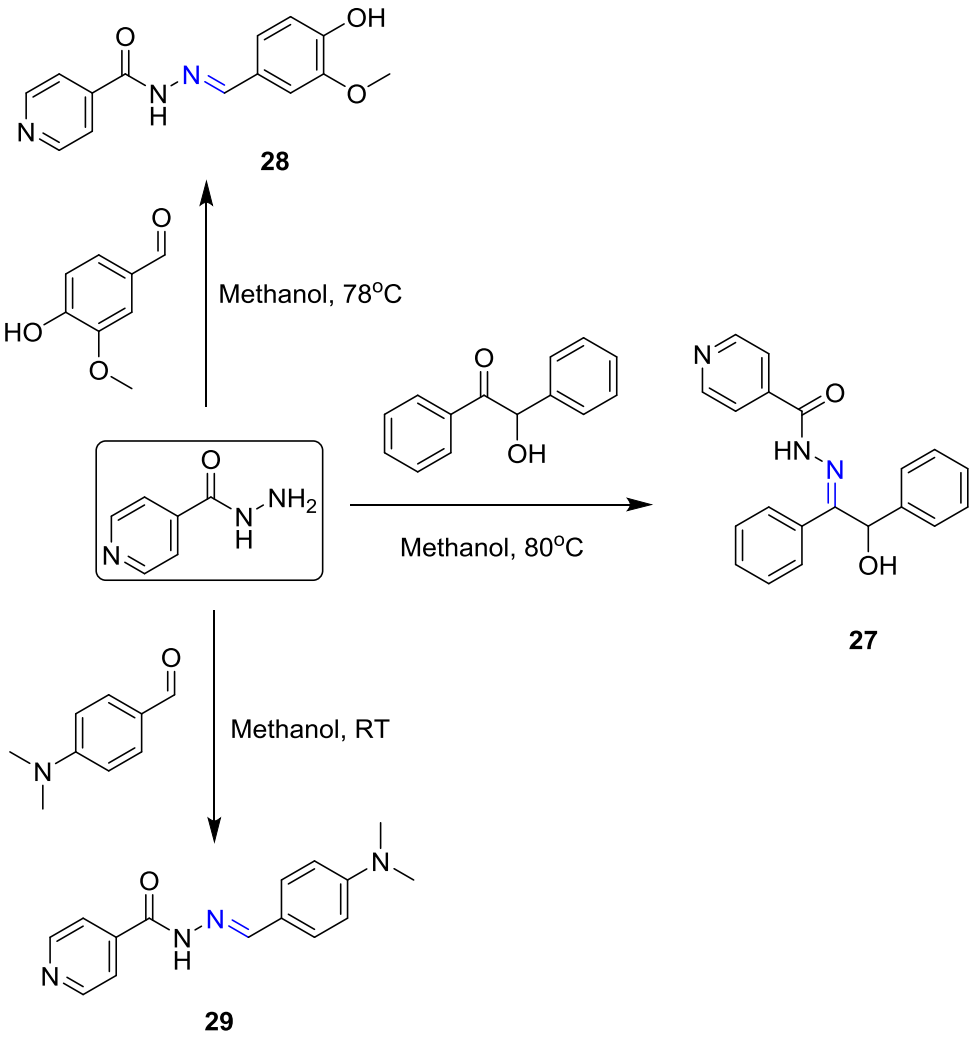

Scheme 2: Synthesis of Schiff base derivatives of isonicotinic acid hydrazide (**27** to **29**)

3.2.2. NMR Spectroscopic Technique

NMR spectra were recorded using a Bruker Avance DMX400 FT-NMR spectrometer (Bruker, Billerica, Massachusetts, USA) operating at 400 MHz for ^{1}H-NMR and 100 MHz for ^{13}C-NMR at room temperature. Tetramethyl silane (TMS) and deuterated dimethyl sulfoxide (DMSO-d_6) served as internal and external references respectively. The ^{1}H-NMR scanning range was 0-16 ppm, and for ^{13}C-NMR, it was 0-210 ppm. Chemical shifts (δ) and coupling constants (J) were expressed in ppm and Hz, respectively. Signal multiplicities in ^{1}H-NMR signals were denoted as *s* (singlet), *d* (doublet) and *m* (multiplets).

3.2.3. Determination of *In vitro* Antimicrobial Activities

3.2.3.1. Antibacterial Assay

The disc diffusion method was used to carry out the *in vitro* antibacterial assay, allowing for the comparison of the test samples' zones of inhibition (ZOI) with ciprofloxacin. In the process, sterile McCartney bottles were filled with two sets of dilution (200 µg/ml) of each test sample dissolved in 1% DMSO and ciprofloxacin also dissolved in 1% DMSO. After that, sterile Petridishes were filled with molten media to create serial nutrient agar plates, which were then incubated for 24 hours at 37 ºC to look for contamination.

Subsequently, the inoculums were evenly swabbed with different sterile cotton buds and given five minutes to dry. Next, the filter paper discs (Whatman no. 1) measuring 6 mm were impregnated with the test sample stock solution (200 µg/ml) and/or ciprofloxacin, which was then applied to the medium's surface. Following a 24-hours incubation period at 37 ^{0}C, the diameter of the inhibition zone was measured in mm for each Petridish. To compare the corresponding ZOI for ciprofloxacin, a similar procedure was used (Lalitha, 2004; Hudzicki, 2009; Schumacher *et al.*, 2018).

3.2.3.2. Antifungal Assay

Using the disc diffusion method, which is also used to determine antibacterial activity, the antifungal potential of the test samples (1500 µg/mL) was assessed against fungal pathogens on Saborauds dextrose agar media. After three days of room temperature incubation, the diameter of the ZOI in the Petri dishes was measured in mm. Griseofulvin, an antifungal agent, served as the benchmark.

3.2.3.3. Minimum Inhibitory Concentrations (MIC)

By using the broth dilution method, which employed nutrient agar and Sabourads dextrose agar for bacterial and fungal growth, respectively, the MIC value was determined. The synthesised

compounds dissolved in DMSO were used in concentrations of 5, 10, 25, 50, 100, 200, 400, and 800 μg/mL for the antibacterial activity test and 50, 100, 200, 400, 800, 1000, 1500, and 2000 μg/mL for the antifungal activity test. A sterility test was also performed (the growth control used DMSO and nutrient broth with no antimicrobials). For fungi and bacteria, the test and growth control wells were incubated at 25 ºC and 37 ºC. Additionally, a sterility control was performed (growth control used DMSO and nutrient broth without any antimicrobials). For fungi and bacteria, respectively, each test and growth control well was incubated at 25 ºC and 37 ºC (Andrews, 2001; Koeth *et al.*, 2015).

3.2.4. *In silico* Studies

3.2.4.1. Molecular Docking Study

Molecular docking of the synthesized compounds was performed on the FabF-platensimycin co-crystallized enzyme of *E. coli* (PDB ID: 3HNZ) as potential targets for antibacterial activity using Maestro V.13.5 software by Schrodinger 2023-1 Suite. The docking results of all synthesized compounds were subsequently compared to the redocked native ligands, namely, platensimycin.

3.2.4.1.1 Protein Preparation

The X-ray crystallography structure of *E. coli* FabF (PDB ID: 3HNZ) chain A; resolution: 2.75 Å complexed with platensimycin was downloaded from the protein data bank (PDB). The 3HNZ structure consists of 427 amino acid chain sequence, complexed with platensimycin (Singh *et al.*, 2009). Using Maestro V13.5 Protein Preparation Workflow module (Schrödinger 2023-1), the 3D structure of *E. coli* FabF protein in complex with platensimycin (PDB ID: 3HNZ, chain A) was prepared by standard procedures. This involved correcting charges, bond orders, and atom types, removing water molecules beyond 5 Å from the het group, and filling in missing side chains and loops. The Optimized Potentials for Liquid Simulations 4(OPLS4)

force field was applied for energy optimization and steric hindrance removal (Madhavi Sastry *et al.*, 2013).

3.2.4.1.2. Ligand Preparation

The structure of compounds **27**-**29** was drawn using ChemDraw Ultra (2022) in MDL SD file format. Ligands were prepared with Maestro V13.5, Schrödinger Suite 2023-1, utilizing the Ligprep module. The OPLS4 force field was applied at a physiological pH of 7.0 ± 2.0, generating low-energy, three-dimensional structures with variations in conformations, ionization states, and tautomers based on molecular weight or specified functional group criteria, up to 5Å for all ligand conformations for each structure with low energy.

3.2.4.1.3. Receptor Grid Generation

In order to see the receptor's active site during glide ligand docking, we created the receptor grid box. The protein structure was selected on the workspace to define the ligand-binding site, which has a radius of 6.0 Å. The van der Waals radii of the receptor atoms was set with partial atomic charge scaling factor of 0.8 and partial cut-off of 0.15 to soften the receptor's nonpolar parts.

3.2.4.1.4. Ligand docking

We docked compounds **27**–**29** into the prepared protein's active binding site using the extra precision (XP) mode of the Glide program. Previously, in order to forecast binding affinity and molecular interaction, we docked the co-crystallized ligand into the protein's active site. A binding pose analysis was conducted using docking scores expressed in kcal/mol. The Schrodinger program suite was used for all of the analyses and procedures.

3.2.4.1.5. Validation of Docking Procedure (Redocking Method)

The docking protocol was validated through redocking, involving the native ligand (platensimycin) into the active binding site of the FabF enzyme. This crucial step assessed the

accuracy of the docking protocol, ensuring reliability, and enhancing computational predictions in drug discovery studies.

3.2.4.2. Pharmacokinetic Prediction Study

Understanding the characteristics of absorption, distribution, metabolism, and excretion (ADME) is essential because most pharmaceuticals do not pass clinical trials. Using QikProp, GLIDE, Maestro V13.5, Schrödinger Suite 2023-1, drug likeness and ADME characteristics of the synthesised compounds were ascertained. The LigPrep module of Schrodinger V 13.5 was utilized to generate the ligand in Maestro format for ADME investigation. Then, in order to obtain the ADME parameters, we set to work by navigating the QikPro dialogue box and inserting the ligand preparation file for the synthesised compounds.

4. Results and Discussion

4.1. Synthesis of Compounds 27 to 29

Three compounds (**27**, **28** and **29**) were synthesized through a modified SB condensation reaction. This reaction involved INH and substituted aromatic aldehydes or ketones, with glacial acetic acid serving as a catalyst. The process led in the formation of imines (C=N bonds) through nucleophilic addition between an aldehyde or ketone and a primary amine compound in the presence of an acid catalyst. Physical properties of the synthesised compounds are presented in Table 1 as shown below.

Table 1: Physical properties data of synthesised compounds **27**, **28** and **29**

Compound	Molecular Formula	Predicted MW(g/mol)	Physical State	Color	% Yield	R_f value
27	$C_{20}H_{17}N_3O_2$	331.37	Crystal	Colorless	24	0.31
28	$C_{14}H_{13}N_3O_3$	271.27	Powder	Yellowish-white	92	0.21
29	$C_{15}H_{16}N_4O$	268.31	Crystal	Yellow	84	0.28

Solvent system: Chloroform: Methanol (7:1), TLC silica gel HF-254, R_f =Retention factor

4.1.1. Synthesis of Compound 27

Compound **27** was synthesized through the SB reaction involving isoniazid (INH) and benzoin in the presence of glacial acetic acid. The synthesis comprises multiple steps. Firstly, the benzoin's carbonyl carbon is protonated by acetic acid to enhance its electrophilicity. Subsequently, the primary amine of INH undergoes a nucleophilic attack on the carbonyl carbon, leading to the formation of an unstable intermediate known as carbinolamine via proton transfer. Acetic acid then protonates the oxygen in the carbinolamine, followed by the elimination of a water molecule, resulting in the formation of an iminium ion. Finally, the iminium ion is deprotonated by the acetate ion, leading to the formation of an imine, identified as the proposed compound **27**. The detailed reaction mechanism is illustrated in Scheme 3.

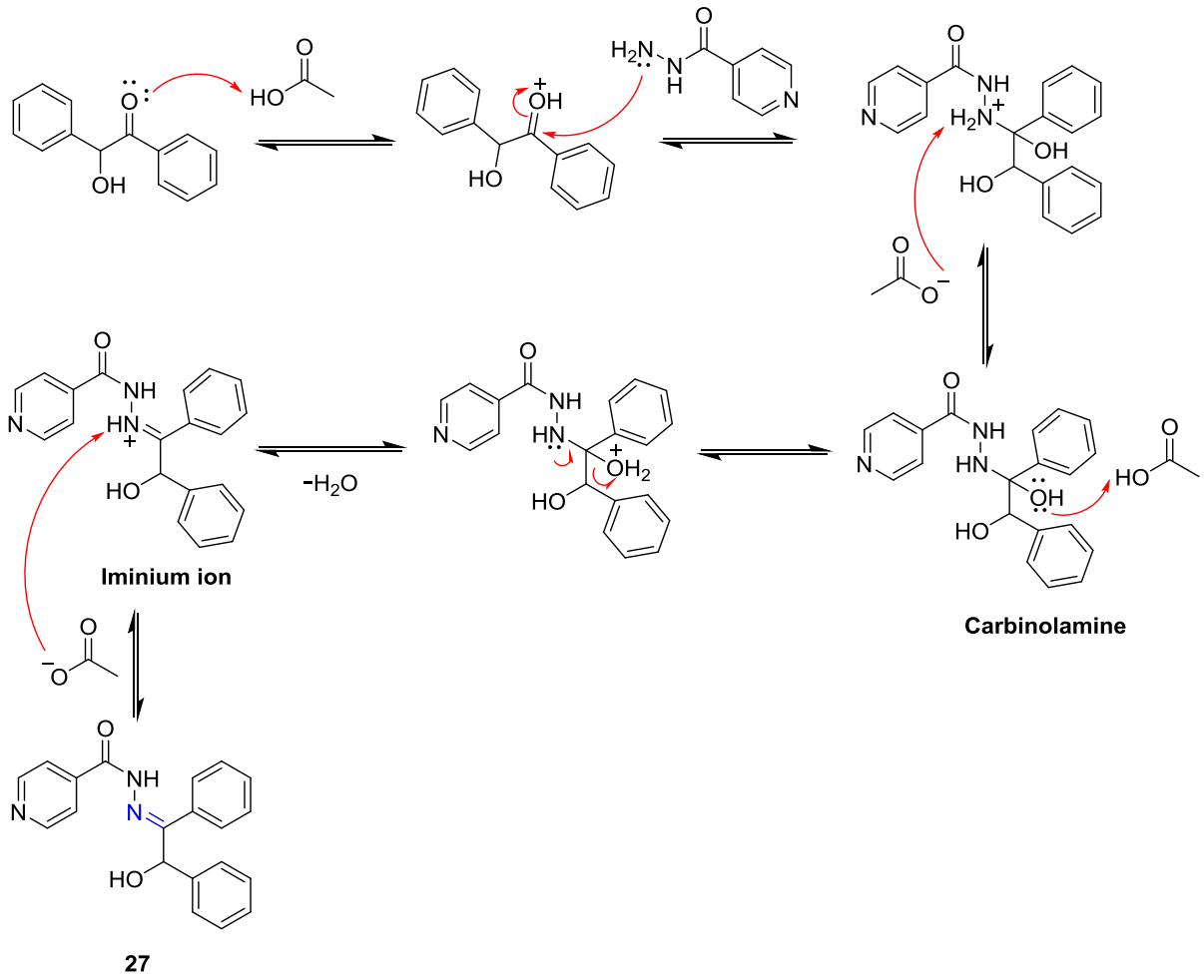

Scheme 3: Proposed mechanism of reaction for synthesis of compound **27**

4.1.2. Synthesis of Compound 28

Compound **28** was also synthesized through an SB reaction involving INH and vanillin (4-hydroxy-3-methoxybenzaldehyde) in the presence of glacial acetic acid. The reaction mechanism of compound **28** follows the same steps as previously outlined in the synthesis of compound **27**. Scheme 4 illustrates the reaction mechanism for compound **28**.

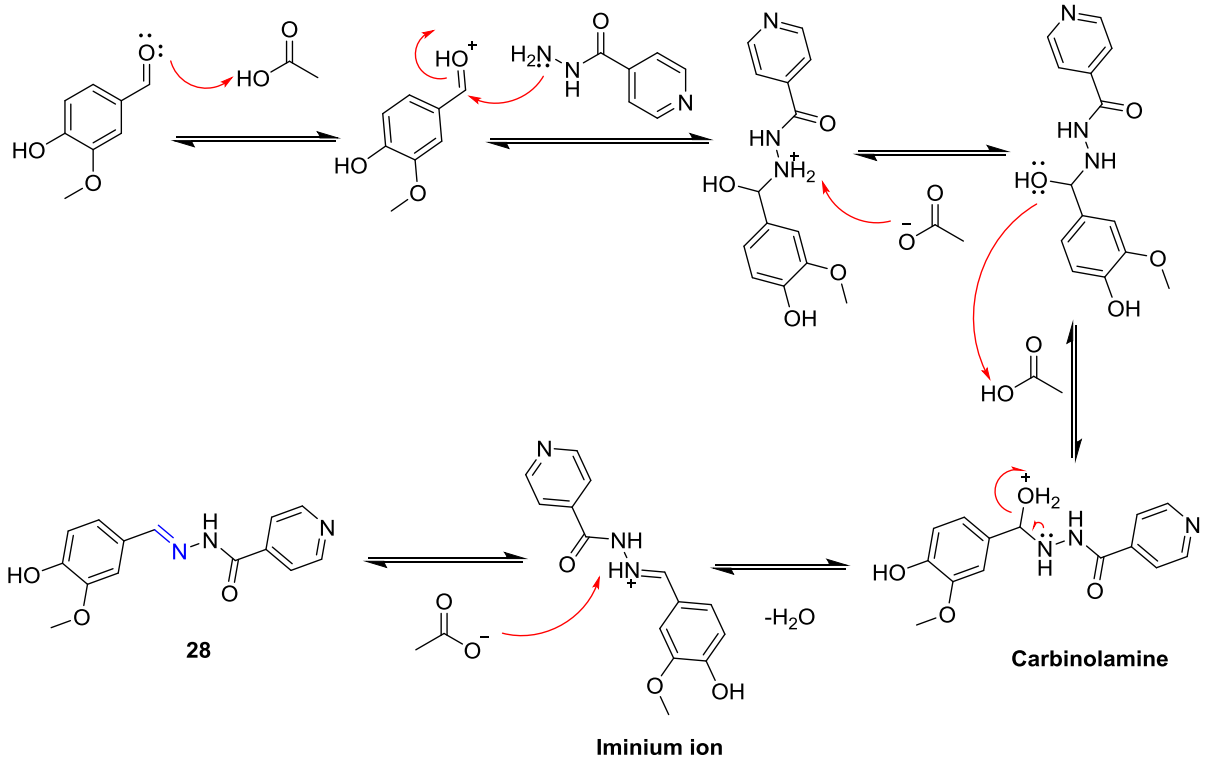

Scheme 4: Proposed mechanism reaction in the synthesis of compound **28**

4.1.3. Synthesis of Compound 29

SB reaction between INH and DABA in the presence of glacial acetic acid led to the formation of compound **29**. The reaction mechanism for the synthesis of compound **29** closely resembles that of compounds **27** and **28**. Scheme 5 provides an illustration of the reaction mechanism for the synthesis of compound **29**.

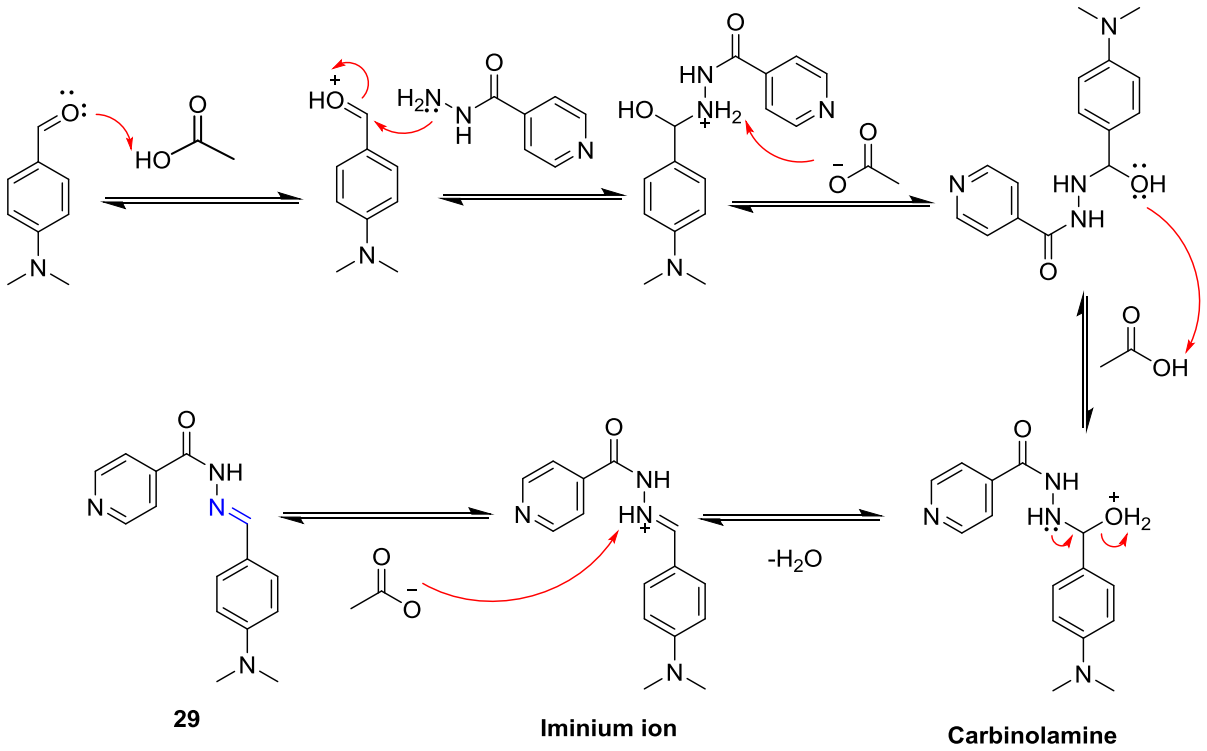

Scheme 5: Proposed mechanism of reaction for synthesis of compound **29**

4.2. Structural Elucidation of the Synthesized Compounds 27 to 29

Compound **27** was obtained as a colorless crystal (2.16 mmol, 24%; w/w). The ^{1}H-NMR spectrum of compound **27** revealed the presence of an amide proton, evident by a singlet signal at δ 12.88. The presence of an amide functional group was further confirmed by a signal resonating at δ 160.96 in the ^{13}C-NMR spectrum. Additionally, two ortho aromatic protons at δ 7.64 (2H, *d*, J= 5.0 Hz) indicated the presence of a phenyl group adjacent to the azomethine group. Another signal at δ 155.54 in the ^{13}C-NMR spectrum was assigned to the azomethine carbon (C-1′; -C=N-). This distinctive pattern was indicative of the formation of the (-C=N-) functional group in compound **27**.

It was also interesting to note that only fourteen signals were apparent in the ^{13}C-NMR spectrum of compound **27**. Upon closer examination, it became evident that six of these signals overlapped due to their magnetic equivalence. Consequently, compound **27** is composed of a total of 20 carbon atoms. A similar pattern was observed in the DEPT-135 spectrum, revealing

fourteen aromatic methine carbons (six equivalent carbons and two different carbons) and one signal from an aliphatic methine carbon in compound **27**. All chemical shifts of proton and carbon signals are clearly assigned in Table 2.

Table 2: ^{1}H-NMR and ^{13}C-NMR spectral data of compound **27** in DMSO-d_6

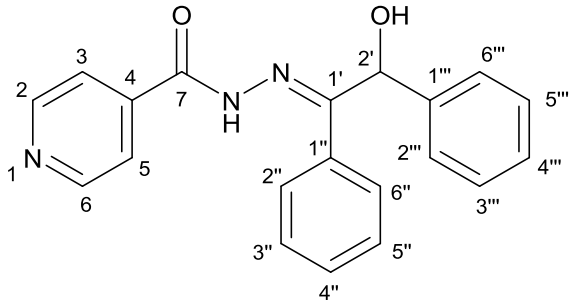

Compound **27**

Position	**δC(ppm)**	**δH(ppm)**
2, 6	151.30	8.81(*d*, J=5.0Hz, 2H)
3, 5	121.16	7.82(*d*, J=5.3Hz, 2H)
4	139.78	-
7(CONH)	160.96	12.88 (*s*, NH, 1H)
1′	155.45	-
2′	73.46	6.42 (*s*, 1H)
1″	136.51	-
2″, 6″	128.52	7.64(*d*, J=5.1Hz, 2H)
3″,5″,2‴, 6‴,4‴,3‴,5‴	128.97, 130.16, 126.90, 129.28, 127.68	7.46 – 7.26 (*m*, 8H)
1‴	140.78	-

Compound **28** was obtained as a yellowish-white solid powder (7.45mmol, 92%; w/w). The ^{1}H-NMR spectrum exhibited a distinct characteristic signal for the azomethine group at δ 8.37 (1H, *s*), while the ^{13}C-NMR spectrum displayed a signal at δ 149.77. These findings unequivocally confirmed the formation of an imine through a Schiff condensation reaction.

Furthermore, the presence of amide and phenolic hydroxyl groups in compound **28** was evident by signals resonating at δ 11.95 and δ 9.68 in the ^{1}H-NMR spectrum, respectively.

Table 3: ^{1}H-NMR and ^{13}C-NMR spectral data of compound **28** in DMSO-d_6

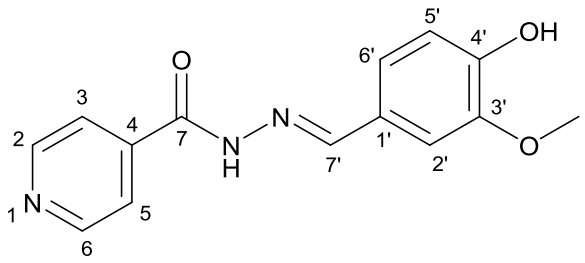

Compound **28**

Position	**δC(ppm)**	**δH(ppm)**
2, 6	150.74	8.78(*d*, J=4.5Hz, 2H)
3, 5	121.99	7.83(*d*, J=4.5Hz, 2H)
4	141.12	-
7(CONH)	161.89	11.95 (*s*, NH, 1H)
1′	125.83	-
2′	109.41	7.35 (*s*, 1H)
3′	148.54	-
3′(-OCH_3)	55.98	3.84(*s*, CH_3, 3H)
4’(Ar-OH)	150.10	9.68 (*s*, Ar-OH, 1H)
5′	115.92	6.87(*d*, J= 8.1Hz, 1H)
6′	123.02	7.12(*d*, J=8.1Hz, 1H)
7′	149.77	8.37 (*s*, 1H)

The ^{13}C-NMR spectrum of compound **28** apparently displayed only twelve signals. Upon closer examination, it was revealed that two sets of equivalent aromatic carbons were present in the spectrum. Consequently, compound **28** comprised of a total of fourteen carbon atoms. Among these, a carbon signal resonating at δ 161.89 indicated the presence of an amide group.

Furthermore, the existence of a methoxy group was supported by the signal at δ 55.98. The chemical shifts for both protons and carbons of compound **28** are detailed in Table 3.

Compound **29** was obtained as a yellow crystalline solid (2.47 mmol, 84%; w/w). Compound **29** displayed a distinct azomethine group, evident by signals at δ 8.33 (*s*) and δ 150.35 in the ^{1}H and ^{13}C-NMR spectra, respectively. The presence of an amide group was confirmed by signals at δ 11.81 (amide proton) and δ 161.56 (amide carbonyl) in the ^{1}H and ^{13}C-NMR spectra. Additionally, a signal at δ 2.97 (*s*), integrating for six protons, indicated the presence of the $N(CH_3)_2$ group.

Table 4: ^{1}H-NMR and ^{13}C-NMR Spectral Data of compound **29** in DMSO-d_6

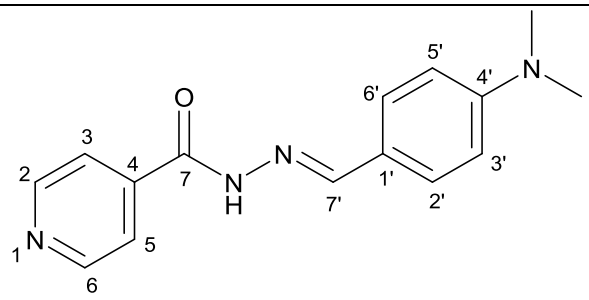

Compound **29**

Position	**δC(ppm)**	**δH(ppm)**
2, 6	150.72	8.77(*d*, J=4.8Hz, 2H)
3, 5	121.95	7.82(*d*, J=4.6Hz, 2H)
4	141.27	-
7(C<u>O</u>N<u>H</u>)	161.56	11.81 (*s*, NH, 1H)
1′	121.60	-
2′, 6′	129.16	7.57 (*d*, J = 8.6 Hz, 2H)
3′, 5′	112.22	6.75 (*d*, J = 8.6 Hz, 2H)
4′	152.15	-
4′(N-(<u>C</u>H$_3$))$_2$	40.18	2.97 (*s*, 6H)
7’	150.35	8.33(*s*, 1H)

The ^{1}H-NMR spectrum revealed signals at δ 6.75 (2H, *d*, J=8.6 Hz) and δ 7.57 (2H, *d*, J=8.6 Hz), confirming the presence of a para-disubstituted benzene group. The ^{13}C-NMR and DEPT-90 spectral data for compound **29** displayed ten signals corresponding to 10 sets of carbon atoms (CH_3 (x2), 5CH (9), and 4C). The chemical shifts for ^{1}H and ^{13}C-NMR are listed in Table 4.

4.3. Antimicrobial Activity of Compounds 27 to 29

4.3.1. Antibacterial Activity

The synthesized compounds were tested *in vitro* antibacterial activity against 26 bacterial strains; five GPB strains including MDR microbes *S. aureus* MDR1, and *S. aureus* MDR2; and 21 GNB strains including drug resistant pathogen *P. aeruginosa* MDR 1 using the disc diffusion method. It's interesting to note that, as shown in Table 5, all compounds showed notable activity against every tested strain of bacteria, with MIC values ranging from 25 µg/ml to 400 µg/ml. Compound **29**, with MIC of 10µg/ml, was discovered to be the most potent antibacterial agent against *P. aeruginosa* MDR 1,which can cause a variety of diseases, including pneumonia, bloodstream infection and UTI (M Campos *et al*., 2020). At 200µg/ml concentration, compound **29** exhibits a greater ZOI (13.5mm) against *S. aureus* MDR 1 in comparison to the standard drug ciprofloxacin (11.5mm). In the case of *S. aureus* ML 267, compound **27** has nearly closed to the standard drug ciprofloxacin (18 mm) in the ZOI (17 mm) at a concentration of 200µg/ml. *S. aureus* is the main culprit behind skin and soft tissue infections, including cellulitis, furuncles, and abscesses (boils) (Del Giudice, 2020). Their MIC of 400µg/ml indicates that they are all very weakly active against *B. pumilus* 82. Furthermore, compound **28** exhibits very little activity (MIC value 400µg/ml) against *B. subtilis* ATCC 6633, *S. aureus* MDR 1, and *S. aureus* MDR 2. Compound **28**, as synthesized and reported by Sethiya *et al*. (2023), has an MIC value of 31.25µg/ml against *E. coli*, whereas our result demonstrates (MIC = 25ug/ml) which verifies that the finding somewhat in align with other studies.

Table 5: Zone of inhibition (ZOI) and minimum inhibitory concentration (MIC) of the synthesized compounds against the tested bacterial strains

Bacterial strains	ZOI in mm(200µg/ml)				MIC(µg/ml)		
	Cpd **27**	Cpd **28**	Cpd **29**	Cipro	Cpd **27**	Cpd **28**	Cpd **29**
B. pumilus 82	8.0	7.5	8.0	19.0	400	400	400
B. subtilis ATCC 6633	8.0	7.5	8.0	18.0	400	400	200
E. coli 3:37C	13.0	13.5	14.0	16.5	50	25	25
E. coli 872	13.0	14.5	14.0	16.0	50	25	25
E. coli C600	12.0	12.5	11.5	13.5	50	50	25
E. coli CD/99/1	13.5	15.0	15.0	17.0	50	25	25
E. coli HB101	13.0	12.0	13.5	14.0	50	50	25
E. coli K88	13.5	14.0	14.5	17.0	50	25	25
E. coli LT37	13.0	15.0	13.5	16.0	50	25	25
E. coli NCTC 5933	13.0	14.0	14.0	16.0	50	25	25
E. coli NCTC 7360	14.0	14.5	14.5	17.0	50	25	25
E. coli ROW 7/12	13.5	13.0	14.5	16.5	50	25	25
P. aeruginosa MDR 1	11.0	11.0	12.0	12.5	50	100	10
S. aureus ML 267	17.0	15.0	16.0	18.0	25	50	50
S. aureus MDR 1	10.5	10.0	13.5	11.5	100	400	100
S. aureus MDR 2	11.0	10.0	11.0	12.0	100	400	100
S. boydii D13629	13.5	12.5	14.0	20.0	100	50	100
S. dysentery 8	14.5	14.0	13.5	20.0	50	100	100
S. enterica TD 01	15.0	14.5	13.5	19.0	50	100	100
S. flexneri Type 6	13.0	12.5	14.0	20.5	100	50	100
S. soneii 1	14.0	14.0	13.0	19.5	50	50	100
S. typhi Ty2	14.0	14.0	13.0	16.0	50	100	100
V. cholerae NCTC 10732	13.0	13.0	14.5	19.0	50	50	50
V. cholerae NCTC 11501	13.5	12.0	14.0	18.5	50	50	50
V. cholerae NCTC 4693	13.0	12.0	15.0	17.5	50	50	50
*V.cholerae*NCTC5596	13.0	12.5	14.0	18.5	50	50	50

Cpd = Compound, Cipro = Ciprofloxacin, MDR= Multidrug resistant

Compound **27** exhibits weak activity (MIC 400µg/ml) against *B. subtilis* ATCC 6633 in a similar manner. *B. subtilis* is a spore-forming GPB, which is linked to septicemia, pneumonia, endocarditis, wound infection, and intraocular inflammation in addition to meningitis (Tokano *et al.*, 2023). With MICs ranging from 25 to 50 µg/ml, the synthesized compounds demonstrated good activity against all strains of *E. coli*, which is the primary cause of UTIs (Klein and Hultgren, 2020).

4.3.2. Antifungal Activity

The fungi tested in the present study were shown to have good susceptibility to all the three compounds. Among the fungal strains tested, *C. albicans*, the primary fungal agent that causes nosocomial invasive candidiasis globally (Bongomin *et al*., 2017), was found to be more susceptible (MIC = 200–800 µg/ml) to the test compounds than the other fungal pathogens (Table 6).

Table 6: Zone of inhibition (ZOI) and minimum inhibitory concentration (MIC) of the synthesized compounds against the tested fungal strains

Fungal strain	ZOI in mm(1500µg/ml)				MIC(µg/ml)		
	Cpd **27**	Cpd **28**	Cpd **29**	Gris	Cpd **27**	Cpd **28**	Cpd **29**
C. albicans ATCC 10231	11.5	12.5	13.0	15.0	800	400	200
A. niger ATCC 6275	12.5	12.0	13.0	14.5	800	400	400
P. notatum ATCC 11625	13.5	11.5	10.5	13.0	800	800	1000
P. funiculosum NCTC 287	13.0	12.0	10.0	13.0	400	800	1000

Cpd = Compound, Gris = Griseofulvin

Among the compounds, compound **27** has better ZOI than the remaining compounds. Moreover, compound **27**(at 13.5mm diameter) shows greater ZOI than the standard drug griseofulvin (13.0 mm diameter) against P. notatum ATCC 11625 and equal ZOI to griseofulvin against P. funiculosum NCTC 287. Furthermore, when compared to the positive control griseofulvin (13.0mm) against *P. notatum* ATCC 11625, compound **27** has a higher

ZOI (13.5mm). Compound **29** exhibits lower MIC value (200µg/ml) against *C. albicans* ATCC 10231in comparison to the other two compounds.

4.4. *In silico* Studies

4.4.1. Molecular Docking of Synthesised Compounds

The primary goal of the *in silico* studies is to save time and money by avoiding needless costs associated with biological assays of compounds with a high likelihood of presenting future pharmacokinetic problems, as these parameters have an impact on pharmacokinetic properties (Brito, 2011). In this study, we evaluated the antibacterial target potential of synthesized compounds by comparing their docking scores with the redocked native ligand platensimycin (compound **25**). The binding affinity of these synthesized compounds with the *E. coli* FabF protein (PDB ID: 3HNZ) was determined using Schrödinger software. Additionally, the well-known inhibitor platensimycin was redocked to validate the docking protocol on the energy-minimized fatty acid synthase enzyme of *E. coli*. The docking scores for compounds **27-29** and redocked platensimycin are presented in Table 7, where a more negative score indicates a stronger binding between the ligand and its target.

Table 7: Docking scores of the synthesised compounds with 3HNZ as predicted by Schrodinger 2023 suite docking software

Ligand	Binding energy (Kcal/mol) with **3HNZ**
Platensimycin(25)	**-9.345**
27	**-8.665**
28	**-5.123**
29	**-5.070**

In Table 7, it is evident that compound **27** achieved the highest docking score (-8.665 kcal/mol) at the active binding site of the *E. coli* enzyme 3HNZ, followed by compound **28** (-5.123 kcal/mol) and compound **29** (-5.070 kcal/mol). Figure 9 illustrates the 3D and 2D interactions between compound **27** and the *E. coli* FabF (PDB ID: 3HNZ). Compound **27** demonstrated

favourable interactions with FabF binding sites, forming five hydrogen bonds with amino acid residues THR-270, THR-305, THR-307, HIE-303, and GLY-310 (Figure 9(**C**)). Additionally, compound **27** also exhibited pi-pi stacking interactions with amino acid residues PHE-400 and PHE-229 in the FabF subunit, enhancing its strong interaction with the enzyme.

Compounds **28** and **29** also exhibited favourable interaction with the active site of the FabF enzyme, each forming a hydrogen bond. Specifically, the amide oxygen of compound **28** formed a hydrogen bond with THR-307 (Figure V, Appendices: 3), while the amide oxygen of compound **29** formed a hydrogen bond with HIE-303 amino acid residue (Figure VI, Appendices: 3) within the active site of the FabF enzyme. It is also noted that aside from these hydrogen bonds, neither compound **28** nor **29** displayed any other significant interactions with the enzyme's active site.

The binding model presented here suggests that these SB derivatives of INH (compounds **27-29**) act as inhibitors of FabF, emphasizing crucial structural elements that need consideration for future optimization efforts.

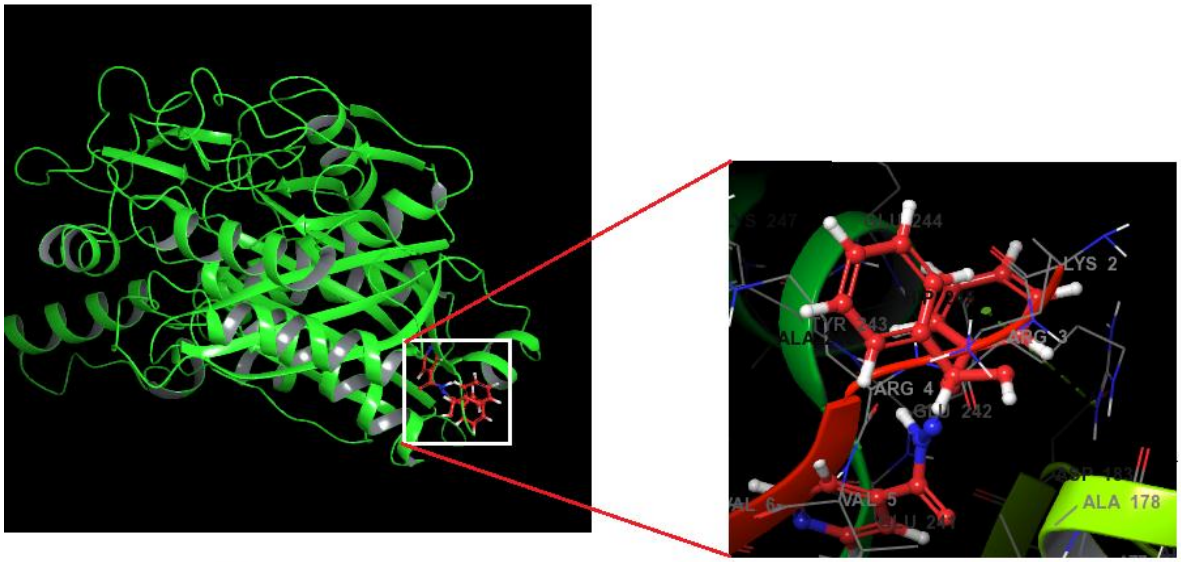

(A) (B)

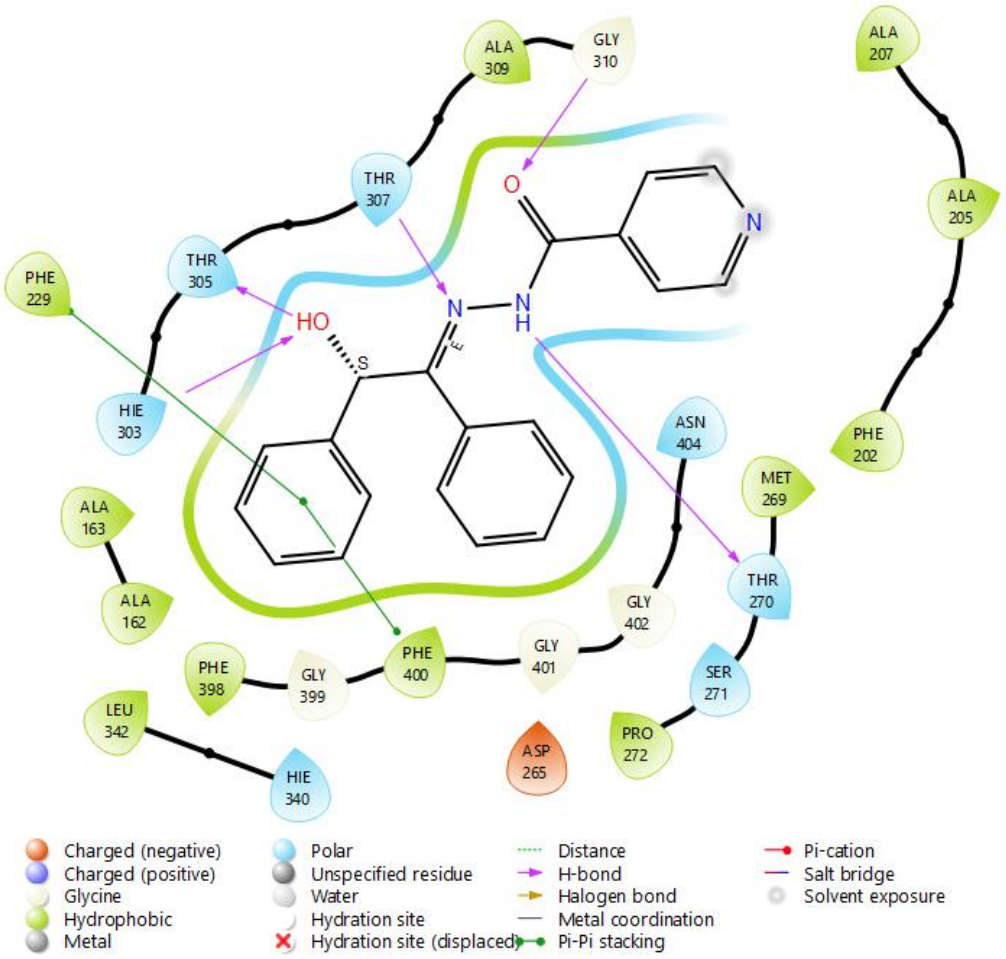

(C)

Figure 9: 3D and 2D interaction between compound **27** and *E. coli* FabF (PDB ID: 3HNZ)

4.2.2. Pharmacokinetic Prediction of Synthesized Compounds

The widely used ADME analysis is essential as it clarifies how a pharmaceutical compound is processed within an organism, thereby influencing the pharmacological activity of the compound (Mali and Chaudhari, 2019). We used Maestro V.13.5's Qikprop (ligand-based ADME analysis) module for this investigation, which offers ranges for comparing a given molecule's properties with those of 95% of known drugs (Mali and Chaudhari, 2018). Our compounds submit to an ADME analysis and the compounds exhibit good drug-like qualities, and Lipinski's rule of five violation was not seen (as shown in Table 8). A drug candidate's molecular weight, QPlogPo/w (which predicts octanol/water partition coefficient), QPPCaco (which predicts permeability of a molecule for the gut-blood barrier through passive transport),

percentage of oral absorption by humans, and the number of H-bonds the solute molecule would donate to the water molecules in the aqueous solution (donor HB) are just a few of the critical properties that must be taken into account. The theoretical drug-like behavior of these compounds is suggested by the ADME analysis results, which are very encouraging and may help with additional laboratory research on them.

Table 8: ADME data of synthesised compounds calculated using Qik Prop Simulation

Ligand	MW	QPlogPo/w	Accept HB	Donor HB	QPlogBB	QPPCaco	Human oral absorption	Ro5
27	331.373	3.420	5.2	2	-1.101	589.426	3	0
28	271.275	1.863	5.5	2	-1.225	398.688	3	0
29	268.318	2.944	5	1	-0.724	1144.936	3	0

MW, not more than 500 Da, QPlogPo/w(accepted range: -2.0 – 6.5), (Hydrogen bond donor (Accepted Limit: ≤ 5), Hydrogen bond acceptor (Accepted Limit: ≤ 10), Log P less than 5, Human oral absorption: 1, 2, or 3 for low, medium, or high, QPlogBB range from: -3.0 to 1.2, QPPCaco(<25 poor, >500 great), Lipinski's rule of five (Ro5)(violating not more than 1)

All of the synthesized compounds displayed remarkable antimicrobial activity, suggesting their potential for further *in vivo* studies. Notably, these compounds exhibited strong antibacterial effects against certain GNB, such as *E, coli, S. typhi, V. cholerae,* known for their resistance challenges, attributed to their additional barriers. Furthermore, all the compounds demonstrated remarkable activities against MDR microbes, including *S. auereus* and *P. auruginosa*.

FabF is one of the crucial FAS-II enzymes that is unique to the prokaryotic kingdom and is essential for the survival of all bacterial species. Inhibiting FabF disrupts FAS, leading to cell death (Davies *et al*., 2000; Wang *et al*., 2006; Belete, 2019). Given its vital role in bacterial survival, FabF has garnered interest as a target for antibacterial drugs (Wang *et al*., 2006).

Considering the synthesized compounds demonstrated promising antimicrobial activity, we considered it necessary to elucidate the likely mechanism of action.

The 2.6-Å structure of *E. coli* FabF in complex with platensimycin reveals that the antibiotic binds to the malonyl subsite of FabF. The active-site histidine residues (HIE 303 and HIE 340) of the conserved HIS-HIS-CYS catalytic triad are crucial. Additionally, the side chain of THR 307, the amide carbonyl of THR 270, and ALA 309 play significant roles in hydrogen bond formation. The open conformation of PHE 400, the gatekeeper residue that separates the malonyl-binding and acyl-binding subsites, is also vital for the interaction between the ligand and enzyme (Wang *et al*., 2006). The synthesized compounds displayed strong binding interactions within the enzyme's active site, as evident by the docking results and the involvement of key side chains of amino acid residues. In a detailed examination of the ligand-enzyme 2D interaction (Figure 9(**C**)), it is noted that compound **27** in conjunction with *E. coli'*s FabF demonstrates interactions nearly identical to the platensimycin-FabF interaction (Figure VII, Appendices:3). This similarity suggests that the compounds hold promise as potential antimicrobial agents, supported by both their antimicrobial activity and docking results.

5. Conclusion

In this study, three SB derivatives of INH were successfully synthesized through the SB condensation reaction. The synthesized compounds exhibited promising antimicrobial activities against a wide range of tested bacterial and fungal strains. Among the synthesised compounds, compound **29** demonstrated better activity (with MIC value of 10µg/ml) than the other two compounds (**27** and **28**) against *P. aeruginosa* MDR 1. Molecular docking results indicated that compound **27** exhibited better interactions with the target protein (FabF enzyme) compared to compounds **28** and **29**. The ADME prediction of the compounds indicated that all of them adhered to Lipinski's rule of five. In the end, SB derivatives of INH show great potential as lead compounds in the development of novel antimicrobial agents to combat the increasing risks of AMR and infectious diseases. These findings underscore the importance of further research into synthesizing additional derivatives to evaluate potential antifungal and antibacterial properties.

6. Recommendations

The following suggestions are made in light of the current study's finding:

- Anti-tubercular activity assay of these compounds will be recommended, since the starting scaffold is well known anti-tubercular agent.
- Performing experimental validation is necessary for all *in silico* analysis results.
- *In vivo* evaluation is suggested because *in vitro* study is insufficient to consider the compounds as good candidates of antimicrobial agents.

References

Abirami, M. & Nadaraj, V. 2014. Synthesis of Schiff Base Under Solvent-free Condition: As A Green Approach. *International Journal of ChemTech Research,* 6 (4)**,** pp 2534-2538.

Aboul-Fadl, T., Radwan, A. A., Abdelaziz, H. A., Baseeruddin, M., Attia, M. I. & Kadi, A. 2012. Novel Schiff Bases of Indoline-2,3-Dione and Nalidixic Acid Hydrazide: Synthesis *In vitro* Antimycobacterial and *In silico Mycobacterium tuberculosis*(*Mtb*) DNA Gyrase Inhibitory Activity. *Digest Journal of Nanomaterials & Biostructures,* 7 (1)**,** pp 329 - 338.

Afridi, H. H., Shoaib, M., Ali Shah, S. W., Hussain, H., Shafiullah & Ghias, M. 2021. *In vivo* Analgesic Potential of Enantiomerically Pure Schiff Bases Using Animal Model. *Bioscience Research,* 18 (1)**,** pp 685-694.

Al-Hiyari, B. A., Shakya, A. K., Naik, R. R. & Bardaweel, S. 2021. Microwave-Assisted Synthesis of Schiff Bases of Isoniazid and Evaluation of Their Anti-Proliferative and Antibacterial Activities. *Molbank,* 2021 (1)**,** pp M1189.

Amorim, C. R., Pavani, T. F., Lopes, A. F., Duque, M. D., Mengarda, A. C., Silva, M. P., de Moraes, J. & Rando, D. G. 2020. Schiff Bases of 4-Phenyl-2-Aminothiazoles as Hits to New Antischistosomals: Synthesis, *In vitro*, *In vivo* and *In silico* Studies. *European Journal of Pharmaceutical Sciences,* 150, pp. 105371.

Andrews, J. M. 2001. Determination of Minimum Inhibitory Concentrations. *Journal of Antimicrobial Chemotherapy,* 48 (suppl_1)**,** pp 5-16.

Aochar, R. B., Mahale, R. G. & Dhivare, R. S. 2022. Synthesis, Physicochemical, Morphological, and Antimicrobial Study of Schiff-Base Ligands Metal Complexes. *Journal of Research in Pharmaceutical Science,* 8 (2)**,** pp 01-06.

Asadi, A., Razavi, S., Talebi, M. & Gholami, M. 2019. A Review on Anti-Adhesion Therapies of Bacterial Diseases. *Infection,* 47, pp. 13–23.

Bauer, D. J., Apostolov, K. & Selway, J. W. T. 1970. Activity of Methisazone against Viruses. *Annals of the New York Academy of Sciences,* 173 (1)**,** pp 314-319.

Bloom, D. E., Black, S. & Rappuoli, R. 2017. Emerging Infectious Diseases: A Proactive Approach. *Proceedings of the National Academy of Sciences,* 114 (16)**,** pp 4055-4059.

Bongomin, F., Gago, S., Oladele, R. O. & Denning, D. W. 2017. Global and Multi-National Prevalence of Fungal Diseases-Estimate Precision. *Journal of Fungi,* 3 (4)**,** pp 57.

Brito, M. A. D. 2011. Pharmacokinetic Study with Computational Tools in the Medicinal Chemistry Course. *Brazilian Journal of Pharmaceutical Sciences,* 47, pp. 797-805.

Brown, G. D., Denning, D. W., Gow, N. A., Levitz, S. M., Netea, M. G. & White, T. C. 2012. Hidden Killers: Human Fungal Infections. *Science Translational Medicine,* 4 (165)**,** pp 165rv13-165rv13.

Casadevall, A. 2018. Fungal Diseases in the 21st Century: The Near and Far Horizons. *Pathogens and Immunity,* 3 (2)**,** pp 183-96.

Coates, A., Hu, Y., Bax, R. & Page, C. 2002. The Future Challenges Facing the Development of New Antimicrobial Drugs. *Nature Reviews Drug discovery,* 1 (11)**,** pp 895-910.

Das, M., Ghosh, P. S. & Manna, K. 2016. A Review on Platensimycin: A Selective FabF Inhibitor. *International Journal of Medicinal Chemistry*.

Davies, C., Heath, R. J., White, S. W. & Rock, C. O. 2000. The 1.8 Å Crystal Structure and Active-Site Architecture of β-ketoacyl-Acyl Carrier Protein Synthase III (FabH) from Escherichia coli. *Structure,* 8 (2)**,** pp 185-195.

Del Giudice, P. 2020. Skin Infections Caused by Staphylococcus aureus. *Acta dermato-venereologica,* 100 (9)**,** pp 208-215.

Desai, D. D. & Desai, G. C. 2014. Hydrazones: Synthesis, Biological Activity and Their Spectral Characterization. *Journal of Chemical and Pharmaceutical Research,* 6 (7)**,** pp 1704-1708.

Dewangan, D., Vaishnav, Y., Mishra, A., Jha, A. K., Verma, S. & Badwaik, H. 2021. Synthesis, Molecular Docking, and Biological Evaluation of Schiff Base Hybrids of 1,2,4-triazole-pyridine as Dihydrofolate Reductase Inhibitors. *Current Research in Pharmacology and Drug Discovery,* 2, pp. 100024.

Doron, S. & Gorbach, S. L. 2008. Bacterial Infections: Overview. *International Encyclopedia of Public Health.*

Falk, N., Berenstein, A. J., Moscatelli, G., Moroni, S., González, N., Ballering, G., Freilij, H. & Altcheh, J. 2022. Effectiveness of Nifurtimox in the Treatment of Chagas Disease: A Long-Term Retrospective Cohort Study in Children and Adults. *Antimicrobial Aents and Chemotherapy,* 66 (5)**,** pp e02021-21.

Feng, Y., Zhang, H., Wu, Z., Wang, S., Cao, M., Hu, D. & Wang, C. 2014. *Streptococcus suis* Infection: An Emerging/Reemerging Challenge of Bacterial Infectious Diseases? . *Virulence,* 5 (4)**,** pp 477-497.

Fernandes, G. F. D. S., Salgado, H. R. N. & Santos, J. L. D. 2017. Isoniazid: A Review of Characteristics, Properties and Analytical Methods. *Critical Reviews in Analytical Chemistry,* 47 (4)**,** pp 298-308.

Flores-Mireles, A. L., Walker, J. N., Caparon, M. & Hultgren, S. J. 2015. Urinary Tract Infections: Epidemiology, Mechanisms of Infection and Treatment Options. *Nature Rviews Mcrobiology,* 13 (5)**,** pp 269-284.

Fonkui, T. Y., Ikhile, M. I., Njobeh, P. B. & Ndinteh, D. T. 2019. Benzimidazole Schiff Base Derivatives: Synthesis, Characterization and Antimicrobial Activity. *BMC Chemistry,* 13 (1)**,** pp 1-11.

García-Lara, J., Masalha, M. & Foster, S. J. 2005. Staphylococcus aureus: The Search for Novel Targets. *Drug Discovery Today,* 10 (9)**,** pp 643-651.

Grzegorzewicz, A. E., Eynard, N., Quémard, A., North, E. J., Margolis, A., Lindenberger, J. J., Jones, V., Korduláková, J., Brennan, P. J., Lee, R. E. & Ronning, D. R. 2015. Covalent Modification of the Mycobacterium tuberculosis FAS-II Dehydratase by Isoxyl and Thiacetazone. *ACS Infectious Diseases,* 1 (2)**,** pp 91−97.

Habala, L., Varényi, S., Bilková, A., Herich, P., Valentová, J., Kožíšek, J. & Devínsky, F. 2016. Antimicrobial Activity and Urease Inhibition of Schiff Bases Derived from Isoniazid and Fluorinated Benzaldehydes and of Their Copper (II) Complexes. *Molecules,* 21 (12)**,** pp 1742.

Hall, R. A. & Noverr, M. C. 2017. Fungal Interactions with the Human Host: Exploring the Spectrum of Symbiosis. *Current Opinion in Microbiology*, 40, pp. 58–64.

Hegde, P., Boshoff, H. I., Rusman, Y., Aragaw, W. W., Salomon, C. E., Dick, T. & Aldrich, C. C. 2021. Reinvestigation of the Structure-Activity Relationships of Isoniazid. *Tuberculosis,* 129, pp. 102100.

Hemalatha, K. & Madhumitha, G. 2016. Study of Binding Interaction Between Anthelmintic 2, 3-dihydroquinazolin-4-ones with Bovine Serum Albumin by Spectroscopic Methods. *Journal of Luminescence,* 178, pp. 163–171.

Holmes, C. L., Anderson, M. T., Mobley, H. L. & Bachman, M. A. 2021. Pathogenesis of Gram-Negative Bacteremia. *Clinical Microbiology Reviews,* 34 (2)**,** pp 10-1128.

Hudzicki, J. 2009. Kirby-Bauer Disk Diffusion Susceptibility Test Protocol. *American society for microbiology,* 15, pp. 55-63.

Ikuta, K. S., Swetschinski, L. R., Aguilar, G. R., Sharara, F., Mestrovic, T., Gray, A. P., Weaver, N. D., Wool, E. E., Han, C., Hayoon, A. G. & Aali, A. 2022. Global Mortality associated with 33 Bacterial Pathogens in 2019: A Systematic Analysis for the Global Burden of Disease Study 2019. *Lancet*, 400 (10369)**,** pp 2221–2248.

Jia, Q., Song, Q., Li, P. & Huang, W. 2019. Rejuvenated Photodynamic Therapy for Bacterial Infections. *Advanced Healthcare Materials,* 8 (14)**,** pp 1900608.

Johnson, J. R., Delavari, P. & Azar, M. 1999. Activities of a Nitrofurazone-Containing Urinary Catheter and a Silver Hydrogel Catheter Against Multidrug-Resistant Bacteria Characteristic of Catheter-Associated Urinary Tract Infection. *Antimicrobial Agents and Chemotherapy,* 43 (12)**,** pp 2990–2995.

Kadhim, Y. M., Lafta, S. J. & Mahdi, M. F. 2020. Synthesis in Microwave, Pharmacological Evaluation, Molecular Docking and ADME Studies of Schiff Bases of Diclofenac Targeting COX-2. *Journal of Biochemical Technology Society*, 11 (2)**,** pp 88-101.

Kapoor, G., Pathak, D. P., Bhutani, R., Husain, A., Jain, S. & Iqbal, M. A. 2019. Synthesis, ADME, Docking Studies and *In vivo* Anti-Hyperglycaemic Potential Estimation of Novel Schiff Base Derivatives from Octadec-9-enoic Acid. *Bioorganic Chemistry*, 84, pp. 478–492.

Khabbaz, R. F., Moseley, R. R., Steiner, R. J., Levitt, A. M. & Bell, B. P. 2014. Challenges of Infectious Diseases in the USA. *The Lancet,* 384 (9937)**,** pp 53–63.

Kizilkaya, H., Dag, B., Aral, T., Genc, N. & Erenler, R. 2020. Synthesis, Characterization, and Antioxidant Activity of Heterocyclic Schiff Bases. *Journal The Chinese Chemical Society,* 67 (9)**,** pp 1696–1701.

Klein, R. D. & Hultgren, S. J. 2020. Urinary Tract Infections: Microbial Pathogenesis, Host–Pathogen Interactions and New Treatment Strategies. *Nature Reviews Microbiology,* 18 (4)**,** pp 211-226.

Koçyiğit-Kaymakçıoğlu, B., Oruç-Emre, E. E., Ünsalan, S., Tabanca, N., Khan, S. I., Wedge, D. E., İşcan, G., Demirci, F. & Rollas, S. 2012. Synthesis and Biological Activity of Hydrazide–hydrazones and Their Corresponding 3-acetyl-2, 5-disubstituted-2, 3-dihydro-1, 3, 4-oxadiazoles. *Medicinal Chemistry Research,* 21, pp. 3499-3508.

Koeth, L. M., DiFranco-Fisher, J. M. & McCurdy, S. 2015. A Reference Broth Microdilution Method for Dalbavancin *In vitro* Susceptibility Testing of Bacteria that Grow Aerobically. *JoVE (Journal of Visualized Experiments),* 103, pp. e53028.

Krátký, M., Bősze, S., Baranyai, Z., Stolaříková, J. & Vinšová, J. 2017. Synthesis and Biological Evolution of Hydrazones Derived from 4-(trifluoromethyl) benzohydrazide. *Bioorganic & medicinal chemistry letters,* 27 (23)**,** pp 5185-5189.

Krause, T., Gerbershagen, M. U., Fiege, M., Weisshorn, R. & Wappler, F. 2004. Dantrolene – A Review of Its Pharmacology, Therapeutic Use and New Developments. *Anaesthesia,* 59 (4)**,** pp 364–373.

Kumar, M., Padmini, T. & Ponnuvel, K. 2017. Synthesis, Characterization and Antioxidant Activities of Schiff Bases are of Cholesterol. *Journal of Saudi Chemical Society,* 21, pp. S322-S328.

Lalitha, M. K. 2004. Manual on Antimicrobial Susceptibility Testing. Performance Standards for Antimicrobial Testing. *Twelfth Informational Supplement,* 56238, pp. 454-456.

Lazar, V., Ditu, L. M., Pircalabioru, G. G., Gheorghe, I., Curutiu, C., Holban, A. M., Picu, A., Petcu, L. & Chifiriuc, M. C. 2018. Aspects of Gut Microbiota and Immune System Interactions in Infectious Diseases, Immunopathology, and Cancer. *Frontiers in Immunology,* 9, pp. 1830.

Los, F. C., Randis, T. M., Aroian, R. V. & Ratner, A. J. 2013. Role of Pore-Forming Toxins in Bacterial Infectious Diseases. *Microbiology and Molecular Biology Reviews,* 77 (2)**,** pp 173–207.

M Campos, J. C. D., Antunes, L. C. & Ferreira, R. B. 2020. Global Priority Pathogens: Virulence, Antimicrobial Resistance and Prospective Treatment Options. *Future Microbiology,* 15 (8)**,** pp 649-677.

M'ikanatha, N. M., Lynfield, R., Julian, K. G., Van Beneden, C. A. & De Valk, H. 2007. Infectious Disease Surveillance: A Cornerstone for Prevention and Control. *In:* Nkuchia M. M'ikanatha, Ruth Lynfiel, Chris A. Van Beneden & Valk, H. d. (eds.) *Infectious Disease Surveillance.* First ed. USA: Blackwell Publishing.

Madhavi Sastry, G., Adzhigirey, M., Day, T., Annabhimoju, R. & Sherman, W. 2013. Protein and Ligand Preparation: Parameters, Protocols, and Influence on Virtual Screening Enrichments. *Journal of computer-aided molecular design,* 27, pp. 221–234.

Malhotra, M., Sharma, G. & Deep, A. 2012. Synthesis and Characterization of (E)-N'-(substituted benzylidene) Isonicotinohydrazide Derivatives as Potent Antimicrobial and Hydrogen Peroxide Scavenging Agents. *Acta Poloniae Pharmaceutica-Drug Research,* 69 (4)**,** pp 637-644.

Mali, S. N. & Chaudhari, H. K. 2018. Computational Studies on Imidazo [1, 2-a] pyridine-3-carboxamide Analogues as Antimycobacterial Agents: Common Pharmacophore

Generation, Atom-based 3D-QSAR, Molecular Dynamics Simulation, QikProp, Molecular Docking and Prime MMGBSA Approaches. *Open Pharmaceutical Sciences Journal,* 5 (1)**,** pp.

Mali, S. N. & Chaudhari, H. K. 2019. Molecular Modelling Studies on Adamantane-based Ebola Virus GP-1 Inhibitors using Docking, Pharmacophore and 3D-QSAR. *SAR and QSAR in Environmental Research,* 30 (3)**,** pp 161-180.

Manjunath, M., Kulkarni, A. D., Bagihalli, G. B., Malladi, S. & Patil, S. A. 2016. Bio-important Antipyrine Derived Schiff Bases and Their Transition Metal Complexes: Synthesis, Spectroscopic Characterization, Antimicrobial, Anthelmintic and DNA Cleavage Investigation. *Journal of Molecular Structure,* 1127, pp. 314-321.

Martens, E. & Demain, A. L. 2011. Platensimycin and Platencin: Promising Antibiotics for Future Application in Human Medicine. *The Journal of Antibiotics,* 64 (11)**,** pp 705–710.

Meles, G. G., Ayele, G., Gutema, B. T., Kondale, M., Zerdo, Z., Merdekios, B., Tsalla, T., Kote, M., Baharu, A., Bekele, A. & Gebremeskel, F. 2023. Causes and Trends of Adult Mortality in Southern Ethiopia: An Eight-Year Follow Up Database Study. *BMC Infectious Diseases,* 23 (1)**,** pp 29.

Misganaw, A., Haregu, T. N., Deribe, K., Tessema, G. A., Deribew, A., Melaku, Y. A., Amare, A. T., Abera, S. F., Gedefaw, M., Dessalegn, M. & Lakew, Y. 2017. National Mortality Burden due to Communicable, Non-communicable, and Other Diseases in Ethiopia, 1990–2015: Findings from the Global Burden of Disease Study 2015. *Population Health Metrics,* 15 (29)**,** pp 1-17.

Mojzych, M. & Sebela, M. 2015. Synthesis and Biological Activity Evaluation of Schiff Bases of 5-Acyl-1,2,4-Triazine. *Journal of Chemical Society Pak.,* 37 (2)**,** pp 300-305.

Netea, M. G. & Brown, G. D. 2012. Fungal Infections: The Next Challenge. *Current Opinion in Microbiology,* 15, pp. 403–405.

Pahlavani, E., Kargar, H. & Rad, N. S. 2015. A study on Antitubercular and Antimicrobial Activity of Isoniazid Derivative. *Zahedan Journal of Research in Medical Sciences,* 17 (7)**,** pp e1010.

Pappas, P. G., Kauffman, C. A., Andes, D., Benjamin Jr, D. K., Calandra, T. F., Edwards Jr, J. E., Filler, S. G., Fisher, J. F., Kullberg, B. J., Ostrosky-Zeichner, L. & eboli, A. C. 2009. Clinical Practice Guidelines for the Management of Candidiasis: 2009 Update by the Infectious Diseases Society of America. *Clinical Infectious Diseases,* 48 (5)**,** pp 503–535.

Phillips, K. F. & Hailey, F. J. 1987. Furazolidone for Treatment of Diarrhoeal Disease. *Tropical Doctor,* 17 (2)**,** pp 89-91.

Popiołek, Ł. 2017. Hydrazide–Hydrazones as Potential Antimicrobial Agents: Overview of the Literature since 2010. *Medicinal Chemistry Research,* 26, pp. 287-301.

Porreca, A., D'Agostino, D., Romagnoli, D., Del Giudice, F., Maggi, M., Palmer, K., Falabella, R., De Berardinis, E., Sciarra, A., Ferro, M. & Artibani, W. 2021. The Clinical Efficacy of Nitrofurantoin for Treating Uncomplicated Urinary Tract Infection in Adults: A Systematic Review of Randomized Control Trials. *Urologia Internationalis,* 105 (7-8)**,** pp 531–540.

Qi, G. B., Zhang, D., Liu, F. H., Qiao, Z. Y. & Wang, H. 2017. An "On-Site Transformation" Strategy for Treatment of Bacterial Infection. *Advanced Materials,* 29 (36)**,** pp 1703461.

Raczuk, E., Dmochowska, B., Samaszko-Fiertek, J. & Madaj, J. 2022. Different Schiff Bases—Structure, Importance and Classification. *Molecules,* 27 (3)**,** pp 787.

Rathelot, P., Vanelle, P., Gasquet, M., Delmas, F., Crozet, M. P., Timon-David, P. & Maldonado, J. 1995. Synthesis of Novel Functionalized 5-Nitroisoquinolines and Evaluation of *In vitro* Antimalarial Activity. *European Journal of Medicinal Chemistry,* 30 (6)**,** pp 503-508.

Reddy, G. K. K., Padmavathi, A. R. & Nancharaiah, Y. V. 2022. Fungal Infections: Pathogenesis, Antifungals and Alternate Treatment Approaches. *Current Research in Microbial Sciences,* 3, pp. 100137.

Rock, K., Brand, S., Moir, J. & Keeling, M. J. 2014. Dynamics of Infectious Diseases. *Reports on Progress in Physics,* 77 (2)**,** pp 026602.

Rokas, A. 2022. Evolution of the Human Pathogenic Lifestyle in Fungi. *Nature Microbiology,* 7, pp. 607-619.

Roquini, V., Mengarda, A. C., Cajas, R. A., Martins-da-Silva, M. F., Godoy-Silva, J., Santos, G. A., Espírito-Santo, M. C. C., Pavani, T. F., Melo, V. A., Salvadori, M. C. & Teixeira, F. S. 2023. The Existing Drug Nifuroxazide as an Antischistosomal Agent: *In vitro, In vivo,* and *In silico* Studies of Macromolecular Targets. *Microbiology Spectrum,* 11 (4)**,** pp e01393-23.

Sadia, M., Khan, J., Naz, R., Zahoor, M., Shah, S. W. A., Ullah, R., Naz, S., Bari, A., Mahmood, H. M., Ali, S. S. & Ansari, S. A. 2021. Schiff Base Ligand L Synthesis and Its Evaluation as Anticancer and Antidepressant Agent. *Journal of King Saud University-Science,* 33 (2)**,** pp 101331.

Salihović, M., Pazalja, M., Halilović, S. Š., Veljović, E., Mahmutović-Dizdarević, I., Roca, S., Novaković, I. & Trifunović, S. 2021. Synthesis, Characterization, Antimicrobial Activity and DFT Study of Some Novel Schiff Bases. *Journal of Molecular Structure,* 1241, pp. 130670.

Schumacher, A., Vranken, T., Malhotra, A., Arts, J. J. C. & Habibovic, P. 2018. In vitro Antimicrobial Susceptibility Testing Methods: Agar Dilution to 3D Tissue-Engineered Models. *European Journal of Clinical Microbiology & Infectious Diseases,* 37, pp. 187-208.

Selvarajan, V., Obuobi, S. & Ee, P. L. R. 2020. Silica Nanoparticles—A Versatile Tool for the Treatment of Bacterial Infections. *Frontiers in Chemistry,* 8, pp. 602.

Sethiya, A., Joshi, D., Manhas, A., Sahiba, N., Agarwal, D. K., Jha, P. C. & Agarwal, S. 2023. Glycerol Based Carbon Sulfonic Acid Catalyzed Synthesis, *In silico* Studies and *In vitro* Biological Evaluation of Isonicotinohydrazide Derivatives as Potent Antimicrobial and Anti-Tubercular Agents. *Heliyon,* 9 (2)**,** pp.

Shah, M. A., Uddin, A., Shah, M. R., Ali, I., Ullah, R., Hannan, P. A. & Hussain, H. 2022. Synthesis and Characterization of Novel Hydrazone Derivatives of Isonicotinic Hydrazide and Their Evaluation for Antibacterial and Cytotoxic Potential. *Molecules,* 27 (19)**,** pp 6770.

Sharma, P. C., Sharma, D., Sharma, A., Saini, N., Goyal, R., Ola, M., Chawla, R. & Thakur, V. K. 2020. Hydrazone Comprising Compounds as Promising Anti-Infective Agents: Chemistry and Structure-Property Relationship. *Materials Today Chemistry,* 18, pp. 100349.

Singh, S. B., Ondeyka, J. G., Herath, K. B., Zhang, C., Jayasuriya, H., Zink, D. L., Parthasarathy, G., Becker, J. W., Wang, J. & Soisson, S. M. 2009. Isolation, Enzyme-Bound Structure and Antibacterial Activity of Platencin A1 from Streptomyces platensis. *Bioorganic & Medicinal Chemistry Letters,* 19 (16)**,** pp 4756–4759.

Slaihim, M. M., Mohammad, H. J. & Ali, A. H. 2023. Synthesis of a Remarkable New Schiff Bases Series Via an Amino-1, 3-diol Substrate. *Journal of Population Therapeutics & Clinical Pharmacology,* 30 (2)**,** pp 249–256.

Slayden, R. A. & Barry III, C. E. 2000. The Genetics and Biochemistry of Isoniazid Resistance in *Mycobacterium tuberculosis*. *Microbes and Infection,* 2 (6)**,** pp 659-669.

Soni, H. I. & Patel, N. B. 2017. Pyrimidine Incorporated Schiff Base of Isoniazid with Their Synthesis, Characterization and *In vitro* Biological Evaluation. *Asian Journal of Pharmaceutical and Clinical Research,* 10 (10)**,** pp 209-214.

Szklarzewicz, J., Jurowska, A., Hodorowicz, M., Kazek, G., Mordyl, B., Menaszek, E. & Sapa, J. 2021. Characterization and Antidiabetic Activity of Salicylhydrazone Schiff Base Vanadium(IV) and (V) Complexes. *Transition Metal Chemistry,* 46, pp. 201–217.

Tagliabue, A. & Rappuoli, R. 2018. Changing Priorities in Vaccinology: Antibiotic Resistance Moving to the Top. *Frontiers in Immunology,* 9, pp. 1068.

Teran, R., Guevara, R., Mora, J., Dobronski, L., Barreiro-Costa, O., Beske, T., Pérez-Barrera, J., Araya-Maturana, R., Rojas-Silva, P., Poveda, A. & Heredia-Moya, J. 2019. Characterization of Antimicrobial, Antioxidant, and Leishmanicidal Activities of Schiff Base Derivatives of 4-Aminoantipyrine. *Molecules,* 24 (15)**,** pp 2696.

Thomas, A. B., Nanda, R. K., Kothapalli, L. P. & Hamane, S. C. 2016. Synthesis and Biological Evaluation of Schiff's Bases and 2-Azetidinones of Isonocotinyl Hydrazone as Potential Antidepressant and Nootropic Agents. *Arabian Journal of Chemistry,* 9, pp. S79-S90.

Tokano, M., Tarumoto, N., Imai, K., Sakai, J., Maeda, T., Kawamura, T., Seo, K., Takahashi, K., Yamamoto, T. & Maesaki, S. 2023. A Case of Bacterial Meningitis Caused by Bacillus subtilis var. natto. *Internal Medicine,* Internal Medicine 0768-22.

Townsend, A. K., Hawley, D. M., Stephenson, J. F. & Williams, K. E. 2020. Emerging Infectious Disease and the Challenges of Social Distancing in Human and Non-human Animals. *Proceedings of the Royal Society B,* 287 (1932)**,** pp 20201039.

Tsacheva, I., Todorova, Z., Momekova, D., Momekov, G. & Koseva, N. 2023. Pharmacological Activities of Schiff Bases and Their Derivatives with Low and High Molecular Phosphonates. *Pharmaceuticals,* 16 (7)**,** pp 938.

Uddin, M. N., Ahmed, S. S. & Alam, S. R. 2020. Review: Biomedical Applications of Schiff Base Metal Complexes. *Journal of Coordination Chemistry,* 73 (23)**,** pp 3109–3149.

Unissa, A. N., Subbian, S., Hanna, L. E. & Selvakumar, N. 2016. Overviewon Mechanisms of Isoniazid Action and Resistance in Mycobacterium tuberculosis. *Infection, Genetics and Evolution,* 45, pp. 474-492.

Uzzaman, M., Junaid, M. & Uddin, M. N. 2020. Evaluation of Anti-tuberculosis Activity of Some Oxotitanium(IV) Schiff Base Complexes; Molecular Docking, Dynamics Simulation and ADMET Studies. *SN Applied Sciences,* 2, pp. 1-11.

Van Seventer, J. M. & Hochberg, N. S. 2017. Principles of Infectious Diseases: Transmission, Diagnosis, Prevention, and Control. *International Encyclopedia of Public Health.* Second ed. USA: Elsevier.

Vijaya, K., S.,, Damodar, G., Ravikanth, S. & Vijayakumar, G. 2012. An Overview on Infectious Disease. *Indian Journal of Pharmaceutical Science & Research,* 2 (2)**,** pp 63-74.

Wang, J., Soisson, S. M., Young, K., Shoop, W., Kodali, S., Galgoci, A., Painter, R., Parthasarathy, G., Tang, Y. S., Cummings, R. & Ha, S. 2006. Platensimycin is A Selective FabF Inhibitor with Potent Antibiotic Properties. *Nature,* 441 (7091)**,** pp 358-361.

Wang, L., Guo, D. G., Wang, Y. Y. & Zheng, C. Z. 2014. 4-Hydroxy-3-methoxy-benzaldehyde Series Aroyl Hydrazones: Synthesis, Thermostability and Antimicrobial Activities. *RSC Advances,* 4 (102)**,** pp 58895-58901.

West, D. X., El-Sawaf, A. K. & Bain, G. A. 1998. Metal Complexes of N (4)-Substituted Analogues of the Antiviral Drug Methisazone {1- Methylisatin Thiosemicarbazone}. *Transition Metal Chemistry-Winheim,* 23, pp. 1-6.

WHO. 2021. World Health Statistics 2021: Monitoring Health for the SDGs, Sustainable Development Goals, (Geneva).

Wilson, J. W., Schurr, M. J., LeBlanc, C. L., Ramamurthy, R., Buchanan, K. L. & Nickerson, C. A. 2002. Mechanisms of Bacterial Pathogenicity. *Postgraduate Medical Journal,* 78 (918)**,** pp 216–224.

Xavier, A. & Srividhya, N. 2014. "Synthesis and Study of Schiff Base Ligands". *IOSR Journal of Applied Chemistry,* 7 (11)**,** pp 06-15.

Yilmaz, E. & Cukurovali, A. 2019. Synthesis, Characterization, Investigation of Biological Activity, Docking Studies, and Spectroscopic Properties of Hydrazone Compounds Containing Different Substituents. *Canadian Journal of Physics,* 97 (4)**,** pp 408-416.

Appendices

Appendix 1: ^{1}H, ^{13}C, DEPT-90 and DEPT-135 NMR Spectra of Synthesised Compounds

Appendix 1a: ^{1}H, ^{13}C, and DEPT-135 NMR Spectra of Compound **27**

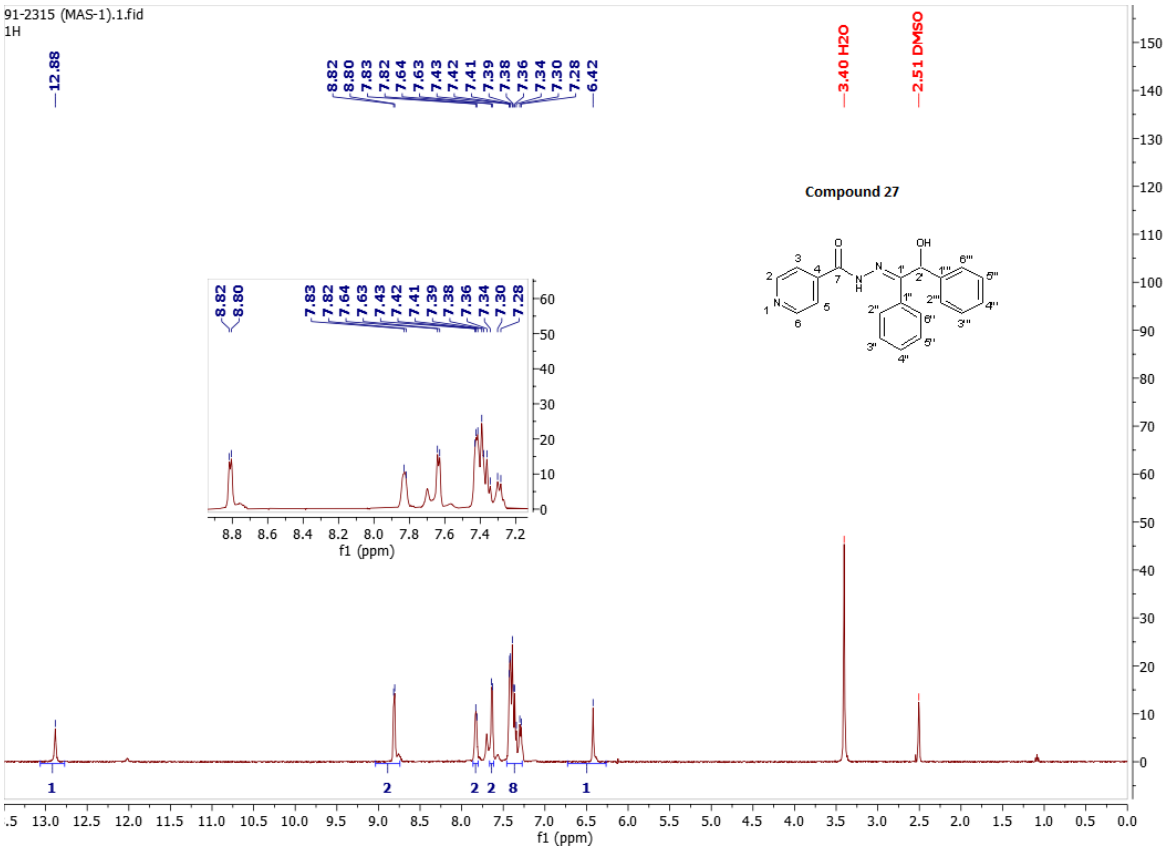

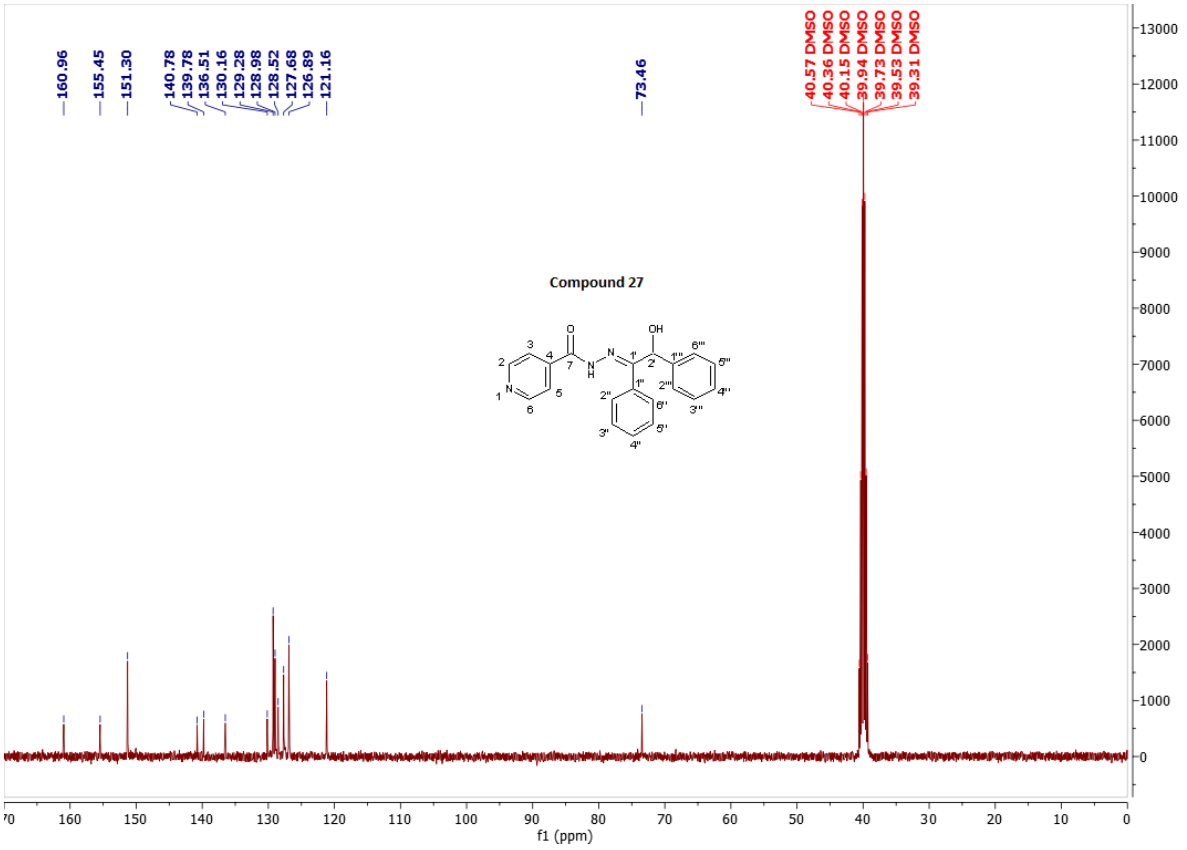
160.96
155.45
151.30
140.78
139.78
136.51
130.16
129.28
128.98
128.52
127.68
126.89
121.16
73.46
40.57 DMSO
40.36 DMSO
40.15 DMSO
39.94 DMSO
39.73 DMSO
39.53 DMSO
39.31 DMSO
Compound 27
f1 (ppm)

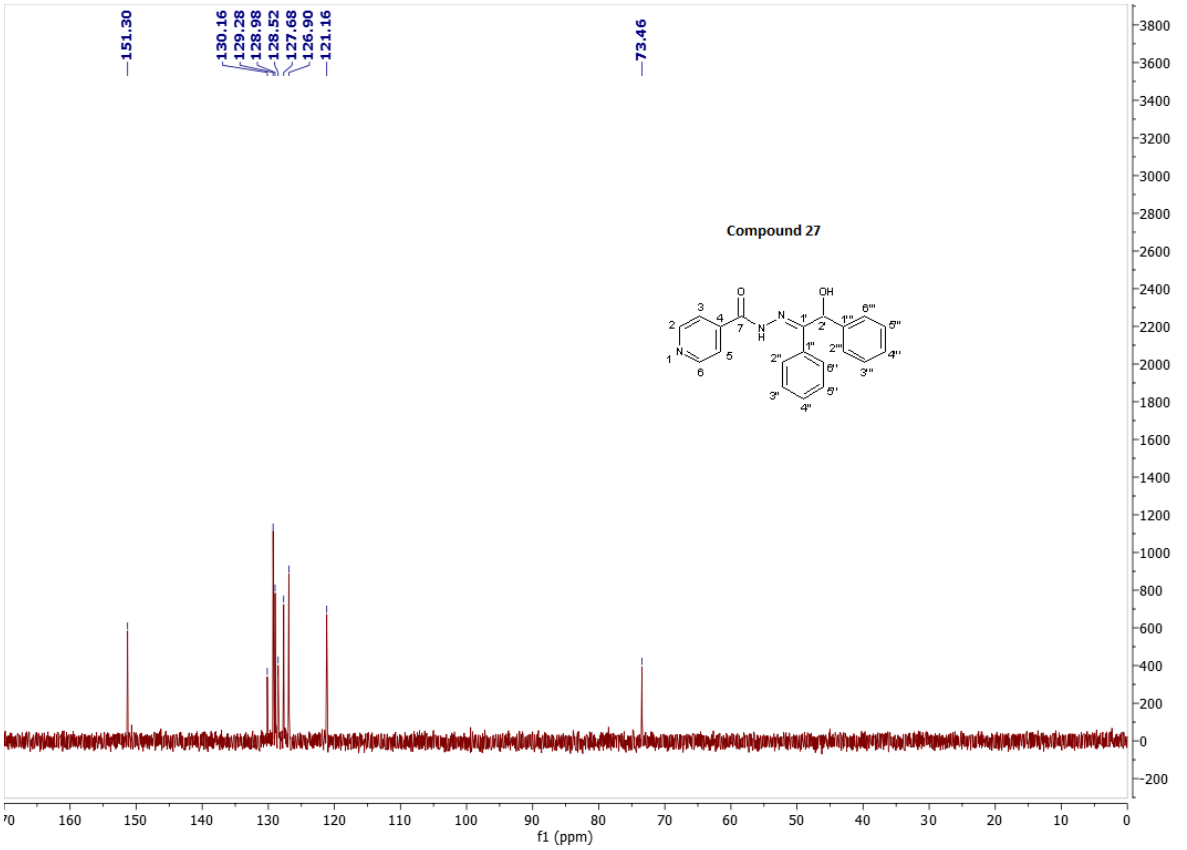
151.30
130.16
129.28
128.98
128.52
127.68
126.90
121.16
73.46
Compound 27
f1 (ppm)

Appendix 1b: ^{1}H, ^{13}C and DEPT-135 NMR Spectra of Compound **28**

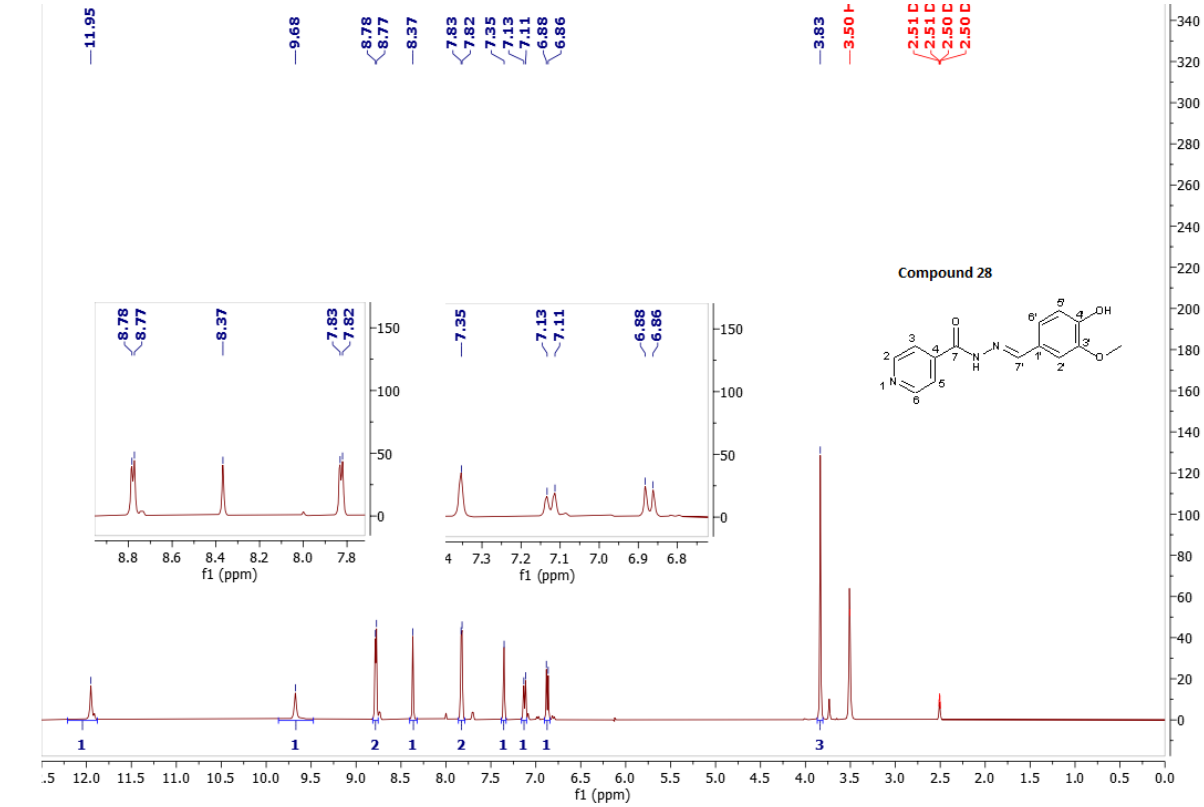

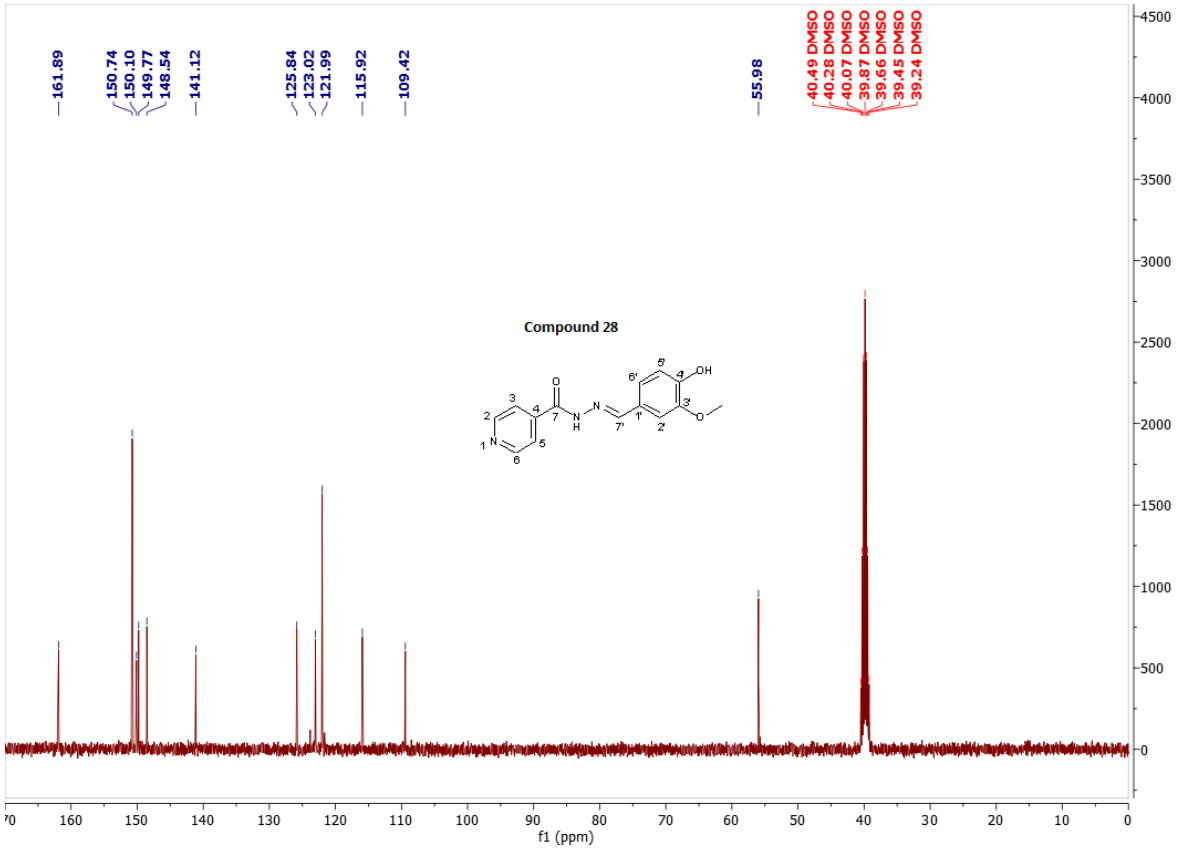

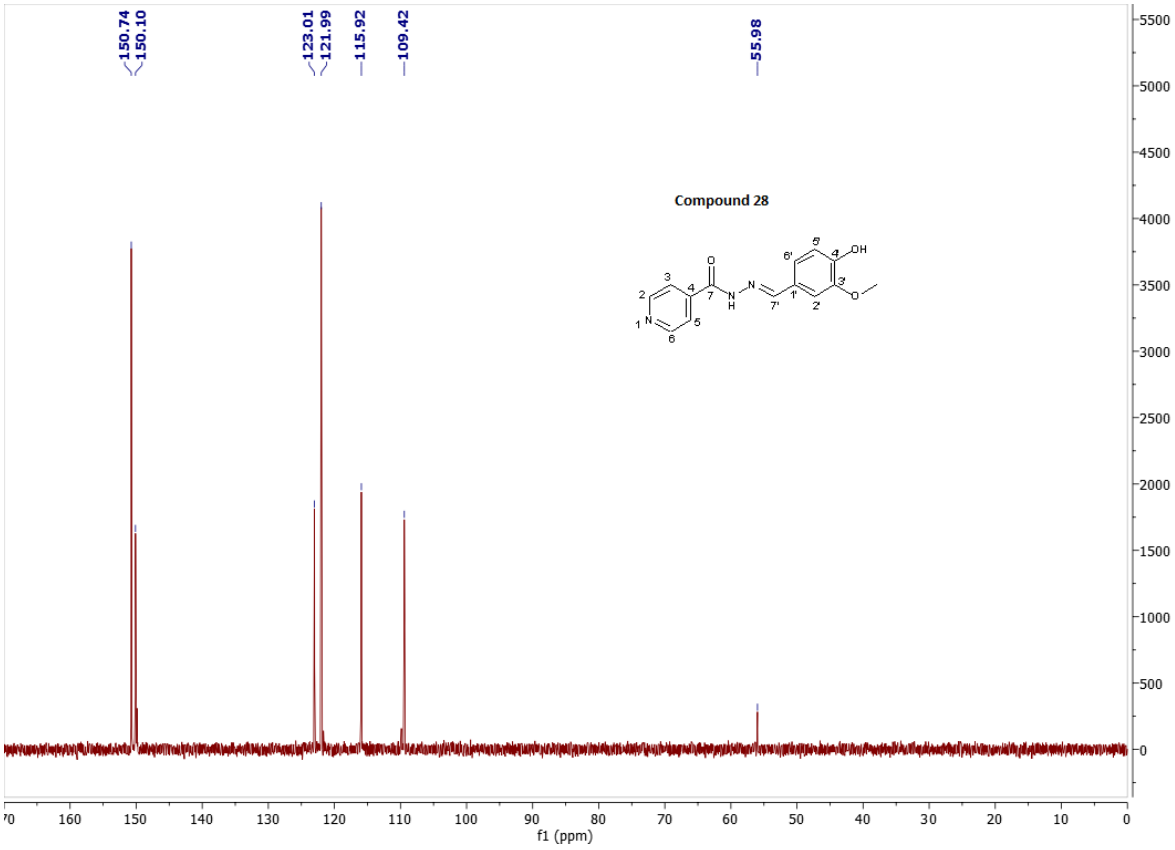

Appendix 1c: ^{1}H, ^{13}C and DEPT-90 NMR spectra of Compound **29**

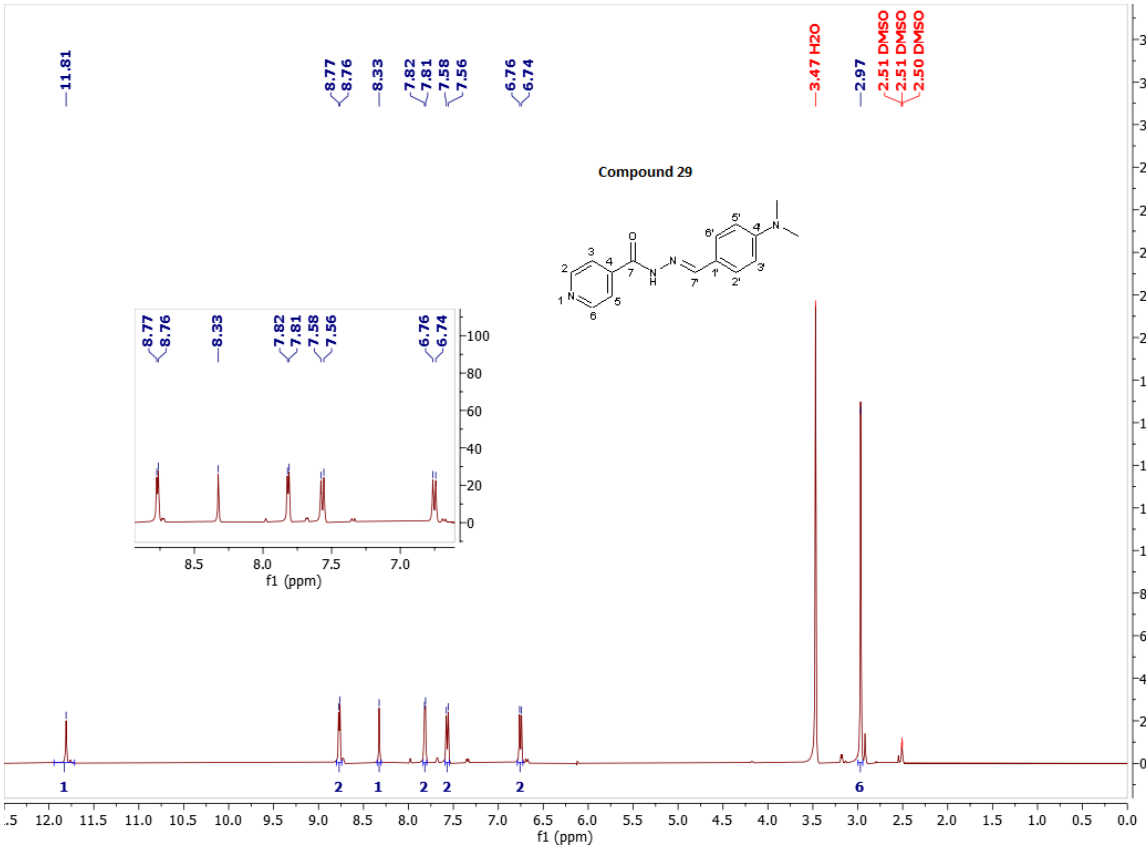

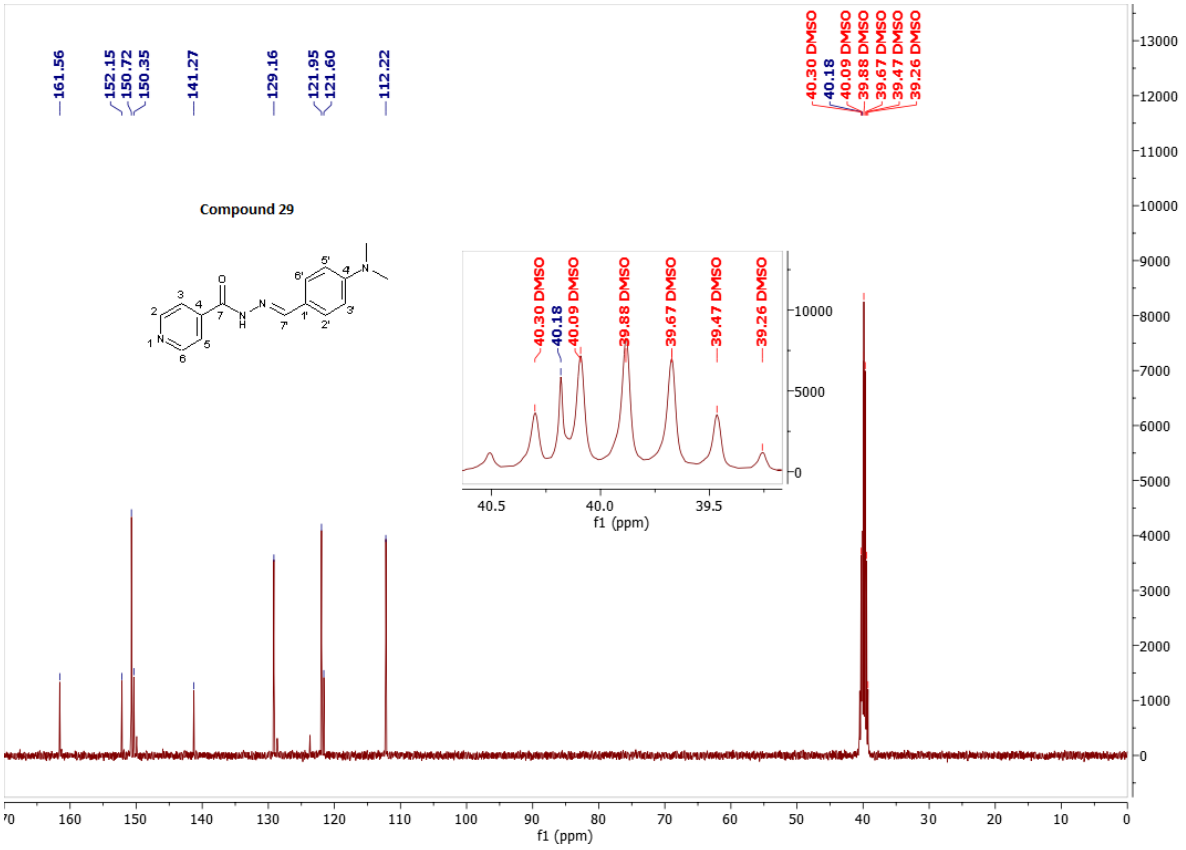
161.56
152.15
150.72
150.35
141.27
129.16
121.95
121.60
112.22
40.30 DMSO
40.18
40.09 DMSO
39.88 DMSO
39.67 DMSO
39.47 DMSO
39.26 DMSO
Compound 29
f1 (ppm)

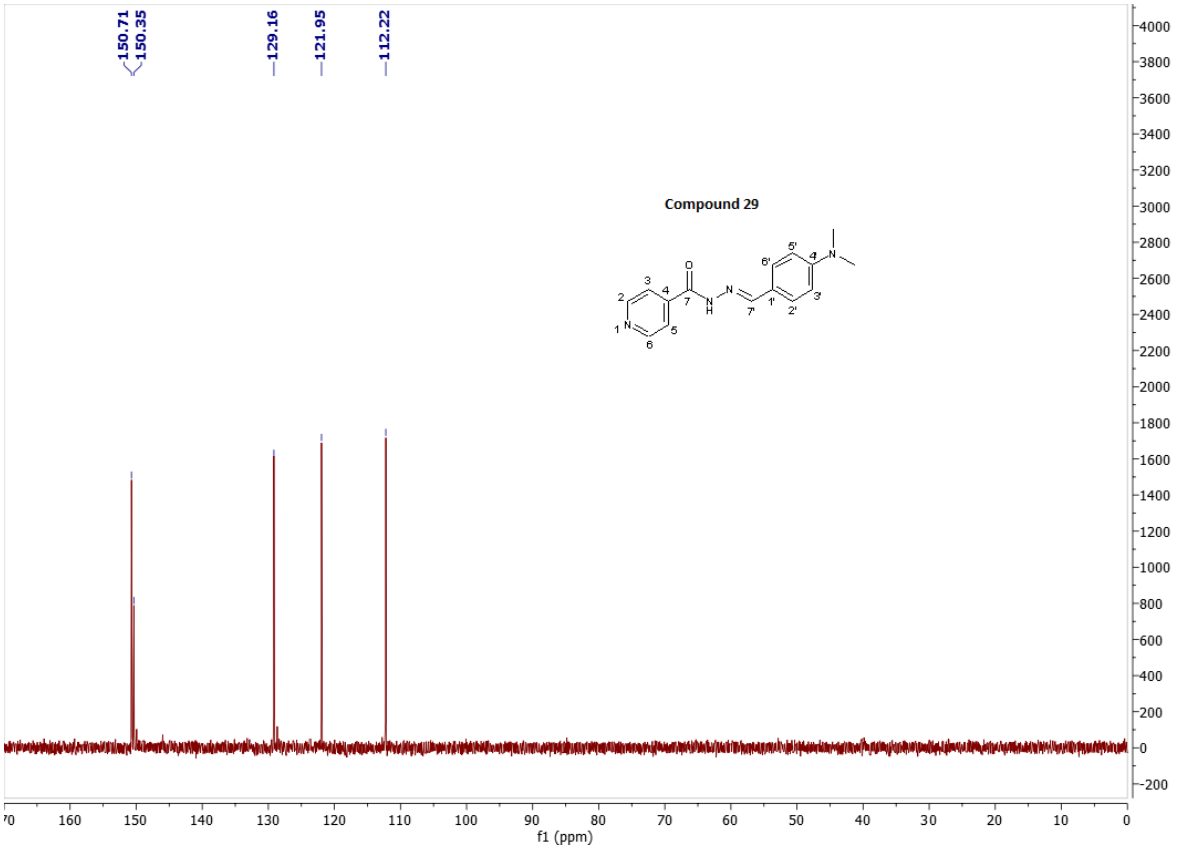
150.71
150.35
129.16
121.95
112.22
Compound 29
f1 (ppm)

Appendix 2: TLC Chromatograms of Synthesised Compounds

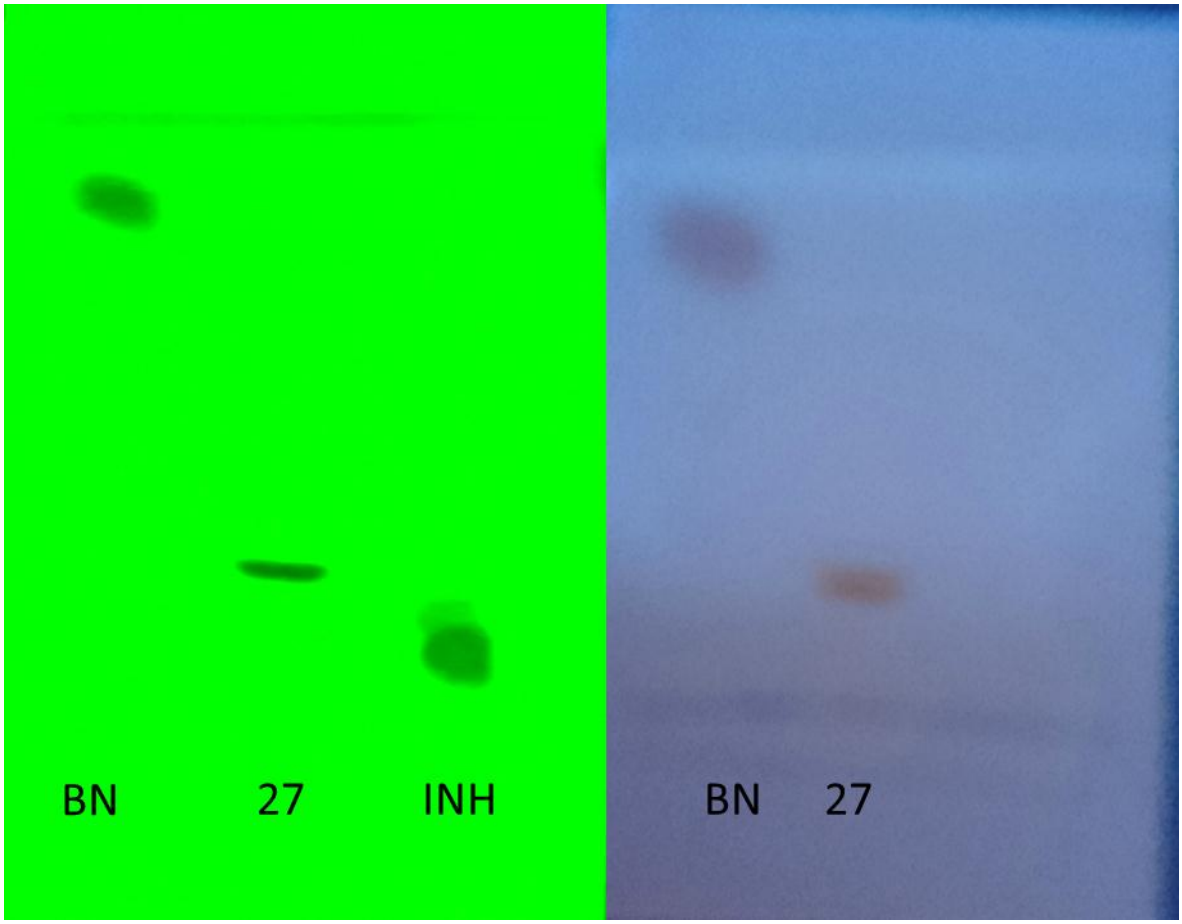

(A) **(B)**

Figure I: Normal phase TLC chromatogram of compound **27** viewed under UV -254(**A**) and UV-366(**B**) light sources with the solvent system $CHCl_3$: MeOH (7:1), BN=Benzoin, INH=Isonicotinic acid hydrazide

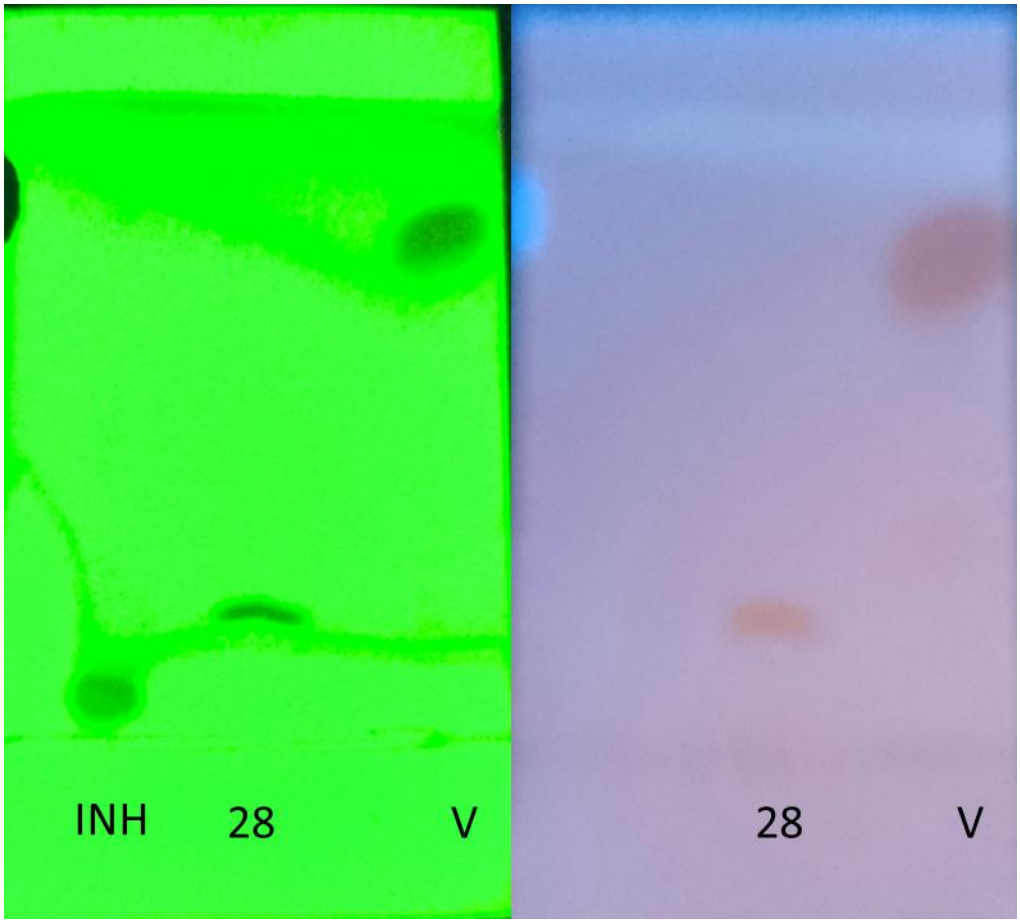

(A) **(B)**

Figure II: Normal phase TLC chromatogram of compound **28** viewed under UV-254 (**A**) and at UV-366(**B**) light sources using mobile phase $CHCl_3$: MeOH(7:1), INH= Isonicotinic acid hydrazide, V= Vanillin

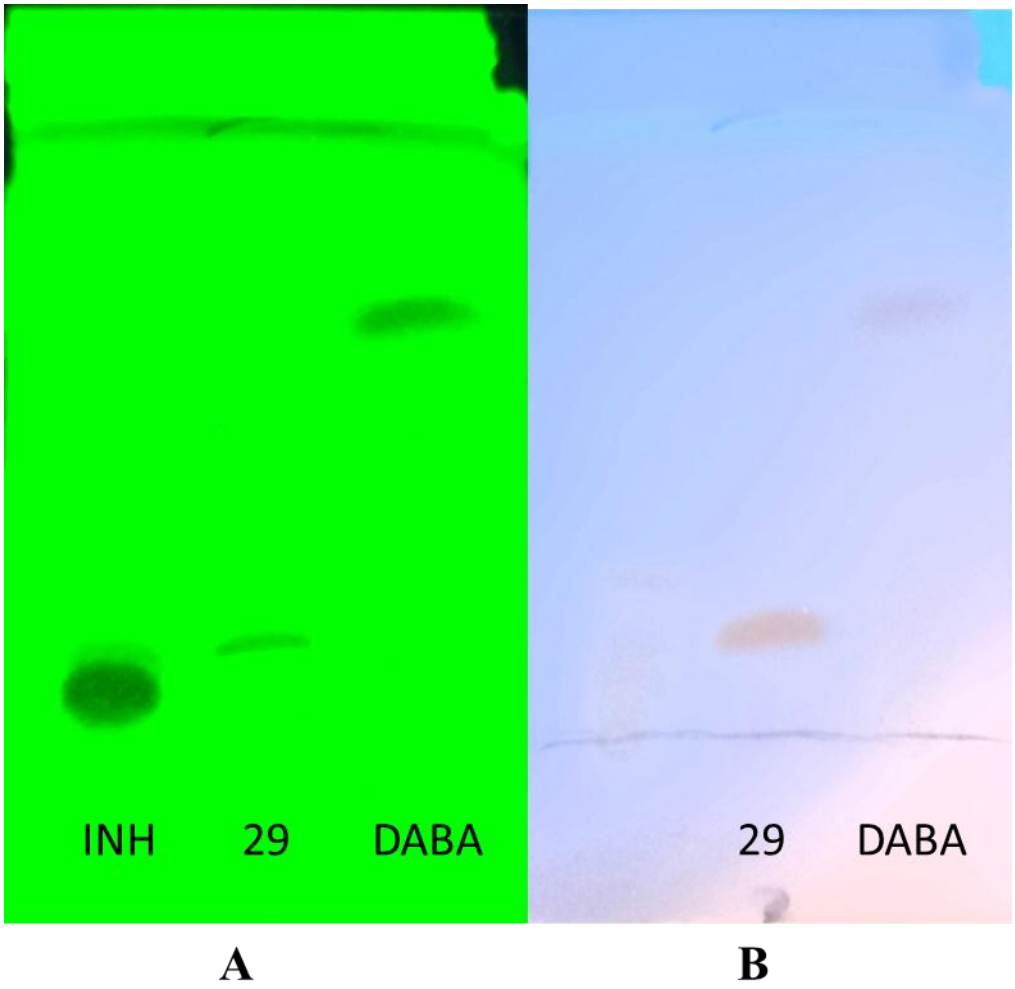

Figure III: Normal phase TLC chromatogram of compound **29** viewed under UV -254(**A**) and UV-366(**B**) light sources with the solvent system $CHCl_3$: MeOH (7:1), INH= Isonicotinic acid hydrazide, DABA= 4-(dimethylamino)benzaldehyde

Appendix 3: Binding Interaction of Synthesised Compounds with FabF of *E. coli* (PDB ID: 3HNZ)

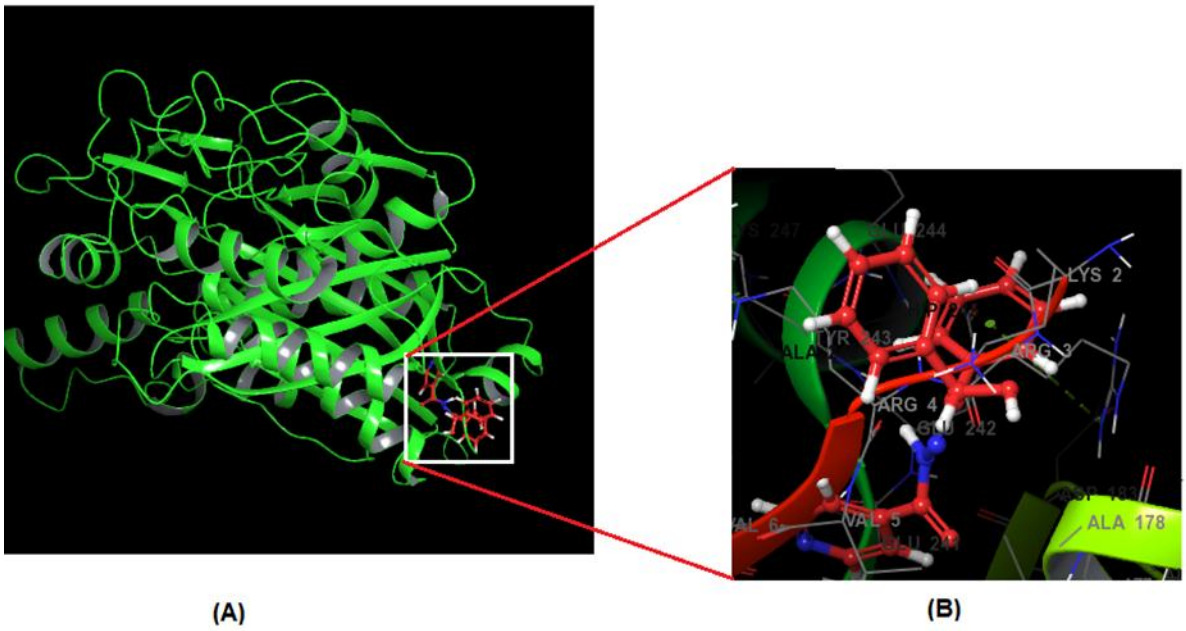

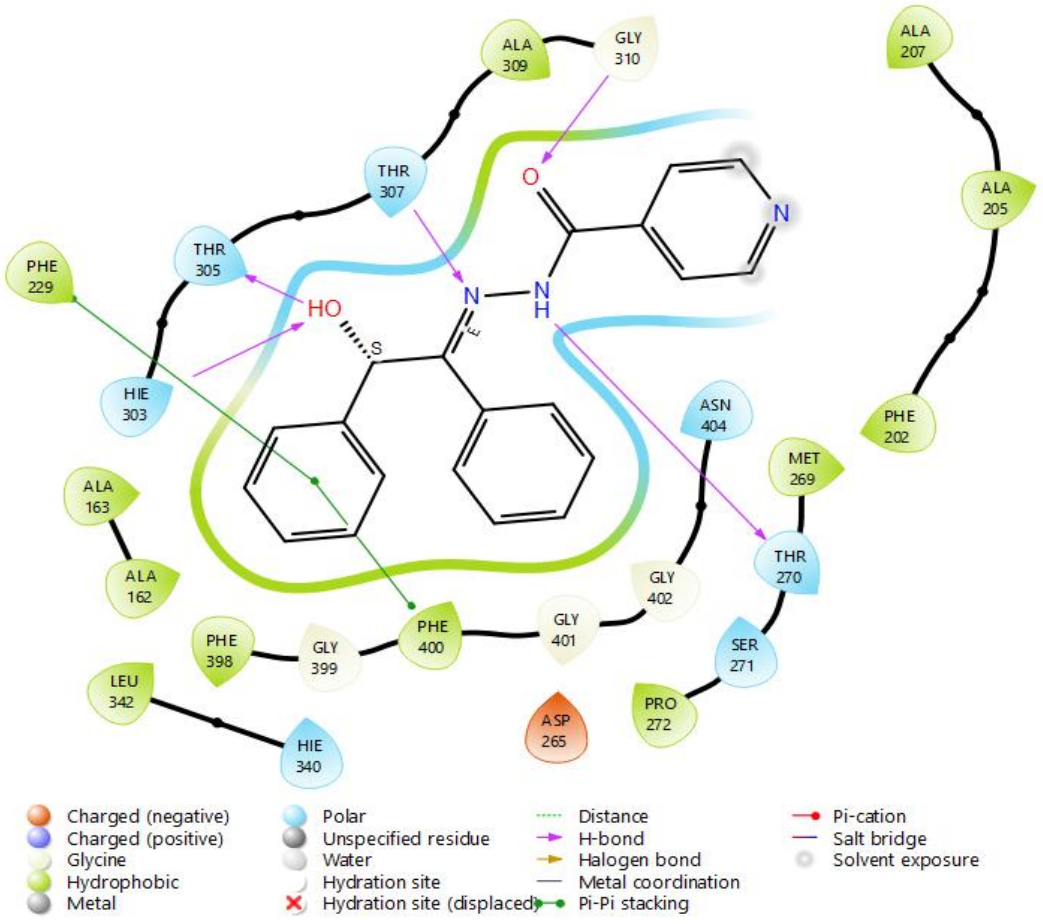

(C)

Figure IV: 3D and 2D interaction between compound **27** and *E. coli* FabF (PDB ID: 3HNZ)

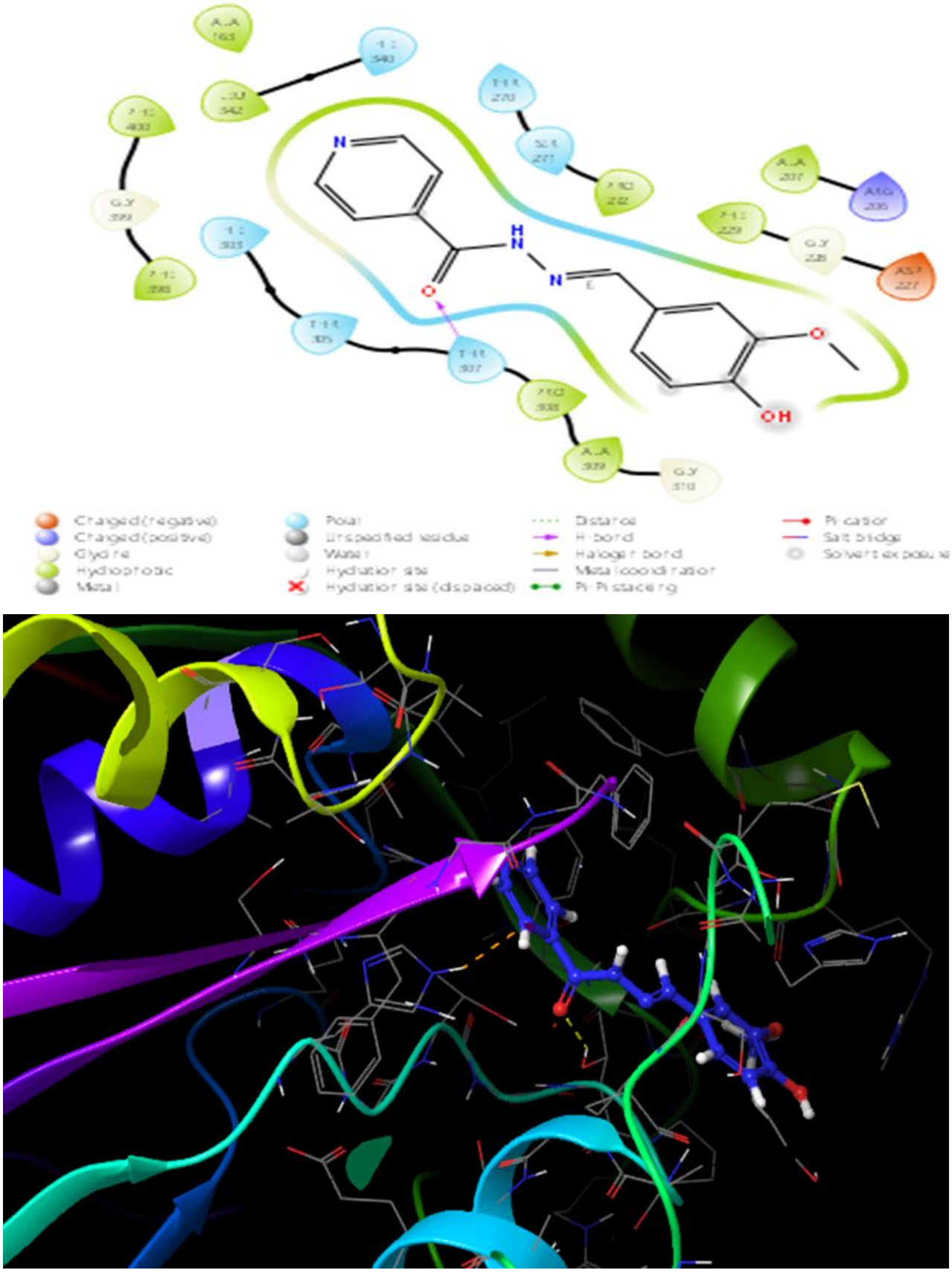

Figure V: 2D and 3D interaction between compound **28** and *E. coli* FabF (PDB ID: 3HNZ)

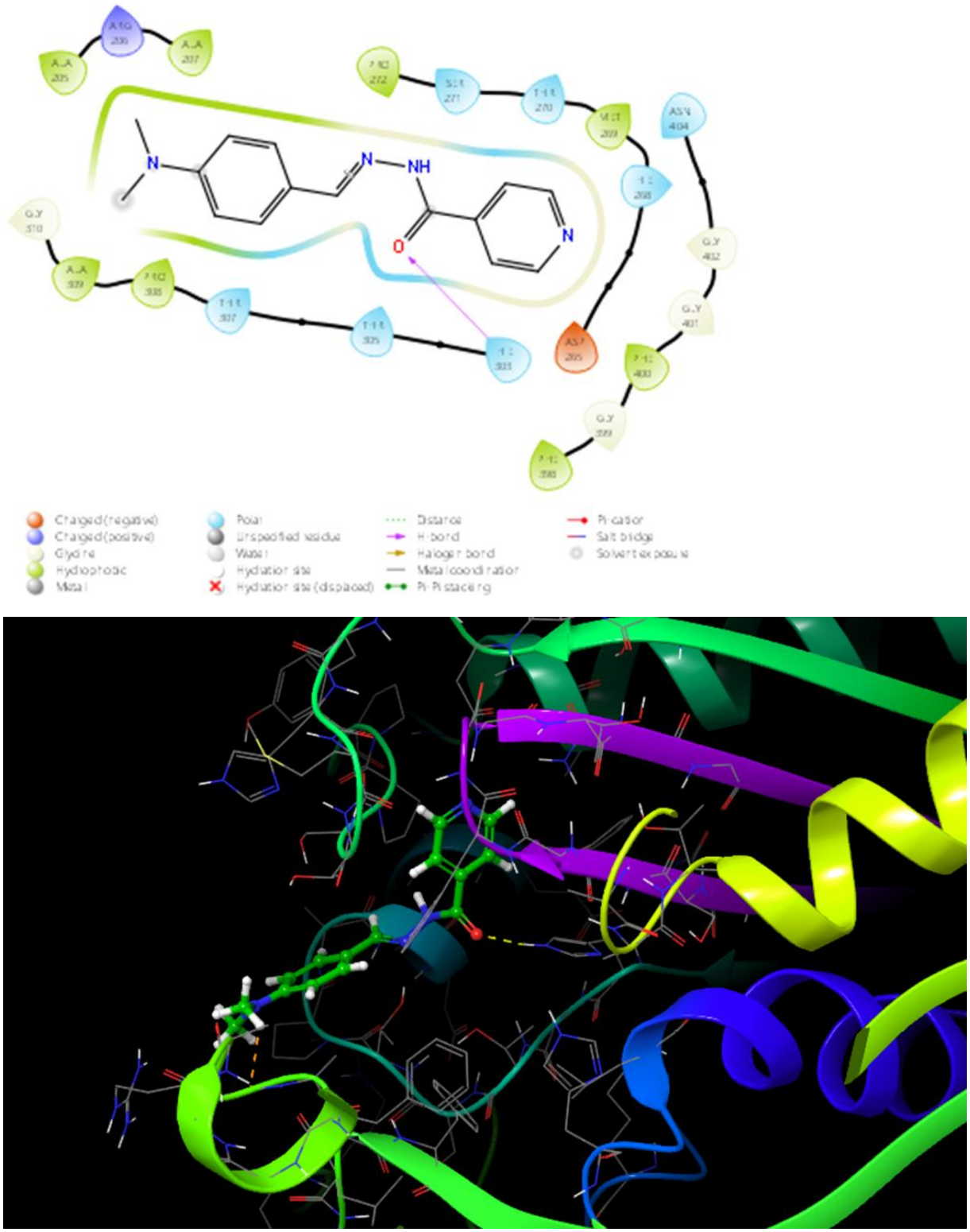

Figure VI: 2D and 3D interaction between compound **29** and *E. coli* FabF (PDB ID: 3HNZ)

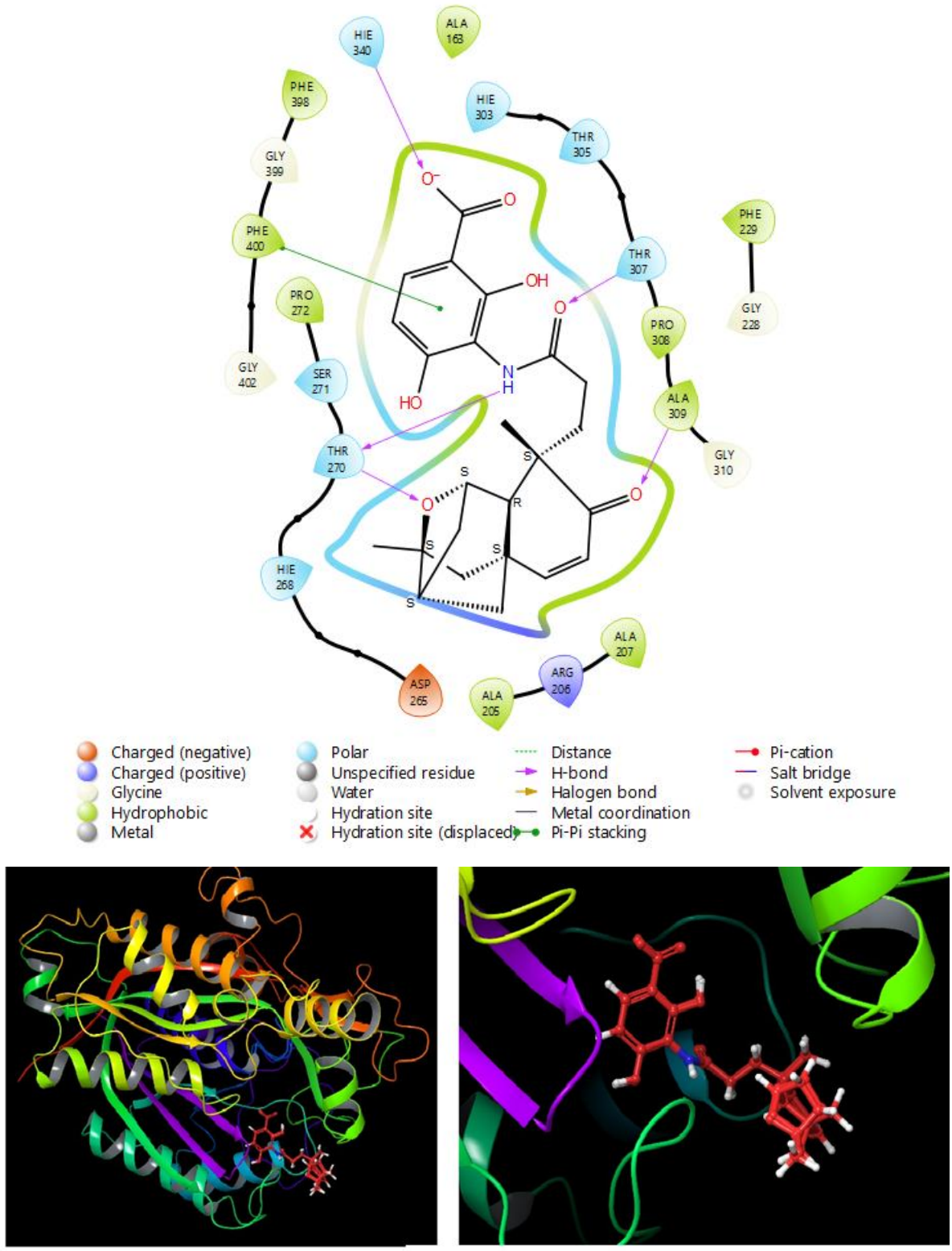

Figure VII: 2D and 3D interaction between platensimycin and *E. coli* FabF (PDB ID: 3HNZ)

Appendix 4: Draft Manuscript from This Thesis

Schiff Base Derivatives of Isonicotinic Acid Hydrazide: Synthesis, *In vitro* Antimicrobial and *In Silico* Studies

Mulugeta Ayele[1], Avijit Mazumder[2], Kaleab Asres[1] and Daniel Bisrat[1]

[1]Department of Pharmaceutical Chemistry and Pharmacognosy, School of pharmacy, College of Health Sciences, Addis Ababa University, Addis Ababa, Ethiopia;
[2]Department of Pharmaceutical Technology, Noida Institute of Engineering and Technology, 19 Knowledge Park II, Institutional Area, Greater Noida, 201306, India

Abstract

Infectious diseases present a substantial global health challenge, exacerbated by increasing antimicrobial resistance and the emergence of new pathogens. Addressing these ongoing challenges requires the development of potent drugs with strong antimicrobial activity. In drug development, compounds with diverse structures, such as Schiff bases, have demonstrated significant pharmacological effects. Isonicotinic acid hydrazide, used to treat tuberculosis caused by *Mycobacterium tuberculosis*, is limited in effectiveness against common Gram-positive and Gram-negative microbes. This study aimed to enhance the antimicrobial efficacy of isonicotinic acid hydrazide through structural modification via synthesis. Utilizing the conventional Schiff base synthesis method, three derivatives were synthesized, namely (E)-N'-(2-hydroxy-1,2-diphenylethylidene) isonicotinohydrazide (**27**), (E)-N'-(4-hydroxy-3-methoxybenzylidene) isonicotinohydrazide (**28**), and (E)-N'-(4-(dimethylamino)benzylidene)isonicotinohydrazide (**29**). Their chemical structures were determined through ^{1}H, ^{13}C-NMR, and DEPT-135 spectral data. The antimicrobial activity of these compounds was assessed against bacterial and fungal strains using disk diffusion and broth dilution methods. Compound **27** demonstrated the highest antibacterial activity, with notable effectiveness against *S. aureus* and comparable performance to ciprofloxacin. Compounds **28** and **29** also displayed antibacterial activity, along with antifungal activity against *C. albicans* and *A. niger*. Molecular docking analysis targeting FabF of *E. coli* predicted favorable ligand-protein interactions, emphasizing the potential of these synthesized compounds, particularly Schiff bases of isonicotinic acid hydrazide, in addressing bacterial and fungal infections.

Keywords: Antimicrobial resistance, isonicotinic acid hydrazide, Schiff bases, antimicrobial activity, *in silico* studies

1. Introduction

An infectious disease is characterized as an illness caused by a pathogen or its toxic product that spreads to a susceptible host via transmission from an infected person, infected animal, or contaminated inanimate object (Van Seventer and Hochberg, 2017). The impact of these illnesses varies widely across populations and regions, with low-income nations experiencing the most severe effects (Khabbaz *et al.*, 2014). For instance, in 2019, communicable diseases accounted for over half of all deaths in Africa (52.9%), 24.3% in the Eastern Mediterranean, and 22.6% in South-East Asia (World Health Statistics 2021)(WHO, 2021).

Schiff's bases (SB) are characterized by a group of compounds consisting of an azomethine group (-HC=N-) in their structures (Abirami and Nadaraj, 2014; Raczuk *et al.*, 2022). They are known to possess a wide range of biological activities due to the presence of bioactive azomethine core (Uddin *et al.*, 2020). Indeed, the azomethine group can be found in some marketed drugs, such as dantrolene, a muscle relaxant used for treatment of skeletal muscle spasticity (Krause *et al.*, 2004), nitrofurantoin, a drug used to treat uncomplicated UTI (Porreca *et al.*, 2021), furazolidone, a drug active against a broad spectrum of bacteria and *Giardia lamblia* (Phillips and Hailey, 1987).

Isonicotinic acid hydrazide (INH) is still one of the most important drugs for tuberculosis treatment (Fernandes *et al.*, 2017). Though INH is effective and potent drug with minimum inhibitory concentration (MIC) in the range of 0.03-.1µg/ml against *M. tuberculosis*, it shows limited action in latent mycobacteria and does not have antibacterial activity to non-mycobacterial species with no inhibition of growth observed even at the maximal concentration of drug tested (100 µM). The aim of this study was to synthesize and characterize some Schiff base derivatives of isonicotinic acid hydrazide, assess their *in vitro* antimicrobial activity, and conduct *in silico* studies.

2. Materials and Methods

2.1. Materials

2.1.1. Chemicals and Reagents

The following chemicals and reagents were used in this study: chloroform, ethyl acetate, methanol, ethanol, distilled water, glacial acetic acid, n-hexane (all Indenta, India), vanillin (BDH, England), INH (BDH, England), benzoin (BDH, England), and 4-

(dimethylamino)benzaldehyde (Hopkin & Williams, England). All the solvents were of analytical grade. The chemicals and reagents were used without further purification process.

3.1.2. Instruments

Nuclear Magnetic Resonance (NMR) spectra were recorded using 400 MHz for proton NMR (^{1}H-NMR) and 100 MHz for carbon-13 NMR (^{13}C-NMR) on a Bruker Avance DMX400 FT-NMR spectrometer (Bruker, Billerica, Massachusetts, USA), tetramethyl silane (TMS) as internal standard and deuterated dimethylsulfoxide (DMSO-d) was used as solvent.

3.2. Methods

3.2.1. Synthesis of Compounds

3.2.1.1 Synthesis of Compound 27

Compound **27** was synthesized via a SB condensation reaction. Benzoin solution was initially prepared by dissolving 2.122 g (0.01 mmol) of benzoin (2-hydroxy-1,2-diphenylethan-1-one) in 15 ml of methanol in a 250 mL round bottom reaction flask. 2 ml of glacial acetic acid was then added to a benzoin solution. Separately, 1.371g (0.01 mmol) of INH was dissolved in 15 ml of methanol in a separate beaker and gradually introduced into the above benzoin-glacial acetic acid solution. The mixture was refluxed for approximately 12 hrs at 80 ºC. The reaction progress was monitored using analytical TLC with chloroform: methanol (7:1) as a mobile phase. After the reaction completion, the mixture was left at room temperature to cool, and crystal growth was observed after 2 days. The crystals was separated, purified by washing with chloroform: methanol (1:1), and filtered using Whatman no.1 filter paper, yielding 0.701g (24%; yield, w/w).

3.2.1.2. Synthesis of Compound 28

Compound **28** was synthesized using the same procedure as described above, with INH and vanillin in the presence of glacial acetic acid.

3.2.1.3. Synthesis of Compound 29

Compound **29** was synthesized using a similar procedure as described above, with INH and 4-(dimethylamino)benzaldehyde (DABA) in the presence of glacial acetic acid.

3.2.3. Antimicrobial Activity Assay

3.2.3.1. Bacterial Strains

In vitro antibacterial assays were carried out against the following Grame-positive bacteria (GPB) strains: *Bacillus pumilus (B. pumilus)* 82, *B. subtilis* ATCC 6633, *S. aureus* ML 267, *S. aureus* MDR1 and *S. aureus* MDR2. The GNB strains used were: *E. coli* 3:37C, *E. coli* 7360,

E. coli 872, *E. coli* CD/99/1, *E. coli* K 88, *E. coli* T 37, *E. coli* ROW 7/12, *E. coli* 5933, *Salmonella enterica(S. enterica)* TD 01, *S. typhi* Ty2, *Shigella boydii(S. boydii)* D13629, *S. dysentery* 8, *Shigella flexneri(S. flexneri*)Type 6, *S. soneii* 1, *V. cholerae* NCTC 5596, *V. cholerae* NCTC 10732, *V. cholerae* NCTC 11501, *V. cholera* NCTC 4693, *E. coli* HB101, *E. coli* C600, and *P. aeruginosa* MDR 1. All the bacterial strains were procured from the Department of Technology, Jadavpur University; Central Drugs Laboratory, Kolkata and Institute of Microbial Technology, Chandigarh, India. The purity of the strains was checked according to the standard microbiological, cultural and biochemical tests prior to sensitivity tests against the test samples.

3.2.3.2. Fungal Strains

Antifungal activity testing was carried out on the following fungal pathogens: *A. niger* ATCC 6275, *C. albicans* ATCC 10231, *Penicillium funiclosum(P.funiclosum)* NCTC 287and *P. notatum* ATCC 11625. All the fungal strains were procured from Central Drugs Laboratory, Kolkata, India.

3.2.3.3. In Vitro Antibacterial Activity Test

In vitro antibacterial assay was screened by the disc diffusion method as described by Mitchell and Carter (Mitchell and Carter, 2000), by determining zones of inhibition produced by the test samples and comparing them with that of ciprofloxacin.

3.2.3.4. In Vitro Antifungal Activity Test

The antifungal potential of the test samples were screened by disc diffusion method (as described for the determination of antibacterial activity) against the fungal pathogens on Saborauds dextrose media. The Petri dishes were incubated at room temperature for 3 days and the diameter of zone of inhibition was measured in mm. Griseofulvin was used as a reference standard.

3.2.3.5. Determination of Minimum Inhibitory Concentration (MIC)

The MIC of the synthesised compounds were determined by the broth dilution method, as described by (Lalitha, 2004).

3.2.4. *In Silico* Studies

3.2.4.1. Molecular Docking Study

Molecular docking of the synthesized compounds was performed on the FabF-platensimycin co-crystallized enzyme of *E. coli* (PDB ID: 3HNZ) as potential targets for antibacterial activity using Maestro V.13.5 software by Schrodinger 2023-1 Suite. The docking results of all

synthesized compounds were subsequently compared to the redocked native ligands, namely, platensimycin.

Our molecular docking study comprised four essential steps: protein preparation, ligand preparation, receptor grid generation, and ligand docking.

3.2.4.2. Pharmacokinetic Prediction Study

Understanding the characteristics of absorption, distribution, metabolism, and excretion (ADME) is essential because most pharmaceuticals do not pass clinical trials. Using QikProp, GLIDE, Maestro V13.5, Schrödinger Suite 2023-1, the likeliness and ADME characteristics of the active compounds were ascertained.

4. Results and Discussion

4.1. Synthesis of compounds 27 to 29

Three compounds (**27**, **28** and **29**) were synthesized through a modified SB condensation reaction. This reaction involved INH and substituted aromatic aldehydes or ketones, with glacial acetic acid serving as a catalyst. The process led in the formation of imines (C=N bonds) through nucleophilic addition between an aldehyde or ketone and a primary amine compound in the presence of an acid catalyst. Physical properties of the synthesised compounds are presented in Table 1 as shown below.

Table 9: Physical properties data of synthesised compounds **27**, **28** and **29**

Compound	**Molecular Formula**	**Predicted MW(g/mol)**	**Physical State**	**Color**	**% Yield**	**R_f value**
27	$C_{20}H_{17}N_3O_2$	331.37	Crystal	Colorless	24	0.31
28	$C_{14}H_{13}N_3O_3$	271.27	Powder	Yellowish-white	92	0.21
29	$C_{15}H_{16}N_4O$	268.31	Crystal	Yellow	84	0.28

Solvent system: Chloroform: Methanol (7:1), TLC silica gel HF-254, R_f =Retention factor

4.1.1. Synthesis of Compound 27

Compound **27** was synthesized through an SB reaction involving INH and benzoin (2-hydroxy-1,2-diphenylethan-1-one) in the presence of glacial acetic acid. The reaction mechanism of compound **27** is illustrated in Scheme 1.

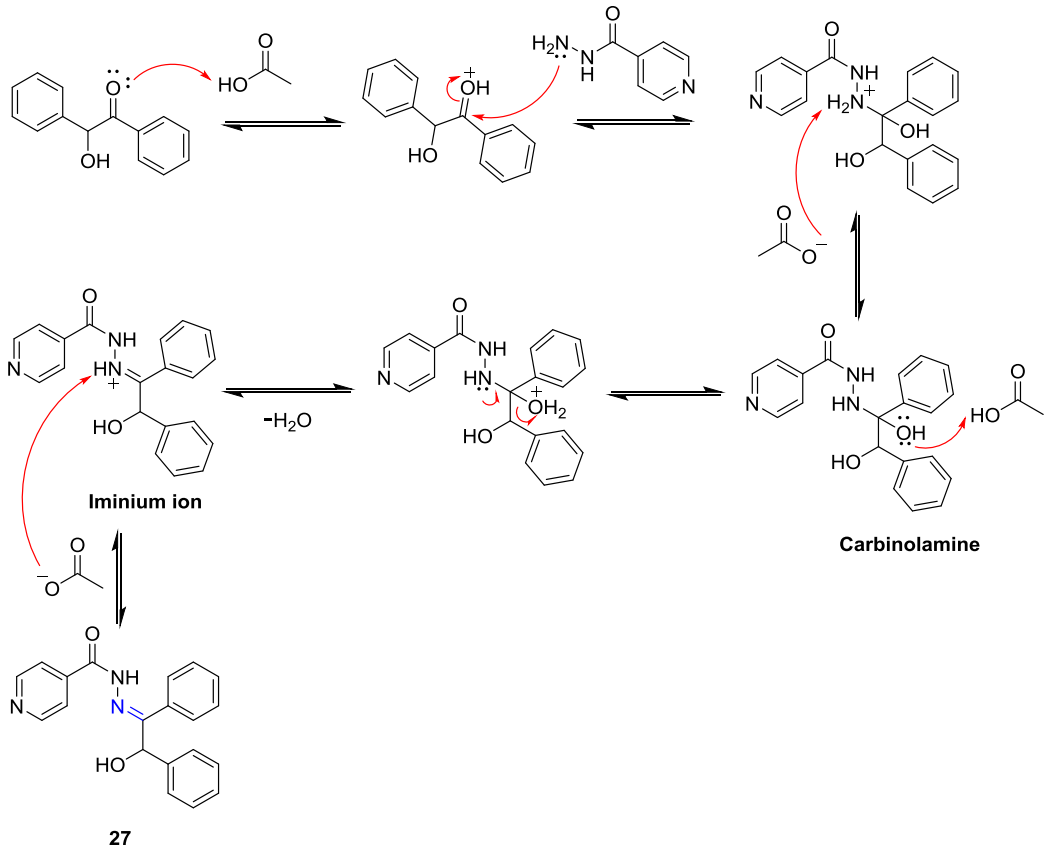

Scheme 1: Proposed mechanism of reaction for synthesis of compound **27**

4.1.2. Synthesis of Compound 28

Compound **28** was also synthesized through an SB reaction involving INH and vanillin (4-hydroxy-3-methoxybenzaldehyde) in the presence of glacial acetic acid. The reaction mechanism of compound **28** follows the same steps as previously outlined in the synthesis of compound **27**. Scheme 2 illustrates the reaction mechanism for compound **28**.

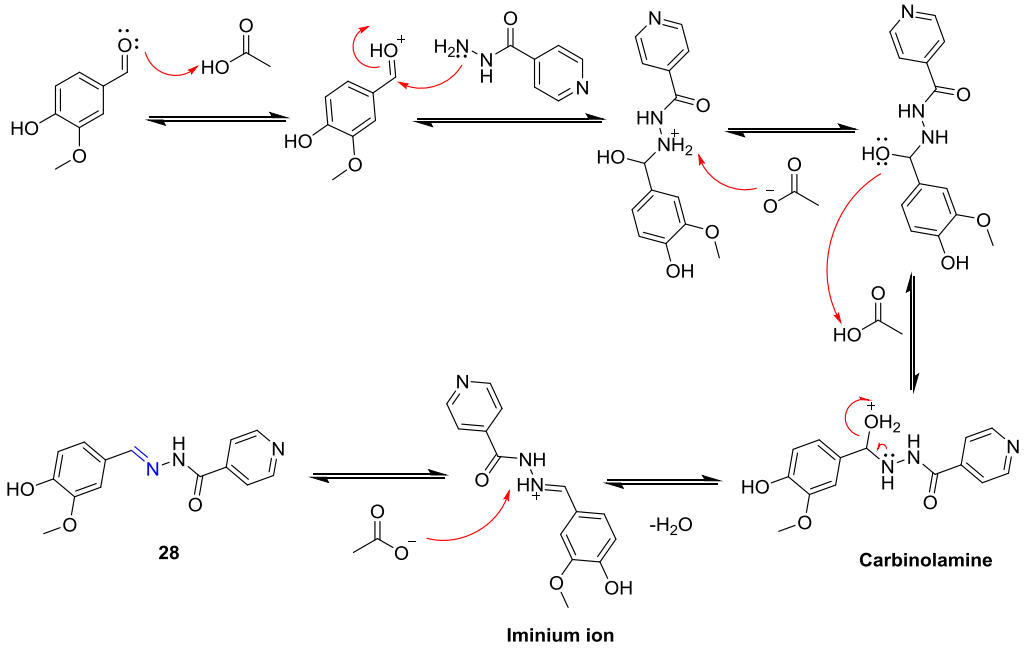

Scheme 2: Proposed mechanism reaction in the synthesis of compound **28**

4.1.3. Synthesis of compound 29

SB reaction between INH and DABA in the presence of glacial acetic acid led to the formation of compound **29**. The reaction mechanism for the synthesis of compound **29** closely resembles that of compounds **27** and **28**. Scheme 5 provides an illustration of the reaction mechanism for the synthesis of compound **29**.

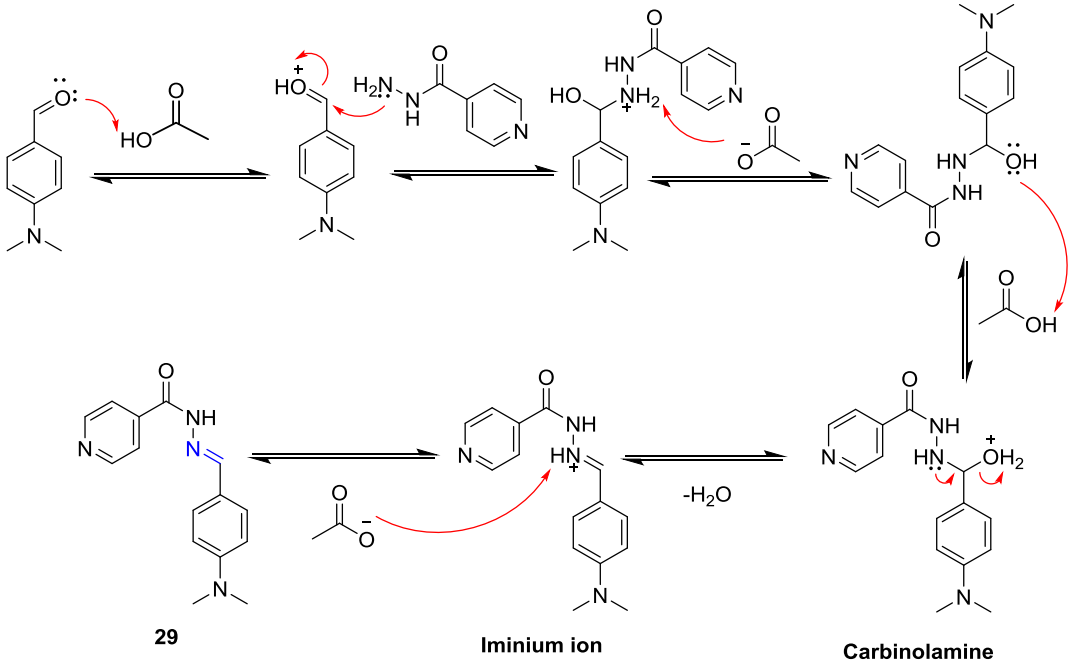

Scheme 3: Proposed mechanism of reaction for synthesis of compound **29**

4.2. Structural Elucidation of the Synthesized Compounds 27 to 29

Compounds **27** to **29** were characterized using ^{1}H, ^{13}C and DEPT-135 spectral data, and the results are presented in Table 2-4

Table 10: ^{1}H-NMR and ^{13}C-NMR spectral data of compound **27** in DMSO-d_6

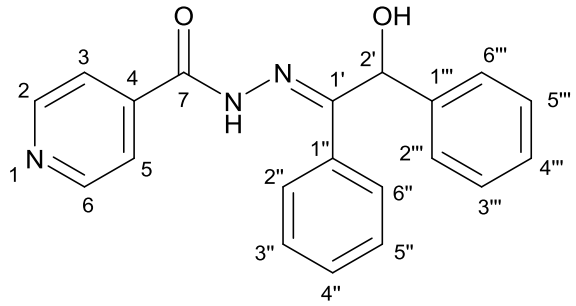

Compound **27**

Position	**δC(ppm)**	**δH(ppm)**
2, 6	151.30	8.81(*d*, J=5.0Hz, 2H)
3, 5	121.16	7.82(*d*, J=5.3Hz, 2H)
4	139.78	-
7(CONH)	160.96	12.88 (*s*, NH, 1H)
1′	155.45	-
2′	73.46	6.42 (*s*, 1H)
1″	136.51	-
2″, 6″	128.52	7.64(*d*, J=5.1Hz, 2H)
3″,5″,2‴, 6‴,4‴,3‴,5‴	128.97, 130.16, 126.90, 129.28, 127.68	7.46 – 7.26 (*m*, 8H)
1‴	140.78	-

Table 11: ^{1}H-NMR and ^{13}C-NMR spectral data of compound **28** in DMSO-d_6

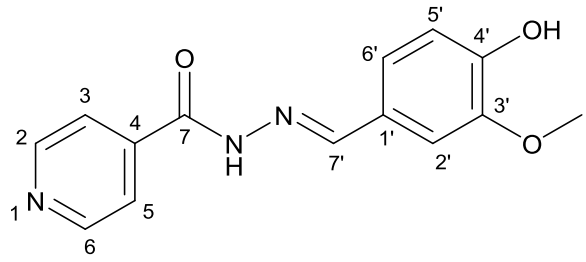

Compound **28**

Position	**δC(ppm)**	**δH(ppm)**
2, 6	150.74	8.78(*d*, J=4.5Hz, 2H)
3, 5	121.99	7.83(*d*, J=4.5Hz, 2H)
4	141.12	-
7(CONH)	161.89	11.95 (*s*, NH, 1H)
1′	125.83	-
2′	109.41	7.35 (*s*, 1H)
3′	148.54	-
3′(-OCH_3)	55.98	3.84(*s*, CH_3, 3H)
4’(Ar-OH)	150.10	9.68 (*s*, Ar-OH, 1H)
5′	115.92	6.87(*d*, J= 8.1Hz, 1H)
6′	123.02	7.12(*d*, J=8.1Hz, 1H)
7′	149.77	8.37 (*s*, 1H)

The ^{1}H-NMR spectrum revealed signals at δ 6.75 (2H, d, J=8.6 Hz) and δ 7.57 (2H, d, J=8.6 Hz), confirming the presence of a para-disubstituted benzene group. The ^{13}C-NMR and DEPT-90 spectral data for compound **29** displayed ten signals corresponding to 10 sets of carbon atoms (CH_3 (x2), 5CH (9), and 4C). The chemical shifts for ^{1}H and ^{13}C-NMR are listed in Table 4.

Table 12: ^{1}H-NMR and ^{13}C-NMR spectral data of compound **29** in DMSO-d_6

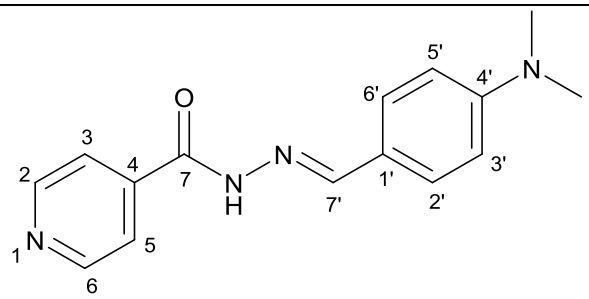

Compound **29**

Position	**δC(ppm)**	**δH(ppm)**
2, 6	150.72	8.77(*d*, J=4.8Hz, 2H)
3, 5	121.95	7.82(*d*, J=4.6Hz, 2H)
4	141.27	-
7(CONH)	161.56	11.81 (*s*, NH, 1H)
1′	121.60	-
2′, 6′	129.16	7.57 (*d*, J = 8.6 Hz, 2H)
3′, 5′	112.22	6.75 (*d*, J = 8.6 Hz, 2H)
4′	152.15	-
4′(N-(CH_3))$_2$	40.18	2.97 (*s*, 6H)
7’	150.35	8.33(*s*, 1H)

4.3. Antimicrobial Activity of Compounds 27 to 29

4.3.1. Antibacterial Activity

The synthesized compounds were tested *in vitro* antibacterial activity against 26 bacterial strains, including five GPB with two different MDR *S. aureus* serotypes(*S. aureus*, *B. subtilis*, *B. pumilus*, *S. aureus* MDR1, and *S. aureus* MDR2) and 21 GNB with 10 serotypes of *E. coli* and 4 different serotypes of *V. cholerea* (*E. coli*, *S. typhi*, *S. enterica*, *S. dysentery*, *S. sonei*, *S. boydii*, *S. flexneri* and *V. cholera*, *E. coli* HB101, *E. coli* C600, *S. aureus* MDR 1, *S. aureus* MDR 2, and *P. aeruginosa* MDR 1) using the disc diffusion method.

It's interesting to note that, as shown in Table 5, all compounds showed notable activity against every tested strain of bacteria, with MIC values ranging from 25 µg/ml to 400 µg/ml. Compound **29**, with MIC of 10µg/ml, was discovered to be the most potent antibacterial agent against *P. aeruginosa* MDR 1. At 200µg/ml concentration, compound **29** exhibits a greater zone of inhibition (13.5mm) against *S. aureus* MDR 1 in comparison to the standard drug, ciprofloxacin (11.5mm).

Table 5: Zone of inhibition (ZOI) and minimum inhibitory concentration (MIC) of the synthesized compounds against the tested bacterial strains

Bacterial strains	ZOI in mm(200µg/ml)				MIC(µg/ml)		
	Cpd **27**	Cpd **28**	Cpd **29**	Cipro	Cpd **27**	Cpd **28**	Cpd **29**
E. coli NCTC 5933	13.0	14.0	14.0	16.0	50	25	25
E. coli K88	13.5	14.0	14.5	17.0	50	25	25
E. coli NCTC 7360	14.0	14.5	14.5	17.0	50	25	25
E. coli LT37	13.0	15.0	13.5	16.0	50	25	25
E. coli 872	13.0	14.5	14.0	16.0	50	25	25
E. coli ROW 7/12	13.5	13.0	14.5	16.5	50	25	25
E. coli 3:37C	13.0	13.5	14.0	16.5	50	25	25
E. coli CD/99/1	13.5	15.0	15.0	17.0	50	25	25
E. coli HB101	13.0	12.0	13.5	14.0	50	50	25
E. coli C600	12.0	12.5	11.5	13.5	50	50	25
S. typhi Ty2	14.0	14.0	13.0	16.0	50	100	100
S. enterica TD 01	15.0	14.5	13.5	19.0	50	100	100
S. dysentery 8	14.5	14.0	13.5	20.0	50	100	100
S. soneii 1	14.0	14.0	13.0	19.5	50	50	100
S. boydii D13629	13.5	12.5	14.0	20.0	100	50	100
S. flexneri Type 6	13.0	12.5	14.0	20.5	100	50	100
S. aureus ML 267	17.0	15.0	16.0	18.0	25	50	50
S. aureus MDR 1	10.5	10.0	13.5	11.5	100	400	100
S. aureus MDR 2	11.0	10.0	11.0	12.0	100	400	100
B. pumilus 82	8.0	7.5	8.0	19.0	400	400	400
B. subtilis ATCC 6633	8.0	7.5	8.0	18.0	400	400	200
V. cholerae NCTC 4693	13.0	12.0	15.0	17.5	50	50	50
*V.cholerae*NCTC5596	13.0	12.5	14.0	18.5	50	50	50
V. cholerae NCTC 10732	13.0	13.0	14.5	19.0	50	50	50
V. cholerae NCTC 11501	13.5	12.0	14.0	18.5	50	50	50
P. aeruginosa MDR 1	11.0	11.0	12.0	12.5	50	100	10

Cpd = Compound, Cipro = Ciprofloxacin, MDR= Multidrug resistant

In the case of *S. aureus* ML 267, compound **27** has nearly closed to the standard drug ciprofloxacin (18 mm) in the zone of inhibition (17 mm) at a concentration of 200µg/ml. *S. aureus* is the main culprit behind skin and soft tissue infections, including cellulitis, furuncles, and abscesses (boils)(Ikuta *et al.*, 2022). Their MIC of 400µg/ml indicates that they are all very weakly active against *B. pumilus* 82. Furthermore, compound 28 exhibits very little activity (MIC value 400µg/ml) against *B. subtilis* ATCC 6633, *S. aureus* MDR 1, and *S. aureus* MDR 2. Compound **27** exhibits weak activity (MIC 400µg/ml) against *B. subtilis* ATCC 6633 in a similar manner. *B. subtilis* is a Gram-positive spore-forming bacterium. *B. subtilis* has been linked to septicemia, pneumonia, endocarditis, wound infection, and intraocular inflammation, in addition to meningitis (Tokano *et al.*, 2023).

4.3.2. Antifungal Activity

The fungi tested in the present study were shown to have good susceptibility to all the three compounds. Among the fungal strains tested, *C. albicans*, the primary fungal agent that causes nosocomial invasive candidiasis globally (Bongomin *et al.*, 2017), was found to be more susceptible (MIC = 200–800 μg/ml) to the test compounds than the other fungal pathogens. Among the compounds, compound **27** has better zone of inhibition than the remaining compounds. Moreover, compound **27**(at 13.5mm diameter) shows greater zone of inhibition than the standard drug griseofulvin (13.0 mm diameter) against *P. notatum* ATCC 11625 and equal zone of inhibition to griseofulvin against *P. funiculosum* NCTC 287.

Table 13: Zone of inhibition (ZOI) and minimum inhibitory concentration (MIC) of the synthesized compounds against the tested fungal strains.

Fungal strain	ZOI in mm(1500μg/ml)				MIC (μg/ml)		
	Cpd **27**	Cpd **28**	Cpd **29**	Gris	Cpd **27**	Cpd **28**	Cpd **29**
C. albicans ATCC 10231	11.5	12.5	13.0	15.0	800	400	400
A. niger ATCC 6275	12.5	12.0	13.0	14.5	800	400	400
P. notatum ATCC 11625	13.5	11.5	10.5	13.0	800	800	1000
P. funiculosum NCTC 287	13.0	12.0	10.0	13.0	400	800	1000

Cpd = Compound, Gris = Griseofulvin

Furthermore, compound **27** shows good MIC (400μg/ml) against *P. funiculosum* NCTC 287 and has equal zone of inhibition (13.0mm) to the standard drug griseofulvin. Compound **28** has greater zone of inhibition (13.5mm) than the positive control griseofulvin (13.0mm) against *P. notatum* ATCC 11625.

4.4. *In Silico* Studies

4.4.1. Molecular Docking of Synthesised Compounds

The primary goal of the *in silico* studies is to save time and money by avoiding needless costs associated with biological assays of compounds with a high likelihood of presenting future pharmacokinetic problems, as these parameters have an impact on pharmacokinetic properties (Brito, 2011). In this study, we evaluated the antibacterial target potential of synthesized compounds by comparing their docking scores with the redocked native ligand platensimycin (compound **25**). The binding affinity of these synthesized compounds with the *E. coli* FabF protein (PDB ID: 3HNZ) was determined using Schrödinger software. Additionally, the well-known inhibitor platensimycin was redocked to validate the docking protocol on the energy-minimized fatty acid synthase enzyme of *E. coli*. The docking scores for compounds **27-29** and

redocked platensimycin are presented in Table 7, where a more negative score indicates a stronger binding between the ligand and its target.

Table 14: Docking scores of the synthesised compounds with 3HNZ as predicted by Schrodinger 2023 suite docking software

Ligand	Binding energy (Kcal/mol) with **3HNZ**
Platensimycin(25)	**-9.345**
27	**-8.665**
28	**-5.123**
29	**-5.070**

In Table 7, it is evident that compound **27** achieved the highest docking score (-8.665 kcal/mol) at the active binding site of the *E. coli* enzyme 3HNZ, followed by compound **28** (-5.123 kcal/mol) and compound **29** (-5.070 kcal/mol). Figure 9 illustrates the 3D and 2D interactions between compound **27** and the *E. coli* FabF (PDB ID: 3HNZ). Compound **27** demonstrated favourable interactions with FabF binding sites, forming five hydrogen bonds with amino acid residues THR-270, THR-305, THR-307, HIE-303, and GLY-310 (Figure 9(C)). Additionally, compound **27** also exhibited pi-pi stacking interactions with amino acid residues PHE-400 and PHE-229 in the FabF subunit, enhancing its strong interaction with the enzyme.

Compounds **28** and **29** also exhibited favourable interaction with the active site of the FabF enzyme, each forming a hydrogen bond. Specifically, the amide oxygen of compound **28** formed a hydrogen bond with THR-307, while the amide oxygen of compound **29** formed a hydrogen bond with HIE-303 amino acid residue within the active site of the FabF enzyme. It is also noted that aside from these hydrogen bonds, neither compound **28** nor **29** displayed any other significant interactions with the enzyme's active site.

The binding model presented here suggests that these SB derivatives of INH (compounds **27-29**) act as inhibitors of FabF, emphasizing crucial structural elements that need consideration for future optimization efforts.

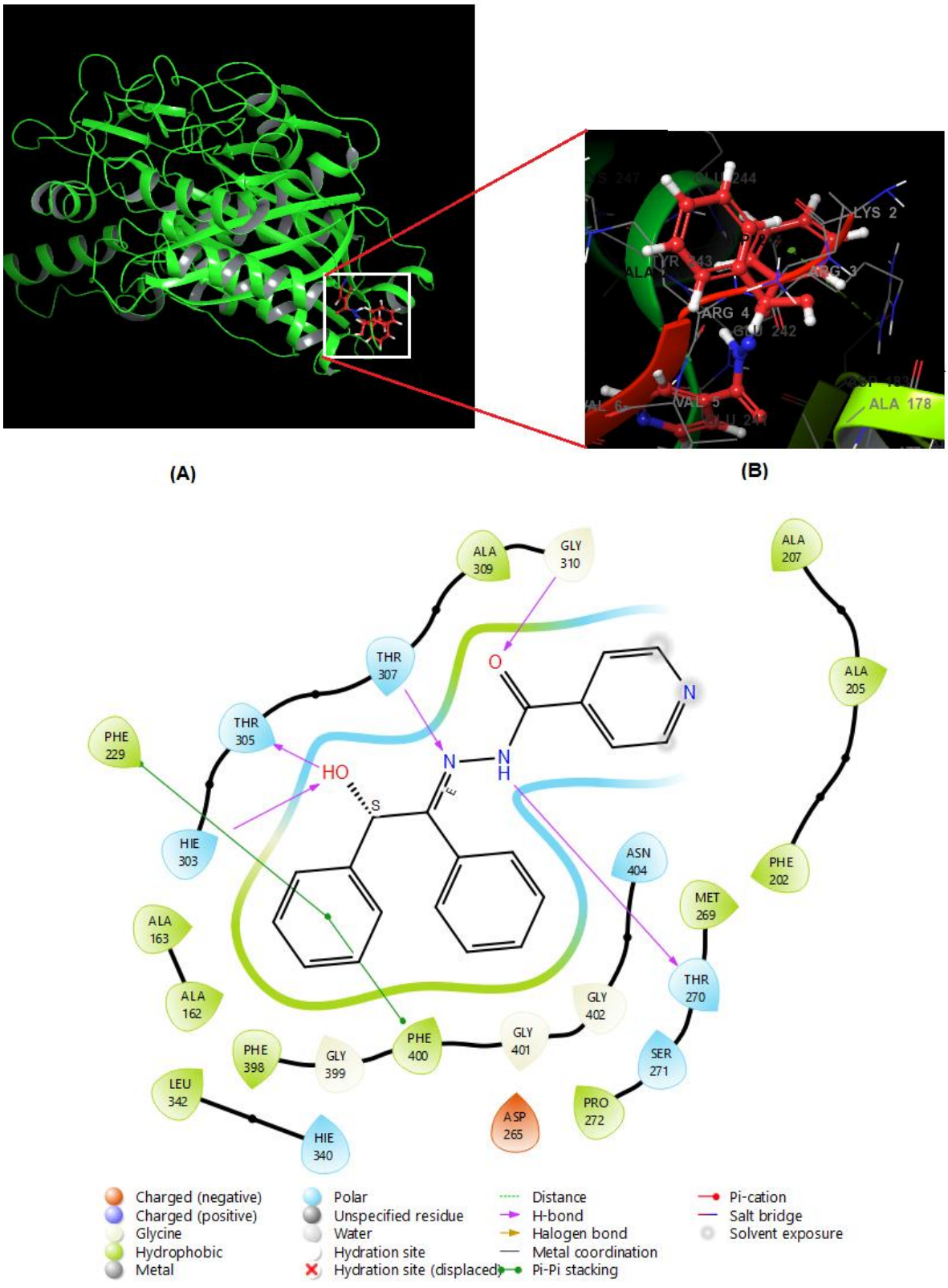

(C)

Figure 3: 3D and 2D interaction between compound **27** and *E. coli* FabF (PDB ID: 3HNZ)

4.2.2. Pharmacokinetic Prediction of Synthesized Compounds

The popular ADME analysis is a crucial analysis that explains how a pharmaceutical compound is disposed of inside an organism and, consequently, affects the pharmacological activity of that compound (Mali and Chaudhari, 2019). We used Maestro V.13.5's Qikprop (ligand-based ADME analysis) module for this investigation, which offers ranges for comparing a given molecule's properties with those of 95% of known drugs (Mali and Chaudhari, 2018). Our compounds submit to an ADME analysis and the compounds exhibit good drug-like qualities, and Lipinski's rule of five violation was not seen (as shown in Table 8). A drug candidate's molecular weight, QPlogPo/w (which predicts octanol/water partition coefficient), QPPCaco (which predicts permeability of a molecule for the gut-blood barrier through passive transport), percentage of oral absorption by humans, and the number of H-bonds the solute molecule would donate to the water molecules in the aqueous solution (donor HB) are just a few of the critical properties that must be taken into account. The theoretical drug-like behavior of these compounds is suggested by the ADME analysis results, which are very encouraging and may help with additional laboratory research on them.

Table 15: ADME data of synthesised compounds calculated using Qik Prop Simulation

Ligand	MW	QPlogPo/w	Accept HB	Donor HB	QPlogBB	QPPCaco	Human oral absorption	Ro5
27	331.373	3.420	5.2	2	-1.101	589.426	3	0
28	271.275	1.863	5.5	2	-1.225	398.688	3	0
29	268.318	2.944	5	1	-0.724	1144.936	3	0

MW, not more than 500 Da, QPlogPo/w(accepted range -2.0 – 6.5), (Hydrogen bond donor (Accepted Limit: ≤ 5), Hydrogen bond acceptor (Accepted Limit: ≤ 10), Log P less than 5, Human oral absorption – 1, 2, or 3 for low, medium, or high, QPlogBB range from -3.0 to 1.2, QPPCaco(<25 poor, >500 great), Ro5(not violating more than 1)

INH has been the primary drug for treating tuberculosis for over 60 years. However, its antibacterial effectiveness against non-mycobacterial species is limited, and it also shows weak antifungal activity (Fernandes et al., 2017; Hegde *et al.*, 2021). Numerous studies have explored the antibacterial and antifungal properties of SB derivatives from hydrazides. This has prompted us to design, synthesize, and evaluate the antimicrobial activities of SB derived from INH. The synthesized compounds showed interesting antimicrobial activity which can be potentially used for further *in vivo* studies. Moreover, molecular docking of the derivatives on FabF enzyme of *E. coli* has been done using Schrodinger docking software and the results demonstrate that the selected enzyme is a promising target for the compounds.

One of the vital FAS-II enzymes, FabF, is unique to the prokaryotic kingdom and is necessary for all bacterial species to survive. When it is inhibited, FAS is disrupted, which leads to cell

death (Davies *et al.*, 2000; Wang *et al.*, 2006; Belete, 2019). Because it is essential for bacterial survival, FabF gained interest as a target for antibacterial drugs (Wang et al., 2006). Considering that the compounds that were synthesized showed promising antimicrobial activity, we felt it was appropriate to elucidate the likely mechanism of action. The 2.6-A° structure of *E. coli* FabF in complex with platensimycin reveals that the antibiotic binds to the malonyl subsite of FabF, and the active-site histidine residues (HIE 303 and HIE 340) of the conserved HIS-HIS-CYS catalytic triad are critical residues. In addition, the side chain of THR 307, the amide carbonyl of THR 270, and ALA 309 play important roles in hydrogen bond formation. The open conformation of PHE 400, the gatekeeper residue that separates the malonyl-binding and acyl-binding subsites, is also important for ligand-enzyme interaction (Wang et al., 2006).

The synthesized compounds exhibit good interaction with the enzyme's active site through the significant side chains of amino acid residues, as demonstrated by the docking results. Upon closer inspection of the ligand-enzyme 2D interaction, compound **27** and *E. coli*'s FabF exhibit nearly identical interactions as compared to platensimycin-FabF interaction. Consequently, the compounds appear to be promising candidates for antimicrobial agents based on their antimicrobial activity as well as their docking results.

5. Conclusion

Antimicrobial resistance remains a significant global threat to public health. One effective strategy to address this challenge involves synthesizing compounds with antimicrobial properties. In this study, we successfully synthesized three Schiff base derivatives of isonicotinic acid hydrazide through the Schiff base condensation reaction. These synthesized compounds exhibited promising antimicrobial activities against a wide range of tested bacterial and fungal strains. Molecular docking results indicated that compound **27** exhibited better interactions with the target protein (FabF enzyme) compared to compounds **28** and **29**. The ADME prediction of the compounds indicated that all of them adhered to Lipinski's rule of five. In the end, Schiff base derivatives of isonicotinic acid hydrazide show great potential as lead compounds in the development of novel antibiotics to combat the increasing risks of antibiotic resistance and infectious diseases. These findings underscore the importance of further research into synthesizing additional derivatives to evaluate potential antifungal and antibacterial properties.

References

Abirami, M. & Nadaraj, V. 2014. Synthesis of Schiff Base Under Solvent-free Condition: As A Green Approach. *International Journal of ChemTech Research,* 6 (4)**,** pp 2534-2538.

Belete, T. M. 2019. Novel Targets to Develop New Antibacterial Agents and Novel Alternatives to Antibacterial Agents. *Human Microbiome Journal,* 11, pp. 100052.

Bongomin, F., Gago, S., Oladele, R. O. & Denning, D. W. 2017. Global and Multi-National Prevalence of Fungal Diseases-Estimate Precision. *Journal of Fungi,* 3 (4)**,** pp 57.

Brito, M. A. D. 2011. Pharmacokinetic Study with Computational Tools in the Medicinal Chemistry Course. *Brazilian Journal of Pharmaceutical Sciences,* 47, pp 797-805.

Davies, C., Heath, R. J., White, S. W. & Rock, C. O. 2000. The 1.8 Å Crystal Structure and Active-Site Architecture of β-ketoacyl-Acyl Carrier Protein Synthase III (FabH) from Escherichia coli. *Structure,* 8 (2)**,** pp 185-195.

Fernandes, G. F. D. S., Salgado, H. R. N. & Santos, J. L. D. 2017. Isoniazid: A Review of Characteristics, Properties and Analytical Methods. *Critical Reviews in Analytical Chemistry,* 47 (4)**,** pp 298-308.

Hegde, P., Boshoff, H. I., Rusman, Y., Aragaw, W. W., Salomon, C. E., Dick, T. & Aldrich, C. C. 2021. Reinvestigation of the Structure-Activity Relationships of Isoniazid. *Tuberculosis,* 129, pp. 102100.

Ikuta, K. S., Swetschinski, L. R., Aguilar, G. R., Sharara, F., Mestrovic, T., Gray, A. P., Weaver, N. D., Wool, E. E., Han, C., Hayoon, A. G. & Aali, A. 2022. Global Mortality associated with 33 Bacterial Pathogens in 2019: A Systematic Analysis for the Global Burden of Disease Study 2019. *Lancet,* 400 (10369)**,** pp 2221–2248.

Khabbaz, R. F., Moseley, R. R., Steiner, R. J., Levitt, A. M. & Bell, B. P. 2014. Challenges of Infectious Diseases in the USA. *The Lancet,* 384 (9937)**,** pp 53–63.

Krause, T., Gerbershagen, M. U., Fiege, M., Weisshorn, R. & Wappler, F. 2004. Dantrolene – A Review of Its Pharmacology, Therapeutic Use and New Developments. *Anaesthesia,* 59 (4)**,** pp 364–373.

Lalitha, M. K. 2004. Manual on Antimicrobial Susceptibility Testing. Performance Standards for Antimicrobial Testing. *Twelfth Informational Supplement,* 56238, pp. 454-456.

Mitchell, J. K. & Carter, W. E. 2000. Modeling Antimicrobial Activity of Clorox (R) Using an Agar-Diffusion Test: A New Twist On an Old Experiment. *Bioscene,* 26 (3)**,** pp 9-13.

Phillips, K. F. & Hailey, F. J. 1987. Furazolidone for Treatment of Diarrhoeal Disease. *Tropical Doctor,* 17 (2)**,** pp 89-91.

Porreca, A., D'Agostino, D., Romagnoli, D., Del Giudice, F., Maggi, M., Palmer, K., Falabella, R., De Berardinis, E., Sciarra, A., Ferro, M. & Artibani, W. 2021. The Clinical Efficacy of Nitrofurantoin for Treating Uncomplicated Urinary Tract Infection in Adults: A Systematic Review of Randomized Control Trials. *Urologia Internationalis,* 105 (7-8)**,** pp 531–540.

Raczuk, E., Dmochowska, B., Samaszko-Fiertek, J. & Madaj, J. 2022. Different Schiff Bases—Structure, Importance and Classification. *Molecules,* 27 (3)**,** pp 787.

Tokano, M., Tarumoto, N., Imai, K., Sakai, J., Maeda, T., Kawamura, T., Seo, K., Takahashi, K., Yamamoto, T. & Maesaki, S. 2023. A Case of Bacterial Meningitis Caused by Bacillus subtilis var. natto. *Internal Medicine,* Internal Medicine, pp.0768-22.

Uddin, M. N., Ahmed, S. S. & Alam, S. R. 2020. Review: Biomedical Applications of Schiff Base Metal Complexes. *Journal of Coordination Chemistry,* 73 (23)**,** pp 3109–3149.

Van Seventer, J. M. & Hochberg, N. S. 2017. Principles of Infectious Diseases: Transmission, Diagnosis, Prevention, and Control. *International Encyclopedia of Public Health.* Second ed. USA: Elsevier.

Wang, J., Soisson, S. M., Young, K., Shoop, W., Kodali, S., Galgoci, A., Painter, R., Parthasarathy, G., Tang, Y. S., Cummings, R. & Ha, S. 2006. Platensimycin is A Selective FabF Inhibitor with Potent Antibiotic Properties. *Nature,* 441 (7091)**,** pp 358-361.

WHO. 2021. World Health Statistics 2021: Monitoring Health for the SDGs, Sustainable Development Goals, (Geneva).